

# **Frequency Domain Analysis and Design of Nonlinear Systems with Application in Chemical Engineering**



**Nik Nor Liyana Nik Ibrahim**

Department of Automatic Control and System Engineering  
University of Sheffield

Thesis submitted for the degree of

*Doctor of Philosophy*

March 2017



I would like to dedicate this thesis to  
my loving parents,  
my sweet husband  
and my family members  
for their endless love, support and encouragement in this long journey.



## **Acknowledgements**

And I would like to thank Prof Zi Qiang Lang, my supportive supervisor, for the knowledge he shared and the opportunity to work under his supervision. I really grateful for all the support and encouragement during his excellent supervision. Thank you for all the valuable and constructive suggestion on my research.

I also would like to acknowledge Ministry of Higher Education (MOHE) and Universiti Putra Malaysia (UPM) in Malaysia for the financial support which allow me to pursue my research interest.

Finally, special thanks to my parents, my husband and my family for their love, support and encouragement along this research journey.



## **Abstract**

Frequency domain analysis are widely done in recent years although it is much more complicated compared to the time domain because it can provide a more physical meaningful insight into the system dynamic behaviours such as stability and resonance. Frequency response function (FRF) is the frequency domain representation of linear systems. However, as most of practical engineering systems could not be modelled as linear systems, nonlinear systems analysis becomes an interesting topic to be researched. Output Frequency Response Function (OFRF) is an extension of FRF to the nonlinear systems. The advantage of using the OFRF method is the link between the parameters that define the system nonlinearity and the output frequency response of the system can be observed and understood. This relationship between the parameters that define the system nonlinearity and the output frequency response of the system provides the important basis for the nonlinear system analysis and design in frequency domain.

This research is concerned with two major scopes:

1. The development of a more effective method for the determination of OFRF for both single input single output (SISO) and multi input multi output (MIMO) nonlinear systems.
  - A new numerical method for determining and expressing the OFRF of nonlinear systems using Associated Linear Equations (ALEs) is discovered for SISO nonlinear systems, where this new methodology provided significant improvement and efficiency in determining the OFRF of the nonlinear system. Using the same

case study, the number of numerical simulations needed to determine OFRF is less compared to the method in the current literature [46]. The mathematical model used in this new method is nonlinear differential equation (NDE).

- However, most of nonlinear engineering systems are MIMO nonlinear systems. Therefore, to make a new contribution to the numerical method in the frequency domain, the new numerical method of determining the OFRF of nonlinear systems using ALEs for SISO nonlinear systems is extended to the MIMO nonlinear systems. Detailed algorithms for the new numerical method are presented and these findings opened a new insight into the understanding of the relationship between the nonlinear parameters and the output of the MIMO nonlinear systems.
- The new numerical method of determining and expressing the OFRF of nonlinear systems using ALEs for the SISO nonlinear system and the MIMO nonlinear system were applied to the passive engine mount system and the earthquake engineering. Detailed process of the determination of OFRFs was presented and the OFRF based analysis was done using the OFRF determined to facilitate the design process of the nonlinear systems. These applications show the efficiency of the new numerical method determined in this research.

2. The application of OFRF approach to the analysis of the output frequency response of chemical engineering systems.

- The current method in the analysis and design in the frequency domain of nonlinear chemical engineering systems cannot provide an explicit relationship between the nonlinear parameters and the output frequency response function. As the OFRF can solve this problem and provide a new understanding of the nonlinear chemical process, the new numerical method presented in this thesis

was applied to the nonlinear non-isothermal continuous stirred tank reactor (CSTR). The technique used to transform the material and energy balance of the system to the NDE model was by using the Taylor series form. Then, from the NDE model, the new numerical method developed in this research was applied and the OFRF of the system was determined. The OFRF provides a good solution to the nonlinear non-isothermal CSTR. The relationship between the nonlinear parameter and the output spectrum of the nonlinear system is analyzed and design of the system can be done from the analysis.

As a conclusion, this research contributes new numerical methods in frequency domain analysis. The new numerical methods presented provide new understanding of the relationship between the parameters that described the nonlinearities and the outputs of the system while making the process of OFRF determination more efficient. It has been applied to the analysis and design of nonlinear chemical engineering process system. It helps in the understanding of the nonlinear chemical process identification and revealing the relationship between the system output frequency response and parameters that define the system nonlinearity.



# Table of contents

<b>List of figures</b>	<b>xv</b>
<b>List of tables</b>	<b>xix</b>
<b>Acronyms</b>	<b>xxi</b>
<b>1 Introduction</b>	<b>1</b>
1.1 Background and motivation . . . . .	1
1.1.1 Background . . . . .	1
1.1.2 Motivation . . . . .	5
1.2 Research objectives . . . . .	8
1.3 Contributions . . . . .	9
1.3.1 Publication . . . . .	11
1.4 Thesis layout . . . . .	12
<b>2 Frequency domain analysis of nonlinear systems and associated chemical engineering background</b>	<b>15</b>
2.1 Overview . . . . .	15
2.2 System Identifications . . . . .	16
2.2.1 Volterra models . . . . .	19
2.2.2 Output Frequency Response Function (OFRF) . . . . .	25
2.3 Chemical Engineering Process Background . . . . .	29

2.3.1	Type of chemical reactors . . . . .	29
2.3.2	Chemical Process Control . . . . .	32
<b>3</b>	<b>A new numerical method for determination of OFRF of SISO nonlinear systems</b>	<b>37</b>
3.1	Introduction . . . . .	37
3.2	A new method for determining the OFRF of the SISO nonlinear systems . . . . .	39
3.2.1	NDE model for SISO nonlinear systems . . . . .	39
3.2.2	The Output Frequency Response Function of the SISO nonlinear systems . . . . .	40
3.2.2.1	OFRF representation of the SISO nonlinear system . . .	40
3.2.2.2	Example . . . . .	42
3.2.3	Derivation of ALEs for SISO nonlinear systems . . . . .	43
3.2.3.1	Associated Linear Equations for SISO nonlinear systems	43
3.2.3.2	Algorithm to determine ALE for the SISO nonlinear system	45
3.2.3.3	Example . . . . .	47
3.2.4	Determination of OFRF of the SISO nonlinear system using ALEs .	49
3.2.4.1	Algorithm to determine OFRF of the SISO nonlinear system using ALEs . . . . .	49
3.2.4.2	Example . . . . .	51
3.3	The OFRF based analysis and design of a passive engine mount . . . . .	53
3.3.1	Passive engine mount . . . . .	53
3.3.2	OFRF representation of the passive engine mount . . . . .	55
3.3.3	ALEs derivation of the passive engine mount . . . . .	56
3.3.4	Determination of OFRF using ALEs . . . . .	57
3.3.5	The results and analysis . . . . .	59
3.4	Conclusion . . . . .	61

<b>4 A new numerical method for determination of OFRFs of MIMO nonlinear systems</b>	<b>63</b>
4.1 Introduction . . . . .	63
4.2 A new numerical method for determining the OFRF of a MIMO nonlinear system . . . . .	65
4.2.1 Nonlinear differential equation (NDE) model for multi input multi output (MIMO) . . . . .	65
4.2.2 The Output Frequency Response Function for MIMO nonlinear system . . . . .	67
4.2.2.1 OFRF representation of the MIMO nonlinear system . . . . .	67
4.2.2.2 Example . . . . .	69
4.2.3 Derivation of ALEs for MIMO nonlinear systems . . . . .	70
4.2.3.1 ALEs for MIMO nonlinear system . . . . .	70
4.2.3.2 Algorithm to determine ALE for MIMO-NDE model . . . . .	73
4.2.3.3 Example . . . . .	74
4.2.4 Determination of OFRF using ALEs for MIMO nonlinear system . . . . .	79
4.2.4.1 Algorithm to determine OFRF using ALEs for MIMO nonlinear system . . . . .	79
4.2.4.2 Example . . . . .	80
4.3 Application study in earthquake engineering . . . . .	84
4.3.1 The model of Sosokan building . . . . .	84
4.3.2 OFRF representation of the Sosokan building . . . . .	89
4.3.3 ALEs derivation of the Sosokan building . . . . .	89
4.3.4 Determination of OFRF using ALEs . . . . .	90
4.3.5 The results and analysis . . . . .	91
4.4 Conclusion . . . . .	93
<b>5 Application of OFRF in non-isothermal Continuous Stirred Tank Reactor (CSTR)</b>	<b>95</b>

5.1	Introduction . . . . .	95
5.2	Implementation of the OFRF into the nonlinear non-isothermal CSTR . . . . .	96
5.2.1	Mathematical model of a nonlinear non-isothermal CSTR . . . . .	96
5.2.2	Output Frequency Response Functions(ORF) representation for nonlinear non-isothermal CSTR . . . . .	103
5.2.3	Derivation of Associated Linear Equations(ALEs) for nonlinear non-isothermal CSTR . . . . .	104
5.2.4	Determination of OFRF of the nonlinear non-isothermal CSTR using ALEs . . . . .	109
5.2.5	OFRF based analysis for the nonlinear non-isothermal CSTR . . . . .	112
5.3	Conclusion . . . . .	119
<b>6</b>	<b>Conclusion and Recommendation for Future Works</b>	<b>121</b>
6.1	Summary and Conclusion . . . . .	121
6.2	Contributions of this research . . . . .	122
6.3	Future works . . . . .	125
<b>References</b>		<b>127</b>
<b>Appendix A</b>	<b>Results for the quadratic nonlinear MIMO system</b>	<b>135</b>
A.1	Comparison between the simulated output and the sum of ALEs . . . . .	135
A.2	Comparison between the simulated output spectrum and the spectrum evaluated using OFRF . . . . .	136
<b>Appendix B</b>	<b>ORF based analysis for the application in the earthquake engineering</b>	<b>139</b>
B.1	The derivation of ALEs for the building system . . . . .	140
B.2	Comparison between the simulated output spectrum and the spectrum evaluated using ORF for even floors . . . . .	144

# List of figures

2.1	The reactors; (a) Batch reactors (b) CSTR (c) PFR. . . . .	30
3.1	The simulated output signal of the system and sum of the signals from the ALEs in the time domain when $a_2 = 500$ and $a_3 = 200$ . . . . .	48
3.2	The simulated output spectrum of the system and sum of the output spectrum from the ALEs in the frequency domain when $a_2 = 500$ and $a_3 = 200$ . . . .	49
3.3	Comparison between the simulated output spectrum and the spectrum evaluated using OFRF when $a_2 = 700$ and $a_3 = 400$ . . . . .	52
3.4	Schematic of the nonlinear passive engine mount. . . . .	55
3.5	Comparison between the simulated output spectrum and the total of ALEs output spectrum when $c_2 = 60 \times 10^3$ and $k_2 = 10 \times 10^3$ . . . . .	59
3.6	Comparison between the simulated output spectrum and the spectrum evaluated using OFRF when $c_2 = 70 \times 10^3$ and $k_2 = 40 \times 10^3$ for the passive engine mount system. . . . .	60
3.7	The relationship between the parameters $c_2$ and $k_2$ and magnitude of the output spectrum at 1.466 rad/s for the passive engine mount system. . . .	61
4.1	The simulated output signals for both $y_1$ and $y_2$ of the system and sum of the signals from the ALEs in the time domain when $a = 50$ and $b = 150$ . . . .	77

4.2	The simulated output spectrum of the system and sum of the output spectrum from the ALEs in the frequency domain when $a = 50$ and $b = 150$ for both $y_1$ and $y_2$ .	78
4.3	Comparison between the simulated output spectrum and the spectrum evaluated using OFRF for output $y_1$ when $a = 90$ and $b = 240$ .	83
4.4	Comparison between the simulated output spectrum and the spectrum evaluated using OFRF for output $y_2$ when $a = 90$ and $b = 240$ .	83
4.5	The picture of Sosokan bulding.	85
4.6	The main shock of the 2011 Great East Japan Earthquake.	86
4.7	The schematic of the building with the nonlinear building isolation system.	88
4.8	Comparison between the simulated output spectrum and the spectrum evaluated using OFRF for the odd floors when $C_2 = 120 \times 10^5$ and $K_2 = 40 \times 10^5$ .	92
4.9	The relationship between the parameters, $C_2$ and $K_2$ and magnitude of the output spectrum at 1.6755 rad/s frequency for the 5F floor.	93
5.1	The frequency of the inlet concentration of the reactant, $C_{in}$ .	99
5.2	The nonlinear nonisothermal CSTR with the a) dimensional parameters and b) dimensionless parameters.	102
5.3	The simulated output signals for both outlet concentration of the reactant, $C$ and temperature in the reactor, $\theta$ and sum of the signals from the ALEs in the dimensionless time domain when $F_s = 1$ .	107
5.4	The simulated output signals for both outlet concentration of the reactant, $C$ and temperature in the reactor, $\theta$ of the system and sum of the signals from the ALEs when $F_s = 1$ .	107
5.5	The simulated output signals for both outlet concentration of the reactant, $c_A$ and temperature in the reactor, $T$ and sum of the signals from the ALEs when $F_s = 1$ .	108

5.6	Comparison between the simulated output spectrum and the spectrum evaluated using OFRF for output $C$ with different values of $F_s$ . . . . .	111
5.7	Comparison between the simulated output spectrum and the spectrum evaluated using OFRF for output $\theta$ with different values of $F_s$ . . . . .	112
A.1	The simulated output signals for both $y_1$ and $y_2$ of the system and sum of the signals from the ALEs in the time domain when $a = 50$ and $b = 150$ . . . . .	135
A.2	The simulated output spectrum of the system and sum of the output spectrum from the ALEs in the frequency domain when $a = 50$ and $b = 150$ for both $y_1$ and $y_2$ . . . . .	136
A.3	Comparison between the simulated output spectrum and the spectrum evaluated using OFRF for output $y_1$ when $a = 90$ and $b = 240$ . . . . .	136
A.4	Comparison between the simulated output spectrum and the spectrum evaluated using OFRF for output $y_2$ when $a = 90$ and $b = 240$ . . . . .	137
B.1	Comparison between the simulated output spectrum and the spectrum evaluated using OFRF for the even floors when $C_2 = 120 \times 10^5$ and $K_2 = 40 \times 10^5$ . . .	145



# List of tables

3.1	Value of $a_2$ and $a_3$ used in the two simulations . . . . .	51
3.2	Value of $c_2$ and $k_2$ used in the three simulations . . . . .	58
4.1	Value of $a$ and $b$ used in the four simulations . . . . .	81
4.2	Value of $C_1$ and $K_1$ used in the analysis. . . . .	87
4.3	Structural parameters of the building at the Keio University . . . . .	87
4.4	Value of $C_2$ and $K_2$ used in the two simulations . . . . .	90
5.1	Definitions of the dimensionless variables. . . . .	99
5.2	Value for the physical parameters . . . . .	102
5.3	Comparison between mean values of the outlet concentration of the reactant, $\bar{c}_A$ using numerical simulation and OFRF. . . . .	113
5.4	Comparison between mean values of the temperature of the reactor, $\bar{T}$ using numerical simulation and OFRF. . . . .	114



# **Acronyms**

ALEs Associated Linear Equations

CSTR Continous stirred tank reactor

FRF Frequency Response Function

GFRFs Generalized Frequency Response Function

IMC Internal model control

MIMO Multi input multi output

MPC Model predictive control

NARMAX Nonlinear AutoRegressive Moving Average with eXogeneous input

NARX Nonlinear AutoRegressive model with eXogeneous input

nCOS nonlinear Characteristics Output Function

NDE Nonlinear Differential Equation

NFR Nonlinear Frequency Response

NIMC Nonlinear internal model control

NMPC Nonlinear model predictive control

OFRF Output Frequency Response Function

PFR Plug flow reactor

PID Proportional-integral-derivative

SISO Single input single output

TTDE Time Delayed Differential Equation

# **Chapter 1**

## **Introduction**

### **1.1 Background and motivation**

#### **1.1.1 Background**

A linear system is easier to be analysed compared to a nonlinear system. However, due to the presence of the nonlinearities, most systems in engineering and real life cannot be represented as a linear system. Thus, more analysis and research need to be done in the nonlinear system area for it to be understood. For the past decades, there is an advance progress in the analysis of the nonlinear systems in both the time and frequency domain. Significant progress that can be seen towards understanding these methods has been made but as the analysis of a nonlinear system is a problem dependent, it is still a great challenge to extract useful information from the system and there are no generic methods to deal with the problems with nonlinearity[28]. Several available techniques that are used in the nonlinear system analysis are for example perturbation method, averaging method and harmonic balance.

Besides these, several studies investigating nonlinear control system analysis have been carried out using mathematical models that can describe nonlinear systems [20, 66]. Mathematical models that are useful in the study of the nonlinear control analysis are Nonlinear Differential

Equation (NDE) [40], Nonlinear AutoRegressive model with eXogenous input(NARX) [65], Nonlinear AutoRegressive Moving Average with eXogenous input (NARMAX) [62], and Time Delayed Differential Equation (TTDE) [33]. Using the mathematical models, researchers are able to get a clear idea of the relationship between the input and the output of the system thus can predict the system behavior.

The NDE model is convenient because it can be formed naturally from the models of physical phenomena. The NARX model is favored when dealing with experimental data [65]. The NARMAX model described a system in terms of a nonlinear functional expansion of lagged input, output and prediction errors [62]. The TDDE is used in describing differential equations system with time delays in the physical process [33]. These mathematical models are widely used in the analysis of nonlinear systems as they can provide better parameter estimation and prediction accuracy compared to linear models.

The nonlinear systems can be separated to the discrete-time process models and the continuous-time process models. The NARMAX model is one of the discrete-time data models that is widely used because it can represent a wide class of nonlinear systems. The NARMAX is useful for a computer-based system, where the input and output data for the system are only available at discrete time instants because the measurements and controls are made at discrete time instants [7]. Examples of the continuous-time process models are Hammerstein and Wiener models [3, 87]. They are usually known as block-oriented models. The Hammerstein and Wiener models are considered as block-oriented nonlinear systems that composed by a cascade combination of a linear dynamic model and a static (memoryless) nonlinear function.

Recently, there have been studies of nonlinear systems that described the system by using the Volterra series [72, 82, 68]. Volterra model can be both continuous-time model and discrete-time model. In [14], it is shown that most of the nonlinear systems can be

represented as Volterra series expansion. The Volterra series also had been used in analysing nonlinear system in the frequency domain as it provides an important theoretical foundation. Any system that possesses a Volterra series representation can be described by a series of associated linear equations (ALEs) [86, 85]. The derivations of ALEs are obtained through manipulations of the Volterra series. From these ALEs, analysis of the output of the nonlinear system can be done order by order.

Based on the Volterra series expansion, the concept of the generalized frequency response function (GFRFs) is proposed in [27]. The GFRF concept is considered as direct extension of the frequency response function (FRF) function to nonlinear systems and is defined as the multidimensional Fourier transform of the Volterra kernels. The GFRF provides a fundamental principle for the study of the nonlinear system in the frequency domain as they can provide great insight about the nonlinear system that had been analysed by highlighting physical properties via a unique system representation. Based on the GFRFs concept, an analytical expression for the output frequency response to a general input that reveals how the nonlinear mechanisms operate on the input spectrum to produce the system output frequency response was derived by Lang [43, 44].

Besides [43] and [44], there are studies that have been focusing on computing the GFRFs of nonlinear systems although these methods asked for more computations compared to linear case. Analysis of nonlinear systems using GFRFs need more efforts as it is not as trivial as a linear system case and the multidimensional nature of nonlinear systems make it hard to interpret and analyse the system properties.

There are several methods to derive the GFRFs for a nonlinear system; the orthogonal functionals [72, 75], the variational approach [72, 74] and the probing method [65]. The GFRFs representation that resulting from these methods are different. For example, the

variational method can only be used when the system has input-output data and the GFRFs can be represented in the nonparametric form [74]. Meanwhile, in harmonic probing, the GFRFs can be obtained through recursive algorithm where higher order GFRFs are computed by using their lower order counterparts. The orthogonal functionals representation was used to deal with convergence problem of the conventional Volterra series, where it was difficult to find convergent Volterra series representation for the given operator [75].

However, there is some limitation in the GFRFs method. There is no revelation in how the system output frequency response depends on the system parameters as the GFRFs concept could not provide clear analytical relationship between the system time domain parameters and the system output frequency response. Graphical analysis of GFRFs method also could not be done in certain analysis or it could be a cost computation except for second order cases, where the GFRFs can be analysed from surface plots.

Hence, based on the Volterra series theory and the GFRF concept of the nonlinear system, the Output Frequency Response Function (OFRF) was proposed by Lang and Billings et al [46]. This concept is the results of a series of studies. The OFRF concept is useful for a wide class of nonlinear systems that can be derived by NDE model. It derived an explicit analytical relationship between the output frequency response and the time domain system coefficients.

By revealing the significant link between the system output frequency response and parameters that define the system nonlinearity, the OFRF concept has provided the important basis for the analysis and design of the nonlinear system. However, the OFRF concept could not be used in analysing a nonlinear system that exhibits sub-harmonics and chaos as the basis of the OFRF concept is the Volterra series approach which occupies the middle ground in generality and applicability of the theories of nonlinear systems [46, 72]. In [59], the

information about the parametric characteristics of the NDE models can be known priori by using a set of algorithms which can be used for the OFRF based analysis of nonlinear systems.

One of the numerical methods that could be used for the estimation of the OFRF is called as nonlinear Characteristic Output Function(nCOS) [38].The OFRF of this method is represented in a different form compared to the method in [46]. This nCOS method required a significant number of numerical simulations to generate system responses under different values of the design parameters which makes the determination of OFRF much more complex [54].

For the estimation of the OFRF, several numerical methods have been developed [37, 39, 46, 35], but since the truncation order of the underlying Volterra series expansion for the nonlinear system is difficult to know in advance and it can be varied with different input magnitudes, biased and even wrong estimation is hard to be avoided. This reduced the reliability and effectiveness of the OFRF based analysis. As a conclusion, in order to achieve a more effective OFRF based nonlinear system analysis and provide significant analysis and design of the nonlinear system in the frequency domain, further research need to be conducted.

### **1.1.2 Motivation**

The frequency domain analysis has been a topic of research for the last few decades. Besides being a topic of interest for engineers that study mechanical systems [18, 58], frequency domain analysis is also of interest to chemical engineer for their chemical process systems analysis [89, 26]. As most practical engineering systems cannot be modelled as a linear system, nonlinear system analysis became the subject of interest to be researched.

The nonlinear system analysis and design in the frequency domain lack of explicit analytical

description that can describe the relationship between the nonlinear parameters and the output frequency response function of the system, which make it more difficult and complicated compared to the linear system analysis. In solving nonlinear chemical process control, the common problems involved are associated with chemical processes like time delays, unmeasured state variables and high-order and distributed processes [9]. Thus, there are several methods and techniques that have been used by the researchers to solve these problems.

Some researchers still use the linear process control techniques for the nonlinear chemical process control as the conventional proportional-integral-derivative (PID) control is still effective if the nonlinearities are mild or the nonlinear process operates over a small range of conditions. For other linear control strategies, the internal model control (IMC), model predictive control (MPC) and adaptive control, they provide adequate performance when the process is sufficiently linear in the region of operation. However, other nonlinear control strategies provide significant improvements over linear control strategies when the process is highly nonlinear [76].

One of the fundamental nonlinear control strategies is feedback linearization, which is based on input-output linearization or state-space linearization. Input-output linearization control is restricted to the process where the nonlinear phase is minimum whereas the state-space linearization exploited the restriction of the input-output linearization where the system has a non-minimum phase nonlinear system and produces a stable internal control [29].

Other methodologies to solve nonlinear chemical process control are Nonlinear Internal Model Control (NIMC) and Nonlinear Model Predictive Control (NMPC) techniques. NIMC can be interpreted as a variant of the input-output linearization technique. This method uses

the two features of the IMC where the controller design is based on the inverse of the process model and the feedback signal is taken from the error between the plan and the model outputs. The NIMC method can be used in the open-loop stable processes only but the main advantage of this method was the main basis of the techniques is on full-state feedback. NMPC was an extended concept of MPC where it provided stability results for the nonlinear system by requiring knowledge of the current state of the nonlinear system and it had the ability to handle all constraints such as control inputs and outputs directly [29].

Most of the methodologies discussed above require an explicit mathematical model of process dynamics. Thus, this makes the development and analysis of the nonlinear process identification important to be studied. The models developed from the analysis of the nonlinear process will be used in the control system design methodologies. For example, there are several nonlinear system representations of pH neutralisation process; NARX models [66], neural networks [10] and Wiener model [41] and these representations were used in different control techniques [66, 91].

In this research, as OFRF concept can provide the explicit relationship between the parameters that describe the nonlinearity of the system and the output spectrum of the nonlinear system, it is interesting to apply OFRF to the nonlinear chemical process. The question rose is if there is any method that can make the determination of OFRF for nonlinear system simpler? Besides, if OFRF to be applied to the nonlinear chemical process which are mostly multi input-multi output (MIMO) nonlinear systems, then there is a need for the extension of the OFRF to MIMO nonlinear system.

Based on the concerns discussed, the OFRF will be the basis of this research. The OFRF concept needs to be understood and a new numerical method to determine OFRF for the nonlinear system will be developed. The new numerical method should increase the efficiency

of the process of OFRF determination. Then, using the new numerical method develops, the OFRF concept need to be extended to MIMO nonlinear systems so that the new numerical method can be applied to MIMO nonlinear chemical process system. Then, an application of analysis and design of an application in chemical engineering using OFRF will be discussed.

## 1.2 Research objectives

This research has two major scopes to be accomplished. First, this research aims to development of a more effective method for the determination of OFRF for both SISO and MIMO nonlinear systems. Secondly, this research involves the application of OFRF approach to the analysis of the output frequency response of chemical engineering systems. There are several objectives to be achieved in this research. The details of the objectives are:

1. To understand the OFRF and ALEs concepts and identify the gaps and future improvement in nonlinear control analysis area. The Volterra series theory in the frequency domain, the OFRF and the ALEs concepts need to be reviewed. Using the understanding of these concepts, a new numerical method can be developed to provide better progress towards understanding the nonlinear control analysis area.
2. To develop a new and more efficient numerical method for the determination of OFRF of SISO nonlinear systems that can facilitate the process of the analysis and design. The new numerical method should increase the efficiency of the determination of OFRF for nonlinear systems by significantly reduce the number of numerical simulations. The new numerical method will utilise the ALEs concept.
3. To develop and extend the new numerical method for the determination of OFRF of the MIMO nonlinear systems. Detailed algorithms will be developed for the determination of OFRF using ALEs for MIMO nonlinear system. The algorithms produced for

MIMO nonlinear systems will open a new journey to understanding the relationship between the nonlinear parameters and the output for MIMO nonlinear system.

4. To test the effectiveness of the new numerical method proposed in this research. Different nonlinear engineering systems will be chosen for the analysis. The simulation studies should demonstrate the effectiveness of the new numerical method proposed in the determination of OFRF. The OFRF based analysis should help the analysis and design of the nonlinear systems.
5. To understand the nonlinear chemical process identification and identify how to reveal the relationship between the system output frequency response and parameters that define the system nonlinearity. A mathematical model is needed thus it is crucial to determine how to represent the nonlinear chemical process system using a NDE model.
6. To implement the new numerical method for the determination of OFRF of the MIMO nonlinear chemical process system. This implementation will help in the understanding of the relationship between the system output frequency response and parameters that define the system nonlinearity of nonlinear chemical engineering process systems. The application is to achieve more effective system analysis and designs.

### 1.3 Contributions

The objectives of this research have been achieved through the following contributions:

- A new numerical method to determine OFRF using ALEs concept is developed. The new numerical method increases the efficiency of determination of OFRF for a nonlinear system. The number of simulations needed to determine OFRF is less compared to the current literature. Detailed algorithms for the new numerical method

are discussed in Chapter 3. In this new numerical method, three algorithms are involved. The OFRF representation of the NDE model can be determined priori using the first derived algorithm. Then, the second algorithm facilitates the derivation of ALEs for the nonlinear system. Finally, the last algorithm uses the results from the first and second algorithm and their relationship to determine the OFRF of the nonlinear system. These algorithms only work for SISO nonlinear system.

- Algorithms to facilitate the process of determination of ALEs for the NDE model for the SISO and MIMO model are presented. These algorithms are developed in this research and useful for the new numerical method proposed in this research. The detailed algorithms to determine ALEs for SISO nonlinear system is presented in Chapter 3 while the detailed algorithms to determine ALEs for MIMO nonlinear system is presented in Chapter 4.
- The new numerical method to determine OFRF using ALEs is extended to MIMO nonlinear systems. This new numerical method also consists of three algorithms and is discussed in Chapter 4. The first algorithm is an algorithm to determine the OFRF representation of the NDE MIMO nonlinear system. Then, the second algorithm is the derivation of ALEs for the MIMO nonlinear system. The last algorithm is the determination of OFRF using ALEs. These algorithms use the same concept and techniques as the new numerical method to determine the OFRF using ALEs for the SISO nonlinear system. The new numerical method to determine the OFRF using ALEs for the MIMO nonlinear system developed in this research provides a better understanding of the relationship between the nonlinear parameters and the output for MIMO nonlinear system.

- The new numerical method proposed is applied to various nonlinear engineering problems. Different SISO nonlinear systems and MIMO nonlinear systems were analysed using the new numerical method. Simulation studies demonstrated the effectiveness of the new numerical method proposed in the determination of OFRF for both SISO and MIMO nonlinear system. The OFRF based analysis and design were done on two different nonlinear systems; the passive engine mount system and the engineering earthquake system.
- In order to analyse the nonlinear chemical process identification and reveal the relationship between the system output frequency response and parameters that define the system nonlinearity, the material and energy balance of the nonlinear non-isothermal CSTR system is transformed to the NDE model. This was done by expanding the nonlinear terms in the Taylor series form.
- The new numerical method proposed in this research is implemented and tested to a nonlinear non-isothermal CSTR system. This system is a periodic operation system. The analysis of the nonlinear non-isothermal CSTR system used the detailed algorithms presented and discussed in Chapter 4. Based on the OFRF determined, the relationship between the system output frequency response and parameters that define the system nonlinearity is analysed. Also, comparing with steady-state operation analysis [49], the result of the OFRF based analysis also consistent with the fact that the periodic operation of a nonlinear system improves the conversion of the product compared to the steady-state operation [19, 71, 73].

### 1.3.1 Publication

The research result was published in the conference proceeding that was attended by the author. The details of the publication is as below: Nik Ibrahim, N. N. L., Lang, Z.Q.

(2016), A new and efficient method for the determination of Output Frequency Response Function of nonlinear vibration system. Proceedings of the International Conference on Smart Infrastructure and Construction (ICSIC 2016), University of Cambridge, Cambridge, United Kingdom, 27-29 June 2016.

The content of Chapters 3, 4 and 5 are currently in progress to be submitted as three different publications.

## 1.4 Thesis layout

Chapter 1 relates to the background and motivation of this research. All the objectives of this research are also listed in details. Lastly, the contributions and publication that achieved through this research are explained.

Chapter 2 discusses the frequency domain analysis for nonlinear systems. A review of system identification and how Volterra models are involved in the development of the studies of nonlinear are done. Then the GFRFs concept is discussed before the OFRF concept is discussed comprehensively as the OFRF concept is the foundation of this research. Chapter 2 also discusses about the chemical process background. Different types of chemical reactors are presented and the background of chemical process control is introduced.

Chapter 3 develops a new numerical method for the determination of the OFRF when the systems are SISO nonlinear systems. The new approach for determining OFRFs is by using the NDE model and exploiting the concept of ALEs. The new numerical method consists of three algorithms. The first algorithm is about the determination of OFRF representation of the SISO nonlinear system. The second algorithm is for the determination of ALEs for the NDE model where the ALEs can be determined easily up to any order. The last algorithm focuses

on the determination of OFRF using the ALEs. This algorithm uses the relationship between the OFRF representation and the ALEs determined in the first two algorithms. Using the new numerical method presented, the OFRF of the SISO nonlinear system can be determined with significantly less number of numerical simulations compared to the previous works. Using the new numerical method presented in this chapter, an OFRF based analysis and design was applied to the nonlinear passive engine mount system.

Chapter 4 discussed the new numerical method for the determination of the OFRF when the systems are MIMO nonlinear systems. It uses the same concepts and techniques presented in Chapter 3 and is an extension of the new numerical method developed in Chapter 3. The new numerical method for the determination of the OFRF for the MIMO nonlinear system also consists of three algorithms. All the algorithms are discussed and presented in details. The new numerical method developed in this chapter provides a better understanding of the relationship between the nonlinear parameters and the output for MIMO nonlinear system. The OFRF based design of a building structure vibration isolation system has then be used to demonstrate how the new numerical method can be applied to implement a design for application in earthquake engineering.

Chapter 5 shows the application of the new numerical method developed in this thesis on chemical engineering system. A periodic operation of a nonlinear non-isothermal CSTR system is chosen for the analysis. The material and energy balance of the nonlinear non-isothermal CSTR system is transformed to the NDE model by expanding the nonlinear terms in the Taylor series form. Then the new numerical method discussed in Chapter 4 is implemented into the nonlinear non-isothermal CSTR system. Using the OFRF determined, the analysis and design of the system are done.

Lastly, Chapter 6 summarises and concludes the main results of this research. All contributions

of the new numerical method proposed in this thesis and its application in the engineering system are listed. In addition, the suggestion of topics that can use the new outcomes proposed in the present study is discussed.

# **Chapter 2**

## **Frequency domain analysis of nonlinear systems and associated chemical engineering background**

### **2.1 Overview**

Studies of a system can be done in either time or frequency domain by using appropriate mathematical models. Most practical systems are using time domain analysis where the input and output signals of the systems are all physical variables changing with time. Although the frequency domain is far more complicated compared to the time domain, the frequency domain can provide a more physical meaningful insight into the systems dynamic behaviours such as stability and resonance. Thus, the analysis in the frequency domains has an excellent opportunity to be developed.

In the early day, the frequency response techniques provide revolution and conceptual framework for control theory and applications in engineering [48]. Thus, extensive studies have been conducted on the system, control, and other relevant subject areas by using

frequency domain analysis and design. Practical systems can be separated into two; linear and nonlinear systems. In comparison, a linear system is easier to be analysed compared to a nonlinear system, but most practical engineering systems cannot be modelled as linear systems. This makes the nonlinear system analysis an interesting topic to be researched.

## 2.2 System Identifications

Intensive studies have been done for linear systems in both the time and frequency domains. In the time domain, for a linear system operator, it can be defined as

$$y(t) = H(u(t)) \quad (2.1)$$

where  $H$  is a mathematical operator that maps an input signal  $u(t)$  to an output signal  $y(t)$ . The system output  $y(t)$  subjected to a general input  $u(t)$  of a linear, stationary, causal and single input-single output (SISO) in the time domain can be represented by the convolution integral [72] as

$$y(t) = \int_{-\infty}^{\infty} h(\sigma)u(t - \sigma)d\sigma \quad (2.2)$$

where  $h(\delta)$  is the impulse response called “kernel” and is assumed to satisfy  $h(t) = 0$  for  $t < 0$ .

Whereas, in the frequency domain, the output frequency response of the linear systems can be described by

$$Y(j\omega) = H(j\omega)U(j\omega) \quad (2.3)$$

when the stable time-invariant linear system is subject to an input whose Fourier transform exist.  $U(j\omega)$  and  $Y(j\omega)$  are the system input and output frequency response which are the Fourier transform of the system output  $y(t)$  and a general input  $u(t)$  in the time domain.  $H(j\omega)$  is the Frequency Response Function (FRF) of the linear system. (2.3) shows that the

output frequency response at any frequency of  $\omega$  of interest is affected by the input spectrum and has been widely applied in systems analysis and controller design for engineering.

However, most systems in engineering and real life cannot be represented as a linear system, due to the presence of nonlinearities. There is an advance progress in the analysis of nonlinear systems in both time and frequency domain, and significant progress towards understanding these methods has been made [46]. But it is still a great challenge to extract useful information from the system, and there is no generic methods to deal with the problems with nonlinearity as the analysis of a nonlinear system is a problem dependent [28]. The nonlinear systems have challenging dynamic behaviours such as input multiplicities [42], chaos [23] and open loop behaviour [83].

There are many mathematical models that have been used to describe nonlinear systems in the study of the nonlinear control analysis such as Nonlinear Differential Equation (NDE), Nonlinear AutoRegressive model with eXogenous input (NARX), Nonlinear AutoRegressive Moving Average with eXogenous input (NARMAX), and Time Delayed Differential Equation (TDDE) [12, 33, 62]. The NDE model is convenient and concise while the NARX model provides practical nonlinear system identification and is used when analysing experimental data. The NARMAX model described a system regarding a nonlinear functional expansion of lagged input, output and prediction errors. Lastly, if there is time delays in the physical process, the TDDE is used in describing differential equations system with time delays in the physical process. These mathematical models are widely used in the analysis of nonlinear systems because they can provide better parameter estimation and prediction accuracy compared to the linear model.

The nonlinear systems can be separated to continuous-time process models and the discrete-time process models. Volterra model can be both continuous-time model and discrete-time model.

The Volterra models will be discussed in the next subsection as it is the basic concept of this research. Closely related to the Volterra models are the block-oriented models. The best-known members of this class are the Hammerstein and Wiener models, which are special kinds of nonlinear systems that have various applications in many practical engineering problems and have been actively researched for a long time. The Hammerstein and Wiener models are considered as block-oriented nonlinear systems that are composed by a cascade combination of a linear dynamic model and a static (memoryless) nonlinear function.

There are several methods for the identification of Hammerstein and Wiener models in the literature [87, 3] such as the iterative method, the stochastic method, the nonlinear least square method, the separable least square method, the blind method and the frequency domain method. These methods have their own advantages and disadvantages.

The iterative method divides parameters into linear and nonlinear parts before optimizing one part and fixing the other parts. The process is repeated where the two parts are switched for the optimization. The iterative method is efficient to be used in the identification of Hammerstein and Wiener model [53, 80]. The stochastic method only needs two data which are white Gaussian input and the system output for the identification. Thus, without knowing the nonlinearity of the system, the identification of the models can be done [11].

For the nonlinear least square method, it only works if certain restrictive conditions are hold [6] while the separable least square method works for hard input nonlinearities [5]. Hard input nonlinearities are difficult because of the coupled unknown parameters of both linear and nonlinear parts. However, for a system where the structure of the input nonlinearities are unknown, the identification of linear and nonlinear parts can be done using the blind method [2]. This makes the blind method works perfectly when no knowledge of the input nonlinearities available.

In the frequency domain identification of the Hammerstein model, the use of sinusoidal inputs makes the identification of the system simpler as the subharmonics and chaos can never happen. Besides, all the signals inside the system consist of frequencies that are an integer multiple of the input frequencies because of the periodicity of the input signals. The output frequency response of the system also can be represented by a Fourier series representation and the Fourier coefficients are invariant to the input frequencies.

There are several approaches to the frequency domain identification of Hammerstein models. In [3], the algorithm discussed how a no priori information on the structure of the nonlinearity and a non-parametric linear part could produce the convergence results in the presence of white noise assumption. The same concept is used in [4] for the Wiener model by making some minor modifications.

For a computer-based system, the input and output data for the system only available at discrete time instants because the measurements and controls are made at discrete time instants. Thus, although continuous time models can be determined from these data, the analysis of the discrete-time system is easier to be done by using discrete-time models themselves. This allows the NARMAX to be popular because it can represent a wide class of nonlinear systems model and one of the discrete-time data models.

### 2.2.1 Volterra models

The Volterra model can be both continuous-time model and discrete-data model. There are research on nonlinear systems that described the system by using the Volterra series [72, 82, 68]. In [14], it is shown that most of the nonlinear systems can be represented as Volterra series expansion. The Volterra series also had been used in analysing nonlinear system in the frequency domain as it provides an important theoretical foundation.

A nonlinear system that is stable at zero equilibrium point which can be approximated by a Volterra series up to maximum order N can be written as [74]

$$y(t) = \sum_{n=1}^N \int_{-\infty}^{\infty} \dots \int_{-\infty}^{\infty} h_n(\tau_1, \dots, \tau_n) \prod_{i=1}^n u(t - \tau_i) d\tau_i \quad (2.4)$$

where  $y(t)$  and  $u(t)$  are the output and input of the system and  $h_n(\tau_1, \dots, \tau_n)$  is the  $n$ th-order Volterra kernel.  $h_n(\tau_1, \dots, \tau_n)$  is a real valued function of  $\tau_1, \dots, \tau_n$ . Equation (2.4) can be expressed as

$$y(t) = \sum_{n=1}^N y_n(t) \quad (2.5)$$

where

$$y_n(t) = \int_{-\infty}^{\infty} \dots \int_{-\infty}^{\infty} h_n(\tau_1, \dots, \tau_n) \prod_{i=1}^n u(t - \tau_i) d\tau_i \quad (2.6)$$

is the contribution of the  $n$ th-order nonlinearity to the system output.

Any system that possesses a Volterra series representation can be described by a series of associated linear equations (ALEs) [84–86]. From these ALEs, analysis of the output of the nonlinear system can be done order by order. The derivations of ALEs are obtained through manipulations of the Volterra series. To understand the concept of ALEs, consider a second-order differential equation described as

$$m\ddot{y}(t) + c\dot{y}(t) + ky(t) + \sum_{j=2}^N k_j y^j(t) = \sum_{j=1}^M a_j u^j(t) \quad (2.7)$$

where  $u$  is the input terms of the system and  $y$  is the output terms of the system. Leaving on the left hand side of the equation only the linear elements, (2.7) will be

$$m\ddot{y}(t) + c\dot{y}(t) + ky(t) = \sum_{j=1}^M a_j u^j(t) - \sum_{j=2}^N k_j y^j(t) \quad (2.8)$$

Knowing that the system possesses a Volterra representation, substitute

$$y(t) = \sum_{n=1}^{\infty} y_n(t) \quad (2.9)$$

into (2.8) form

$$m \sum_{n=1}^{\infty} \ddot{y}_n(t) + c \sum_{n=1}^{\infty} \dot{y}_n(t) + k \sum_{n=1}^{\infty} y_n(t) = \sum_{j=1}^M a_j u^j(t) - \sum_{n=2}^N k_n \left( \sum_{i=1}^{\infty} y_i(t) \right)^j \quad (2.10)$$

Then, by rearranging the sum, grouping the degree of the terms, (2.10) become

$$\begin{aligned} & m \sum_{n=1}^{\infty} \ddot{y}_n(t) + c \sum_{n=1}^{\infty} \dot{y}_n(t) + k \sum_{n=1}^{\infty} y_n(t) \\ &= \sum_{j=1}^M a_j u^j(t) - \left( \sum_{n=1}^{\infty} \sum_{l=2}^n k_l \sum_{j_1=1}^{n-l+1} \dots \sum_{j_i=1}^{n-l+i-j_1-\dots-j_{i-1}} \dots \sum_{j_l=0}^{n-j_1-\dots-j_{i-1}-j_{l-1}} y_{j_1}(t) y_{j_2}(t) \dots y_{j_l}(t) \right) \end{aligned} \quad (2.11)$$

In (2.11), all the elements on the left hand side are linear whereas on the right hand side, all the terms comprise the summation of terms. In ALEs, determination of the total response will be the summation of all the responses.

Based on the Volterra series expansion, the concept of the generalized frequency response function (GFRFs) is proposed in [27]. The  $n$ th-order GFRF of system (2.4) is defined as

$$H_n(j\omega_1, \dots, j\omega_n) = \int_{-\infty}^{\infty} \dots \int_{-\infty}^{\infty} h_n(\tau_1, \dots, \tau_n) \exp(-j(\omega_1 \tau_1, \dots, \omega_n \tau_n)) d\tau_1 \dots d\tau_n \quad (2.12)$$

The GFRF concept is considered as direct extension of the frequency response function (FRF) function to nonlinear systems. The GFRF provides the fundamental principle for

the study of nonlinear systems in the frequency domain as they can provide a great insight about the nonlinear system that had been analysed by highlighting physical properties via unique system representation and is defined as the multidimensional Fourier transform of the Volterra kernels [88]. Billings and Peyton Jones derived the analytical relationship between NDE and GFRFs in [13]. Based on the GFRFs concept, an analytical expression for the output frequency response to a general input that reveals how the nonlinear mechanisms operate on the input spectrum to produce the system output frequency response was derived as [43]

$$\begin{cases} Y(j\omega) = \sum_{n=1}^N Y_n(j\omega) & \text{for } \forall \omega, \\ Y_n(j\omega) = \frac{1/\sqrt{n}}{(2\pi^{n-1})} \int_{\omega_1+\dots+\omega_n=\omega} H_n(j\omega_1, \dots, j\omega_n) \prod_{i=1}^n U(j\omega_i) d\sigma_{n\omega} \end{cases} \quad (2.13)$$

where  $Y_n(j\omega)$  represents the  $n$ th-order output frequency response of the system and  $\int_{\omega_1+\dots+\omega_n=\omega} H_n(j\omega_1, \dots, j\omega_n) \prod_{i=1}^n U(j\omega_i) d\sigma_{n\omega}$  denotes the integration of  $H_n(j\omega_1, \dots, j\omega_n) \prod_{i=1}^n U(j\omega_i)$  over the  $n$ -dimensional hyperplane  $\omega_1, \dots, \omega_n = \omega$ . The term  $H_n(j\omega_1, \dots, j\omega_n)$  is the  $n$ th-order GFRF of the system as defined in (2.12).

In nonlinear systems that can be described by the Volterra series in equation (2.4), the output frequencies at the steady state can be defined as follows

$$f_Y = \bigcup_{n=1}^N f_{Y_n} \quad (2.14)$$

where  $f_Y$  represents the non-negative frequency range of the nonlinear system output and  $f_{Y_n}$  is the non-negative frequency range produced by the  $n$ th-order system nonlinearity. An explicit expression for the nonlinear systems subjected to a general input with a spectrum is

derived as

$$U(j\omega) = \begin{cases} U(j\omega) & \text{when } |\omega| \in (a, b), \\ 0 & \text{otherwise} \end{cases} \quad (2.15)$$

where  $b > a \geq 0$  [44]. The result obtained is as follows

$$\left\{ \begin{array}{l} f_Y = f_{Y_N} \cup f_{Y_{N-(2p^*-1)}}, \\ f_{Y_N} = \begin{cases} \bigcup_{k=0}^{i^*-1} I_k & \text{when } \frac{nb}{a+b} - \left\lfloor \frac{na}{(a+b)} \right\rfloor < 1, \\ \bigcup_{k=0}^{i^*} I_k & \text{when } \frac{nb}{a+b} - \left\lfloor \frac{na}{(a+b)} \right\rfloor \geq 1, \end{cases} \\ i^* = \left\lfloor \frac{na}{(a+b)} \right\rfloor + 1 \quad \lfloor . \rfloor \quad \text{means to take the integer part,} \\ I_k = (na - k(a+b), nb - k(a+b)) \quad \text{for } k = 0, \dots, i^* - 1, \\ I_{i^*} = (0, nb - i^*(a+b)), \\ p^* = 1, 2, \dots, \lfloor N/2 \rfloor. \end{array} \right. \quad (2.16)$$

This result provides a significant analytical description for the output frequencies of the nonlinear system and shows the extension of the output frequencies of the linear system to the nonlinear system. Although these methods asked for more computations compared to the linear case, besides [43, 44], there are studies that have been focusing on computing the GFRFs of nonlinear systems. The analysis of nonlinear systems using GFRFs needs more efforts as it is not as trivial as a linear system case and the multidimensional nature of nonlinear systems make it hard to interpret and analyse the system properties.

There are several methods to derive the GFRFs for a nonlinear system, for example the orthogonal functionals [72, 75], the variational approach [72, 74] and the probing method [13, 65]. These methods produce different GFRFs representations. For example, GFRFs

is represented in the nonparametric form for the variational method and can only be used when the system has input-output data [74]. Meanwhile, in harmonic probing, the GFRFs can be obtained through recursive algorithm where higher order GFRFs are computed by using their lower order counterparts. The orthogonal functionals representation is used to deal with convergence problem of the conventional Volterra series, where it was difficult to find convergent Volterra series representation for the given operator [75].

However, there is some limitation in the GFRFs method. There is no revelation in how the system output frequency response depends on the system parameters. The GFRFs concept could not provide a clear analytical relationship between the system time domain parameters and the system output frequency response. Graphical analysis of GFRFs method also could not be done in certain analysis or it could be cost computations except for second order cases, where the GFRFs can be analysed from surface plots.

Hence, based on the Volterra series theory and the GFRF concept and limitations, the Nonlinear Output Frequency Response Function (NOFRFs) was proposed by Lang and Billings in 2005 [45] the Output Frequency Response Function (OFRF) was proposed by Lang et al in 2007 [46]. These concepts are the results of a series of studies. The NOFRFs method gave better estimation compared to the harmonic balance method [61]. The concept of OFRF will be discussed comprehensively in the next subsection.

The GFRF concept itself is being researched actively to overcome its limitation. In 2012, Bayma produced an algorithm to generate GFRFs from nonlinear system models that can be described by NARX model [8]. This allows GFRFs to be determined up to any arbitrary order. Using the same concept applied to the GFRFs, Bayma developed a new method to determine NOFRFs [7]. The concept of OFRF will be discussed comprehensively in the next subsection.

## 2.2.2 Output Frequency Response Function (OFRF)

The OFRF concept is useful for a wide class of nonlinear system that can be represented by NDE model. It derived an explicit analytical relationship between the output frequency response and the time domain system coefficients.

By revealing the significant link between the system output frequency response and parameters that define the system nonlinearity, OFRF concept has provided an important basis for the analysis and design of the nonlinear system. However, the OFRF concept could not be used in analysing a nonlinear system that exhibits sub-harmonics and chaos as the basis of the OFRF concept is the Volterra series approach which occupies the middle ground in generality and applicability of the theories of nonlinear systems [46, 72].

Consider polynomial-type nonlinear systems, where the system can be described by a differential equation of a polynomial form or known as Nonlinear Differential Equation(NDE) model

$$\sum_{m=1}^M \sum_{\substack{p=0 \\ p+q=m}}^m \sum_{l_1, \dots, l_{p+q}}^L c_{pq}(l_1, \dots, l_{p+q}) \prod_{i=1}^p D^{l_i} y(t) \times \prod_{i=p+1}^{p+q} D^{l_i} u(t) = 0 \quad (2.17)$$

where M and L are the maximum degrees of nonlinearity in terms of  $y(t)$  and  $u(t)$ , and the maximum order of derivative while the operator  $D$  is defined by

$$D^l x(t) = \frac{d^l x(t)}{dt^l} \quad (2.18)$$

This equation explains the relationship between the time and frequency domain representations of nonlinear systems explicitly. By assuming  $c_{(1,0)}(0) \neq 0$ , equation (2.17) can be used to represent a valid input/output map. By rearranging this equation, a nonlinear differential equation model is produced

$$-c_{1,0}(0)y(t) = \sum_{m=1}^M \sum_{\substack{p=0 \\ p+q=m}}^m \sum_{l_1, \dots, l_{p+q}}^L c_{pq}(l_1, \dots, l_{p+q}) \prod_{i=1}^p D^{l_i} y(t) \times \prod_{i=p+1}^{p+q} D^{l_i} u(t) \quad (2.19)$$

For a better of understanding of (2.17), consider a cubic duffing oscillator that was described as

$$10\ddot{y}(t) + 1000\dot{y}(t) + 2.5 \times 10^6 y(t) + 5 \times 10^4 y(t)^3 = 10u(t) \quad (2.20)$$

where the input signal for the output frequency response analysis was  $u(t) = 15\sin(3t)$ ,  $t \in [-20s, 20s]$ . (2.20) is in the form of NDE model in equation (2.17) with  $M = 3$  and  $L = 2$ . The coefficient of this NDE model are  $c_{1,0}(2) = 10$ ,  $c_{1,0}(1) = 1000$ ,  $c_{1,0}(0) = 2.5 \times 10^6$ ,  $c_{3,0}(0,0,0) = 5 \times 10^4$ ,  $c_{0,1}(0) = -10$  and all other  $c_{pq}(.) = 0$ .

For nonlinear systems that can be described by model (2.17), and satisfies the following assumptions:

- The system is stable at zero equilibrium
- The systems can equivalently be described by the Volterra series model with  $N \geq M$  over a regime around the equilibrium,

there exists an explicit analytical relationship between the output frequency response and the model parameters. In [46], the OFRF of a general nonlinear system can be represented as

$$\begin{aligned} \hat{Y}(j\omega) &= \sum_{(j_1, \dots, j_{S_N}) \in J} \gamma_{(j_1, \dots, j_{S_N})}(\omega) x_1^{j_1} \dots x_{S_N}^{j_{S_N}} \\ &= \sum_{j_1}^{m_1} \sum_{j_2}^{m_2} \dots \sum_{j_{S_N}}^{m_{S_N}} \gamma_{(j_1, \dots, j_{S_N})}(\omega) x_1^{j_1} \dots x_{S_N}^{j_{S_N}} \end{aligned} \quad (2.21)$$

where  $m_i$  are the maximum power of  $x_i$ ,  $i = 1, \dots, S_N$ .

The functions  $\gamma_{(j_1, \dots, j_{S_N})}(\omega)$ ,  $j_i = 0, \dots, m_i$ , can be determined as

$$\begin{bmatrix} \underbrace{\gamma_{0, \dots, 0}}_{S_N}(\omega) \\ \vdots \\ \vdots \\ \gamma_{m_1, \dots, m_{S_N}}(\omega) \end{bmatrix} = X_{\bar{M}}^{-1} \begin{bmatrix} Y^1(j\omega) \\ \vdots \\ \vdots \\ Y^{\bar{M}}(j\omega) \end{bmatrix}, \quad (2.22)$$

where  $\bar{M} = (m_1 + 1)(m_2 + 1) \dots (m_{S_N} + 1)$  and

$$X_{\bar{M}} = \begin{bmatrix} (x_{11}^0 \dots x_{S_N 1}^0) \dots \dots (x_{11}^{m_1} \dots x_{S_N 1}^{m_{S_N}}) \\ \vdots \quad \vdots \quad \vdots \quad \vdots \\ \vdots \quad \vdots \quad \vdots \quad \vdots \\ (x_{1\bar{M}}^0 \dots x_{S_N \bar{M}}^0) \dots \dots (x_{1\bar{M}}^{m_1} \dots x_{S_N \bar{M}}^{m_{S_N}}) \end{bmatrix}_{\underbrace{(m_1+1)(m_2+1)\dots(m_{S_N}+1)}_{\bar{M}}} \quad (2.23)$$

$x_i(1), \dots, x_i(m_i + 1)$  are  $m_i + 1$  different values that can be taken by the systems parameter  $x_i, i = 1, \dots, S_N$ . When the parameters  $x_1, \dots, x_{S_N}$  of the systems are taken as  $x_{1\tilde{m}}, \dots, x_{S_N \tilde{m}}$ , with  $\tilde{m} = 1, \dots, \bar{M}, x_{i\tilde{m}} \in \{x_i(1), \dots, x_i(m_i + 1)\}, i = 1, \dots, S_N, \tilde{m} = 1, \dots, \bar{M}, (x_{1i}, \dots, x_{S_N i}) \neq (x_{1v}, \dots, x_{S_N v}), i \neq v$ , the output spectrum of (2.21) can be defined as  $Y^{\tilde{m}}(j\omega)$ . The output spectrum  $Y^{\tilde{m}}(j\omega)$  can be determined from the system output response through experimental tests and simulation analysis [28].

In [59], the information about the parametric characteristics in (2.21) can be known priori by using a set of algorithm. This algorithm provides a good way to determine all the parametric characteristics involved in the OFRF. By knowing the parametric characteristics, a correct OFRF representation of a system can be determined easily. Denote the set of all the

parametric characteristics involved in the representation of  $Y(j\omega)$  given by (2.21) as  $\mathbf{M}_n$  and  $\mathbf{M}_1 = [1]$ , then

1. Set  $N \geq 0$  and  $n = 0, 1, \dots, N$ .
2. Calculate  $\mathbf{M}_n$  by using

$$\begin{aligned} \mathbf{M}_n = & \left[ \bigcup_{l_1, \dots, l_n=0}^L [c_{0n}(l_1, \dots, l_p)] \right] \cup \left[ \bigcup_{q=1}^{n-1} \bigcup_{p=1}^{n-q} \bigcup_{l_1, \dots, l_n=0}^L [c_{0n}(l_1, \dots, l_p) \otimes \mathbf{M}_{n-q,p}] \right] \\ & \cup \left[ \bigcup_{p=2}^n \bigcup_{l_1, \dots, l_p=0}^L [c_{p0}(l_1, \dots, l_p) \otimes \mathbf{M}_{np}] \right] \end{aligned} \quad (2.24)$$

where  $\otimes$  is the Kronecker product, and

$$\mathbf{M}_{np} = \bigcup_{i=1}^{n-p+1} (\mathbf{M}_i \otimes \mathbf{M}_{n-i,p-1}) \quad \text{and} \quad \mathbf{M}_{n1} = \mathbf{M}_n \quad (2.25)$$

3. Lastly, the set of the parametric characteristics in (2.21) can be expressed as

$$\bar{\mathbf{M}}_N = \bigcup_{n=1}^N \mathbf{M}_n \quad (2.26)$$

$\bar{\mathbf{M}}_N$  is the parametric characteristics involved in the OFRF. Using the parametric characteristics, the OFRF representation can be determined.

One of the numerical methods that could be used for the estimation of the OFRF is called as nonlinear Characteristic Output Function(nCOS) [38, 36]. In this method, the nonlinear output spectrum of (3.1) is written as an explicit polynomial function of the characteristic parameters of the system

$$Y(j\omega) = \sum_{n=1}^N \chi_n \cdot \varphi_n(j\omega)^T \quad (2.27)$$

where  $\chi_n$  denotes the  $n$ th-order characteristic parameter vector composed of nonlinear parameters and  $\varphi_n(j\omega)^T$  is the correlative complex-valued function of the  $n$ th-order output

spectrum. Both  $\chi_n$  and  $\varphi_n(j\omega)^T$  can be analytically determined with method in [37] and [38].

By using the  $n$ th-order output spectrum ( $n$ th-OSE) algorithm and  $n$ th-order nCOS estimation ( $n$ th-COSE) algorithm[35], the estimation of OFRF function can be written as

$$\hat{Y}(j\omega) = \rho \hat{Y}_1(j\omega) + \sum_{n=2,3,\dots}^{\chi_{n|\bar{c}=1}} \rho^n \hat{Y}_n(j\omega) + \sum_{n=2,3,\dots}^{\chi_{n|\bar{c}\neq 1}} \rho^n (\hat{Y}_n(j\omega)|_{\bar{c}=0} \chi_{n|\bar{c}} \varphi_n(j\omega)^T) \quad (2.28)$$

where  $\bar{c}$  is the set of the characteristics parameters of the system. The OFRF of this method is represented in a different form compared to that in [46] where it is expressed in a polynomial function that explicitly stated the relationship between the output spectrum and all the system characteristic parameters such as nonlinear parameters and input excitation magnitude.

For the estimation of the OFRF, several numerical methods have been developed [35, 37, 39, 46]. However, biased and even wrong estimation is hard to be avoided since the truncation order of the underlying Volterra series expansion for the nonlinear system is difficult to know in advance and it can be varied with different input magnitudes. This reduced the reliability and effectiveness of the OFRF based analysis. As a conclusion, further research need to be conducted in order to achieve a more effective OFRF based nonlinear system analysis and provide significant analysis and design of the nonlinear system in the frequency domain.

## 2.3 Chemical Engineering Process Background

### 2.3.1 Type of chemical reactors

A chemical process is a process of chemical reaction between two or more reactants resulting in a conversion of chemical substances that involved. A chemical reactor is a vessel where chemicals are made as the product of a chemical process reaction. In designing a chemical reactor, many factors are considered, but the two most important factors are the

thermodynamic and kinetics of the chemical reaction for the system. The chemical reactors can be classified into their mode of operations which are continuous and discontinuous reactors [17]. The two main types of the continuous chemical reactors are continuous stirred tank reactor (CSTR) and plug flow reactor(PFR) whereas batch reactor is a widely used discontinuous reactor. Other types of continuous chemical reactors are fixed bed reactors and fluid bed reactors. Figure 2.1 shows the batch reactor, CSTR, and PFR.

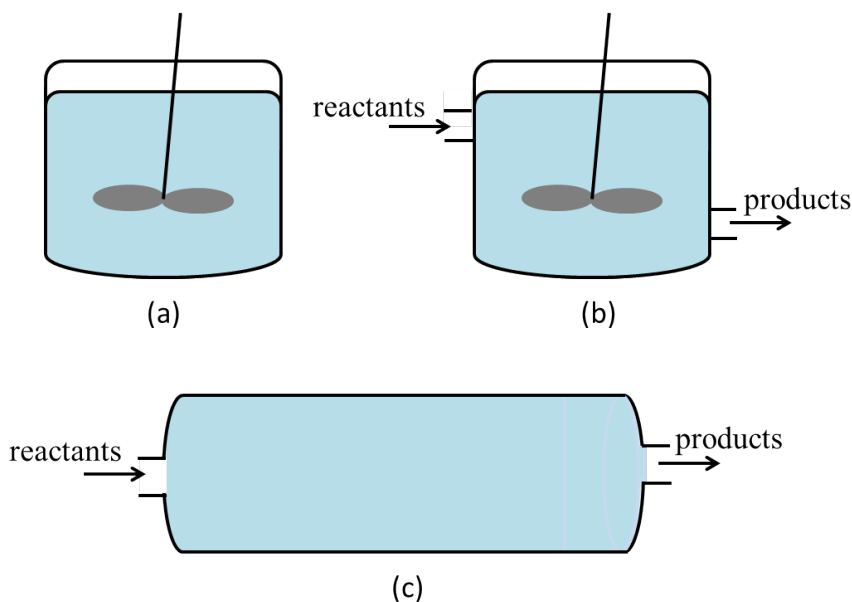


Figure 2.1: The reactors; (a) Batch reactors (b) CSTR (c) PFR.

A batch reactor is a closed thermodynamic reactor system where all reactants are added at the start and no withdrawal is made until the reaction has reached the desired degree of completion. A batch reactor is not suitable for large batch size production but is a good choice of reactor for a small scale production. Thus, the batch reactor is useful in the lab. Besides, the batch reactor can be used for reactions that required long reaction times and reactions that have superior selectivity. As the product of the batch reactor can only be collected once the reaction is completed, the same batch reactor can be used for different chemical processes. Batch reactors are used widely in chemical and food industry such as inks, dyes and polymers productions.

CSTR is a reactor that runs with a continuous flow of reactants and products at a steady-state operation. The benefit of CSTR is good control of the system and continuous operation can be done easily. It is economically advantageous to conduct CSTRs in series and parallel. In the calculation of the performance of CSTR, an assumption of perfect mixing must be made. Besides, the steady-state CSTR produce low conversion per unit volume. Although there is a lot of disadvantages of using CSTR, chemical engineer still prefers CSTR because of its highly flexible condition.

PFR is a tubular reactor that is used for gas reactions. In a PFR, it is assumed that the flow rate and fluid properties are uniform to the fluid motion over any cross-section and there are negligible axial mixing [51]. There could be lateral mixing but there must not be any axial mixing such diffusion [47]. For the same conversion of CSTR and PFR, the volume of PFR is smaller than the volume of CSTR.

There is an interest in the periodic operation of the reactors to improve the conversion of the product. Periodic operation of the chemical reactors had been explored actively when the researchers started to focus on the dynamic behaviour of chemical reactors in the decade 1970-1980 [78, 70, 30]. In [77], Si and Blackburn identified five benefits of the periodic operation of the chemical reactors. First, the improvement of the conversion, where it is better than the optimal steady-state operation [19, 71, 73]. Besides, the periodic operation of the chemical reactors improve the selectivity of the product, thus fewer by-products are produced. Although in the region of high parameter sensitivity, periodic operation allows the reactor to be operated safely. Lastly, another advantage of periodic operation is the reduction rate of catalyst deactivation compared to the steady-state operation [79].

The improvement of the conversion in the periodic operation of chemical reactors is due to the system nonlinearity [24]. However, researchers started to debate whether the results of

the periodic operation is significant. Thus, there are investigations in the optimisation of the periodic operation of the chemical reactors [70, 30]. Overall, these studies provide important insights into the analysis and control of the periodic operation.

### 2.3.2 Chemical Process Control

In chemical process control, there are manipulated variables, controlled variables and processes. The objective of chemical process control is to maintain the process outputs (controlled variables) at the desired operating conditions, efficiently and safely while adjusting the process inputs (manipulated variables). A process is called linear when it can be described by a linear combination of derivatives of the process output  $y(t)$ , the process input  $u(t)$  and a constant. There are two types of linear processes, time-invariant and time-variant linear processes where it depends on the coefficients, if the coefficients are time-invariant, then it became the time-invariant linear process and vice versa. Several control techniques available for linear process are the conventional proportional-integral-derivative (PID) control, internal model control (IMC), model predictive control and adaptive control [76, 81, 90].

However, many important industrial chemical processes exhibit the nonlinear behaviours where the relationship between the controlled and manipulated variables depends on the operating condition. In solving nonlinear chemical process control, the common problems involved are associated with chemical processes like time delays, unmeasured state variables and high-order and distributed processes [9]. Thus, several methods and techniques that have been used by the researchers to solve these problems. The PID control still effective if the nonlinearities are mild or the nonlinear process operates over a small range of conditions [67]. For other linear control strategies, the internal model control, model predictive control and adaptive control, they provide adequate performance when the process is sufficiently linear in the region of operation [50]. Other nonlinear control strategies provide significant improvements over linear control strategies when the process is highly nonlinear.

One of the fundamental nonlinear control strategies is feedback linearization. The feedback linearization is based on input-output linearization or state-space linearization. Input-output linearization control is restricted to the process where the nonlinear phase is minimum whereas the state-space linearization exploited the restriction of the input-output linearization where the system has a non-minimum phase nonlinear system and produces a stable internal control [29].

In solving the nonlinear chemical process control systems, other methodologies that can be used are Nonlinear Internal Model Control (NIMC) and Nonlinear Model Predictive Control (NMPC) techniques [21, 25]. The NIMC method can be interpreted as a variant of the input-output linearization technique and can be used in the open-loop stable processes only but the main advantage of this method was the main basis of the techniques is on full-state feedback. This method uses the two features of the IMC where the controller design is based on the inverse of the process model and the feedback signal is taken from the error between the plan and the model outputs. The NMPC method was an extended concept of MPC where it provided stability results for the nonlinear system by requiring knowledge of the current state of the nonlinear system and it had the ability to handle all constraints such as control inputs and outputs directly [29, 76].

An explicit mathematical model of process dynamics is required for most of the methodologies discussed above. Thus, this makes the development and analysis of the nonlinear process identification important to be studied. The models developed from the analysis of the nonlinear process will be used in the control system design methodologies. There are several nonlinear system representations of pH neutralisation process, for example NARX models [66], neural networks [10] and Wiener model [41] and these representations were used in different control techniques.

Another method to analyse both linear and nonlinear chemical process is understanding the process in the frequency domain. It uses the concept of Fourier transform. In the analysis of the nonlinear chemical process, the concept of higher-order frequency response functions (FRFs) is used where it applicable for weakly nonlinear systems[63]. The higher-order frequency response functions (FRFs) is based on Volterra series and generalised Fourier transform. According to Petkovska and Do [64], the analysis of nonlinear systems in frequency domain gives accurate limits in which linear analysis is applicable and enables nonlinear model parameters estimation.

In chemical process control analysis in the frequency domain, researchers started to use nonlinear frequency response (NFR) approach that was introduced in [64] recently. One of the nonlinear chemical process systems that have been investigated in the frequency domain using the NFR approach is the adsorption process [15, 16, 32]. In [16], analysis of nonisothermal adsorption controlled by macropore diffusion had been done using the NFR approach. This analysis developed NFR approach for investigation of adsorption kinetics and the new approach shows better result compared to the linear FR method.

Besides, continuously stirred tank reactor (CSTR) have been investigated in the frequency domain [55–57]. The basis of this analysis is the periodic operation of CSTR. The CSTR is subjected to a periodic input operation in [55, 56] and to simultaneous periodic modulation of two inputs in [57]. The NFR approach is used in the periodic operation of CSTR and it was found that the results obtained by the NFR method agreed with the results of numerical simulations. Besides, the results of the periodic operation of CSTR also better than the steady-state operation of the CSTR.

Collectively, these studies outline a critical role for analysis of chemical process control to be done in the frequency domain. The NFR approach provides good insight on the investigation

of the chemical process. However, there is no analysis done in the chemical process control that can provide the analytical relationship between the output frequency response and the nonlinear parameters. The OFRF method that was developed by Lang et al. in [46] can provide the analytical relationship between the output frequency response and the nonlinear parameters. Thus, the applicability of the OFRF method in the chemical process control can provide new insight and understanding in the nonlinear chemical process systems.



# **Chapter 3**

## **A new numerical method for determination of OFRF of SISO nonlinear systems**

### **3.1 Introduction**

The Output Frequency Response Function (OFRF) is the basis of this whole research. Why is it important to determine OFRF of nonlinear system? By revealing the significant link between the system output frequency response and parameters that define the system nonlinearity, the OFRF concept has provided an important basis for the analysis and design of nonlinear systems. The OFRF concept can be used in analysing nonlinear systems that can be studied using the Volterra series approach which occupies the middle ground in generality and applicability of the theories of nonlinear systems [46, 72].

This chapter presents three new synergizing algorithms involved in the new numerical method for determining the OFRFs of SISO nonlinear systems. It will begin by defining the nonlinear differential equation (NDE) model as the OFRF concept is useful for a wide class

of nonlinear systems that can be represented by NDE model, showing an explicit analytical relationship between the output frequency response and the time domain system coefficients. Then, the concept of the OFRF for single input single output (SISO) nonlinear systems is introduced and an algorithm is derived where it can determine OFRF representation of the output spectrum of the system to any inputs.

The first algorithm is about the determination of OFRF representation of the SISO nonlinear system. The second algorithm is for the determination of ALEs for the NDE model where the ALEs can be determined easily up to any nth-order. The last algorithm is focusing on the determination of OFRF using the ALEs. This algorithm use the relationship between the OFRF representation and the ALEs determined in the first two algorithms. An example, a simple mechanical system is used to demonstrate the effectiveness of the new numerical method. Then, the new numerical method will be applied to the passive engine mount system and the OFRF based analysis will be done using the OFRF determined to facilitate the design process of the system.

The advantage of the new numerical method is that it allows OFRF, which reveals a significant link between the system output frequency response and the parameters that define the system nonlinearity to be determined with significantly less number of numerical simulations compared to previous works. When the process of determining OFRF is easier, the design of NDE system can be done more efficiently than before.

## 3.2 A new method for determining the OFRF of the SISO nonlinear systems

### 3.2.1 NDE model for SISO nonlinear systems

Consider nonlinear systems which can be described by a differential equation of a polynomial form known as NDE model

$$\sum_{m=1}^M \sum_{\substack{p=0 \\ p+q=m}}^m \sum_{l_1, \dots, l_{p+q}}^L c_{pq}(l_1, \dots, l_{p+q}) \prod_{i=1}^p D^{l_i} y(t) \times \prod_{i=p+1}^{p+q} D^{l_i} u(t) = 0 \quad (3.1)$$

where M is the maximum degree of nonlinearity in terms of  $y(t)$  and  $u(t)$ , L is the maximum order of differential function and the operator  $D$  is defined by

$$D^l x(t) = \frac{d^l x(t)}{dt^l} \quad (3.2)$$

This equation describes the relationship between the time domain input and output of the nonlinear systems.  $u(t)$  and  $p$  are corresponds to the inputs while  $y(t)$  and  $q$  are corresponds to the outputs. This equation also can represent nonlinear systems where its output and inputs terms relate to each other although the presence of such systems are not common. By assuming  $c_{(1,0)}(0) \neq 0$ , equation (3.1) can be used to represent a valid input/output map. By rearranging this equation, a NDE model is produced as

$$-c_{1,0}(0)y(t) = \sum_{m=1}^M \sum_{\substack{p=0 \\ p+q=m}}^m \sum_{l_1, \dots, l_{p+q}}^L c_{pq}(l_1, \dots, l_{p+q}) \prod_{i=1}^p D^{l_i} y(t) \times \prod_{i=p+1}^{p+q} D^{l_i} u(t) \quad (3.3)$$

To illustrate the NDE model, consider a simple mechanical system that is described by

$$240\ddot{y} + 296\dot{y} + 16000y + a_2\dot{y}^2 + a_3\dot{y}^3 = u(t) \quad (3.4)$$

where the input

$$u(t) = \frac{200}{\pi} \frac{[\sin(15t) - \sin(3t)]}{t}, t \in [-40.955s, 40.96s] \quad (3.5)$$

and  $a_2$  and  $a_3$  are the system nonlinear characteristic parameters. This simple mechanical system is in the form for NDE model in equation (3.1) where  $M = 3$  and  $L = 2$ . The coefficients of this specific NDE model are  $c_{0,1}(0) = -1, c_{1,0}(0) = 1600, c_{1,0}(1) = 296, c_{1,0}(2) = 240, c_{2,0}(1,1) = a_2, c_{3,0}(1,1,1) = a_3$  and all other  $c_{pq}(\cdot) = 0$ .

### 3.2.2 The Output Frequency Response Function of the SISO nonlinear systems

#### 3.2.2.1 OFRF representation of the SISO nonlinear system

For nonlinear systems that can be described by model (3.1), and satisfies the following assumptions:

- The system is stable at zero equilibrium
- The systems can equivalently be described by the Volterra series model with  $N \geq M$  over a regime around the equilibrium,

there exists an explicit analytical relationship between the output frequency response and the model parameters. According to [46], the OFRF of a general nonlinear system can be represented as

$$\begin{aligned} \hat{Y}(j\omega) &= \sum_{(j_1, \dots, j_{S_N}) \in J} \gamma_{(j_1, \dots, j_{S_N})}(\omega) x_1^{j_1} \dots x_{S_N}^{j_{S_N}} \\ &= \sum_{j_1}^{m_1} \sum_{j_2}^{m_2} \dots \sum_{j_{S_N}}^{m_{S_N}} \gamma_{(j_1, \dots, j_{S_N})}(\omega) x_1^{j_1} \dots x_{S_N}^{j_{S_N}} \end{aligned} \quad (3.6)$$

where  $x_i, i = 1, \dots, S_N$  are the parameters which define the system nonlinearity;  $m_i$  is the maximum power of  $x_i, i = 1, \dots, S_N$ .  $\gamma_{(j_1, \dots, j_{S_N})}(\omega)$  represents the coefficient of the term  $x_1^{j_1} \dots x_{S_N}^{j_{S_N}}$ .  $x_1^{j_1} \dots x_{S_N}^{j_{S_N}}, (j_1, \dots, j_{S_N}) \in J$  is a set of all monomials involved in the representation of  $\hat{Y}(j\omega)$ .

In order to determine the OFRF representation of the nonlinear system, the set of the monomials involved in the representation of  $\hat{Y}(j\omega)$  up to  $N_{max}$ th-order, denote as  $\mathbf{M}_{N_{max}}$  need to be determined first. Then using the  $\mathbf{M}_{N_{max}}$  determined, the OFRF representation of the nonlinear system can be derived. The OFRF representation of a nonlinear system can be determined by the following algorithm,

1. Set  $n = 1, 2, \dots, N_{max}$  where  $N_{max} \geq 0$ .
2.  $\mathbf{M}_1 = [1]$ . Calculate  $\mathbf{M}_n$  by using

$$\begin{aligned} \mathbf{M}_n = & \left[ \bigcup_{l_1, \dots, l_n=0}^L [c_{0n}(l_1, \dots, l_p)] \right] \cup \left[ \bigcup_{q=1}^{n-1} \bigcup_{p=1}^{n-q} \bigcup_{l_1, \dots, l_n=0}^L [c_{0n}(l_1, \dots, l_p) \otimes \mathbf{M}_{n-q,p}] \right] \\ & \cup \left[ \bigcup_{p=2}^n \bigcup_{l_1, \dots, l_p=0}^L [c_{p0}(l_1, \dots, l_p) \otimes \mathbf{M}_{np}] \right] \end{aligned} \quad (3.7)$$

where  $\otimes$  is the Kronecker product, and

$$\mathbf{M}_{np} = \bigcup_{i=1}^{n-p+1} (\mathbf{M}_i \otimes \mathbf{M}_{n-i,p-1}) \quad \text{and} \quad \mathbf{M}_{n1} = \mathbf{M}_n \quad (3.8)$$

3. The set of the monomials involved in the representation of OFRF is

$$\bar{\mathbf{M}}_{N_{max}} = \bigcup_{n=1}^{N_{max}} \mathbf{M}_n \quad (3.9)$$

4. Lastly, the OFRF representation of the system can be written as

$$\hat{Y}(j\omega) = \sum_{n=1}^{N_{max}} \mathbf{M}_{nf} P_{nf} \quad (3.10)$$

where  $f$  is corresponding to the element number in  $\mathbf{M}_n$ .

This algorithm provides an effective way to determine all the monomials involved in the OFRF (3.6). After knowing these monomials, an OFRF representation of the system can be determined where every monomial is paired with an OFRF "coefficient".

### 3.2.2.2 Example

Consider the simple nonlinear mechanical system that was discussed in the previous subsection, the OFRF representation of the system up to fourth order,  $N_{max} = 4$  can be determined priori using the algorithm that has been discussed as below. In this example, the OFRF that will be determine is a fourth order because it is the same case that was analysed in [46]. Thus a comparison with the number of numerical simulations needed can prove the efficiency of the new method proposed in this research.

Firstly, set  $N_{max} = 4$ ,  $n = 1, 2, 3, 4$  and the monomial for the first order,  $\mathbf{M}_1 = [1]$ . Then calculate each  $\mathbf{M}_n$  using (3.7) resulting in

$$\begin{aligned}\mathbf{M}_1 &= [1] \\ \mathbf{M}_2 &= [a_2] \\ \mathbf{M}_3 &= [a_2^2, a_3] \\ \mathbf{M}_4 &= [a_2 a_3, a_2^3]\end{aligned}\tag{3.11}$$

Then, the set of the monomials involved in the OFRF of the simple nonlinear mechanical system when up to 4-th order system nonlinearity is taken into the account can be expressed as

$$\bar{\mathbf{M}}_4 = \bigcup_{n=1}^4 \mathbf{M}_n = [1, a_2, a_2^2, a_3, a_2 a_3, a_2^3]\tag{3.12}$$

and using this result, the OFRF representation of the system can be written as

$$\begin{aligned}\hat{Y}(j\omega) &= \hat{P}_{11}(j\omega) + a_2 \hat{P}_{21}(j\omega) + a_2^2 \hat{P}_{31}(j\omega) + a_3 \hat{P}_{32}(j\omega) \\ &\quad + a_2 a_3 \hat{P}_{41}(j\omega) + a_2^3 \hat{P}_{42}(j\omega)\end{aligned}\tag{3.13}$$

### 3.2.3 Derivation of ALEs for SISO nonlinear systems

#### 3.2.3.1 Associated Linear Equations for SISO nonlinear systems

Any system that possesses a Volterra series representation can be described by a series of ALEs [86, 85]. From these ALEs, analysis of the output of the nonlinear system can be done order by order. The ALEs can be obtained through manipulations of the Volterra series. In this subsection, as most of the nonlinear systems do not have the terms that represents both inputs and outputs, only nonlinear systems that have the terms that represents only inputs or outputs will be discussed. The basic NDE model that will be used in the derivation of ALEs is

$$\sum_{p=1}^P \sum_{l_1, \dots, l_p}^L c_{p0}(l_1, \dots, l_p) \prod_{i=1}^p D^{l_i} y(t) + \sum_{q=1}^Q \sum_{l_1, \dots, l_q}^L c_{0q}(l_1, \dots, l_q) \prod_{i=1}^q D^{l_i} u(t) = 0 \quad (3.14)$$

where Q is the maximum degree of nonlinearity in terms of the inputs,  $u(t)$  while where P is the maximum degree of nonlinearity in terms of outputs,  $y(t)$ . There is no M and m when compare to equation (3.1) because the inputs and outputs terms are independent.

Then separating the NDE to two different parts for the output, linear and nonlinear parts produces

$$\begin{aligned} & \sum_{l_1=0}^L c_{10}(l_1) D^{l_1} y(t) + \sum_{p=2}^P \sum_{l_1, \dots, l_p}^L c_{p0}(l_1, \dots, l_p) \prod_{i=1}^p D^{l_i} y(t) \\ & + \sum_{q=1}^Q \sum_{l_1, \dots, l_q}^L c_{0q}(l_1, \dots, l_q) \prod_{i=1}^q D^{l_i} u(t) = 0 \end{aligned} \quad (3.15)$$

Using the knowledge that the NDE model posesses a Volterra representation, substitution of

$$y(t) = \sum_{n=1}^{\infty} y_n(t) \quad (3.16)$$

into equation (3.15) yields

$$\begin{aligned} \sum_{l_1=0}^L c_{10}(l_1) \sum_{n=1}^{\infty} D^{l_1} y_n(t) + \sum_{p=2}^P \sum_{l_1, \dots, l_p}^L c_{p0}(l_1, \dots, l_p) \prod_{i=1}^p D^{l_i} \sum_{n=1}^{\infty} y_n(t) \\ + \sum_{q=1}^Q \sum_{l_1, \dots, l_q}^L c_{0q}(l_1, \dots, l_q) \prod_{i=1}^q D^{l_i} u(t) = 0 \end{aligned} \quad (3.17)$$

Then, rearrangement of the nonlinear part of the equation (3.17) is made as

$$\begin{aligned} \sum_{l_1=0}^L c_{10}(l_1) \sum_{n=1}^{\infty} D^{l_1} y_n(t) + \sum_{p=2}^P \sum_{l_1, \dots, l_p}^L c_{p0}(l_1, \dots, l_p) \left( \sum_{n=1}^{\infty} D^0 y_n(t) \right)^{p_0} \left( \sum_{n=1}^{\infty} D^1 y_n(t) \right)^{p_1} \dots \\ \left( \sum_{n=1}^{\infty} D^s y_n(t) \right)^{p_s} + \sum_{q=1}^Q \sum_{l_1, \dots, l_q}^L c_{0q}(l_1, \dots, l_q) \prod_{i=1}^q D^{l_i} u(t) = 0 \end{aligned} \quad (3.18)$$

where  $p_0 + p_1 + \dots + p_s = p$ . Then, leaving on the LHS of the equation only the linear elements, (3.18) will be

$$\begin{aligned} \sum_{l_1=0}^L c_{10}(l_1) \sum_{n=1}^{\infty} D^{l_1} y_n(t) = - \sum_{p=2}^P \sum_{l_1, \dots, l_p}^L c_{p0}(l_1, \dots, l_p) \left( \sum_{n=1}^{\infty} D^0 y_n(t) \right)^{p_0} \left( \sum_{n=1}^{\infty} D^1 y_n(t) \right)^{p_1} \dots \\ \left( \sum_{n=1}^{\infty} D^s y_n(t) \right)^{p_s} - \sum_{q=1}^Q \sum_{l_1, \dots, l_q}^L c_{0q}(l_1, \dots, l_q) \prod_{i=1}^q D^{l_i} u(t) = 0 \end{aligned} \quad (3.19)$$

For the determination of OFRF using ALEs derivation, the systems will be analyzed up to  $N_{max}$  order, thus (3.19) can be written as

$$\begin{aligned} \sum_{l_1=0}^L c_{10}(l_1) \sum_{n=1}^{N_{max}} D^{l_1} y_n(t) = - \sum_{p=2}^P \sum_{l_1, \dots, l_p}^L c_{p0}(l_1, \dots, l_p) \left( \sum_{n=1}^{N_{max}} D^0 y_n(t) \right)^{p_0} \left( \sum_{n=1}^{N_{max}} D^1 y_n(t) \right)^{p_1} \dots \\ \left( \sum_{n=1}^{N_{max}} D^s y_n(t) \right)^{p_s} - \sum_{q=1}^Q \sum_{l_1, \dots, l_q}^L c_{0q}(l_1, \dots, l_q) \prod_{i=1}^q D^{l_i} u(t) = 0 \end{aligned} \quad (3.20)$$

and (3.20) can be simplified as

$$\begin{aligned} \sum_{l_1=0}^L c_{10}(l_1) \sum_{n=1}^{N_{max}} D^{l_1} y_n(t) &= - \sum_{p=2}^P \sum_{l_1, \dots, l_p} c_{p0}(l_1, \dots, l_p) \left( \prod_{s=0}^S \left( \sum_{n=1}^{N_{max}} D^s y_n(t) \right)^{p_s} \right) \\ &\quad - \sum_{q=1}^Q \sum_{l_1, \dots, l_q} c_{0q}(l_1, \dots, l_q) \prod_{i=1}^q D^{l_i} u(t) = 0 \end{aligned} \quad (3.21)$$

where  $S$  is the maximum power of the nonlinear terms for each nonlinear output terms. From equation (3.22), it can be seen the relationship between the linear and nonlinear outputs and the input.

For the determination of OFRF using ALEs, the analysis of the output of the nonlinear system is done order by order where the linear terms on the left-hand side are solved by using nonlinear terms that are one order lower on the right-hand side. Then, the response of the nonlinear system is the total of all the response from the ALEs. The algorithm to determine ALE for the NDE model is described as below.

### 3.2.3.2 Algorithm to determine ALE for the SISO nonlinear system

In ALEs, determination of the total response will be the summation of all the responses. The following algorithm can be used to determined the ALEs for every  $N$ th-order up to any  $N_{max}$ th-order. Consider a NDE model where the linear and nonlinear parts of the outputs had been separated and the input and the output terms independent and not related to each other

$$\begin{aligned} \sum_{l_1=0}^L c_{10}(l_1) \sum_{n=1}^{N_{max}} D^{l_1} y_n(t) &= - \sum_{p=2}^P \sum_{l_1, \dots, l_p} c_{p0}(l_1, \dots, l_p) \left( \prod_{s=0}^S \left( \sum_{n=1}^{N_{max}} D^s y_n(t) \right)^{p_s} \right) \\ &\quad - \sum_{q=1}^Q \sum_{l_1, \dots, l_q} c_{0q}(l_1, \dots, l_q) \prod_{i=1}^q D^{l_i} u(t) \end{aligned} \quad (3.22)$$

where  $P$  is the maximum degree of nonlinearity in terms of  $y(t)$ ,  $Q$  is the maximum degree of nonlinearity in terms of  $u(t)$ ,  $L$  is the maximum order of differential function,  $S$  is the

maximum power of the nonlinear terms for each nonlinear output terms and the operator  $D$  is defined by

$$D^l x(t) = \frac{d^l x(t)}{dt^l} \quad (3.23)$$

The ALEs for every nth-order up to any  $N_{max}$ th-order can be determined using the algorithm below

1. Set  $n = 1, 2, \dots, N_{max}$  where  $N_{max} \geq 0$ .
2.  $J_0 = J_1 = 0$ . The ALEs for every nth-order can be written as

$$\sum_{l_1=0}^L c_{10}(l_1) D^{l_1} y_n(t) = \sum_{l_1, \dots, l_n}^L c_{0n}(l_1, \dots, l_n) \prod_{i=1}^n D^{l_i} u(t) + J_n - J_{n-1} \quad (3.24)$$

where

$$J_n = - \sum_{p=2}^P \sum_{l_1, \dots, l_p}^L c_{p0}(l_1, \dots, l_p) \left( \prod_{s=0}^S \left( \sum_{n=1}^{n-1} D^s y_n(t) \right)^{p_s} \right) \quad (3.25)$$

3. The estimation of the output signal and the output spectrum for the system up to  $N_{max}$ th-order thus can be written as

$$\hat{y}(t) = \sum_{N=1}^{N_{max}} \hat{y}_N(t) \quad (3.26)$$

and

$$\hat{Y}(j\omega) = \sum_{n=1}^{N_{max}} \hat{Y}_n(j\omega) \quad (3.27)$$

This algorithm made the ALEs for every nth-order up to any  $N_{max}$ th-order can be determined more easily.

### 3.2.3.3 Example

To show the effectiveness of this algorithm, the ALEs for simple nonlinear mechanical system up to 4th-order is determined using the steps in the algorithm. First, consider the NDE form of the system as in (3.4). (3.4) can also be written in the (3.22) form as

$$240 \sum_{n=1}^{\infty} D^2 y_n(t) + 296 \sum_{n=1}^{\infty} D^1 y_n(t) + 16000 \sum_{n=1}^{\infty} y_n(t) + \\ a_2 \left( \sum_{n=1}^{\infty} D^1 y_n(t) \right)^2 + a_3 \left( \sum_{n=1}^{\infty} D^1 y_n(t) \right)^3 + \frac{200}{\pi} \frac{[\sin(15t) - \sin(3t)]}{t} = 0 \quad (3.28)$$

where all the condition of the system is the same as before.

As  $N_{max} = 4$ ,  $n = 1, 2, 3, 4$ . Then, the general ALEs for every order up to 4th-order can be written as

$$\begin{aligned} c_{1,0}(2)\ddot{y}_1(t) + c_{1,0}(1)\dot{y}_1(t) + c_{1,0}(0)y_1(t) &= c_{0,1}(l_1)D^{l_1}u(t) + J_1 - J_0 \\ c_{1,0}(2)\ddot{y}_2(t) + c_{1,0}(1)\dot{y}_2(t) + c_{1,0}(0)y_2(t) &= c_{0,2}(l_1, l_2)D^{l_1}u(t)D^{l_2}u(t) + J_2 - J_1 \\ c_{1,0}(2)\ddot{y}_3(t) + c_{1,0}(1)\dot{y}_3(t) + c_{1,0}(0)y_3(t) &= c_{0,3}(l_1, l_2, l_3)D^{l_1}u(t)D^{l_2}u(t)D^{l_3}u(t) + J_3 - J_2 \\ c_{1,0}(2)\ddot{y}_4(t) + c_{1,0}(1)\dot{y}_4(t) + c_{1,0}(0)y_4(t) &= c_{0,4}(l_1, \dots, l_4) \prod_{i=1}^4 D^{l_i}u(t) + J_4 - J_3 \end{aligned} \quad (3.29)$$

where  $J_0 = J_1 = 0$ ,  $c_{0,1}(l_1)D^{l_1}u(t) = u(t)$  and  $c_{0,2}(1) = c_{0,3}(1) = c_{0,4}(1) = 0$ .

Then solving for each  $J_n$ , the ALES for the system up to 4th-order are

$$\begin{aligned} 240\ddot{y}_1(t) + 296\dot{y}_1(t) + 16000y_1(t) &= u(t) \\ 240\ddot{y}_2(t) + 296\dot{y}_2(t) + 16000y_2(t) &= -a_2\dot{y}_1(t)^2 - a_3\dot{y}_1(t)^3 \\ 240\ddot{y}_3(t) + 296\dot{y}_3(t) + 16000y_3(t) &= -a_2(\dot{y}_2(t)^2 + 2\dot{y}_1(t)\dot{y}_2(t)) \\ &\quad - a_3(\dot{y}_2(t)^3 + 3\dot{y}_1(t)^2\dot{y}_2(t) + 3\dot{y}_1(t)\dot{y}_2(t)^2) \end{aligned}$$

$$\begin{aligned}
 240\ddot{y}_4(t) + 296\dot{y}_4(t) + 16000y_4(t) = & -a_2(2\dot{y}_1(t)\dot{y}_3(t) + 2\dot{y}_2(t)\dot{y}_3(t) + \dot{y}_3(t)^2) \\
 & -a_3(3\dot{y}_1(t)\dot{y}_3(t) + 6\dot{y}_1(t)\dot{y}_2(t)\dot{y}_3(t) + 3\dot{y}_1(t)\dot{y}_3(t)^2 \\
 & + 3\dot{y}_2(t)\dot{y}_3(t) + 3\dot{y}_2(t)\dot{y}_3(t)^2 + \dot{y}_3(t)^2)
 \end{aligned} \tag{3.30}$$

Using the ALEs determined, the estimation of the output signal and the output spectrum for the system up to 4th-order thus can be written as

$$\hat{y}(t) = \hat{y}_1(t) + \hat{y}_2(t) + \hat{y}_3(t) + \hat{y}_4(t) \tag{3.31}$$

$$\hat{Y}(j\omega) = \hat{Y}_1(j\omega) + \hat{Y}_2(j\omega) + \hat{Y}_3(j\omega) + \hat{Y}_4(j\omega) \tag{3.32}$$

From (3.31), it can be understandable that the estimation of the output signal is the total of all ALEs responses. Figure 3.1 shows the comparison of the simulated results and the sum of the ALEs results in the time domain to demonstrate the significant of (3.31).

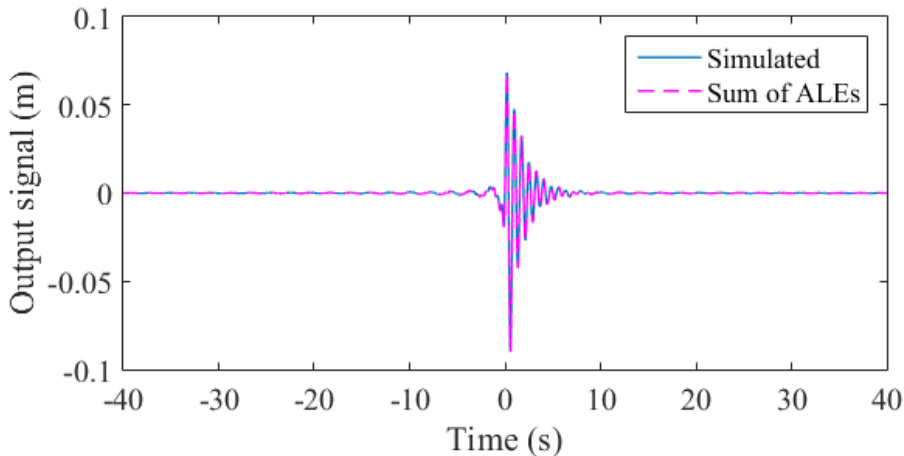


Figure 3.1: The simulated output signal of the system and sum of the signals from the ALEs in the time domain when  $a_2 = 500$  and  $a_3 = 200$ .

From Figure 3.1, it can be said that the sum of the ALEs results in the time domain is in good accuracy to the simulated results. Then, by Fourier transforming all the ALEs results,

the output spectrum can be approximated by the sum of the solutions of the ALE in the frequency domain as described in (3.32). Figure 3.2 shows the comparison of the simulated output spectrum and the sum of the solutions of the ALE in the frequency domain.

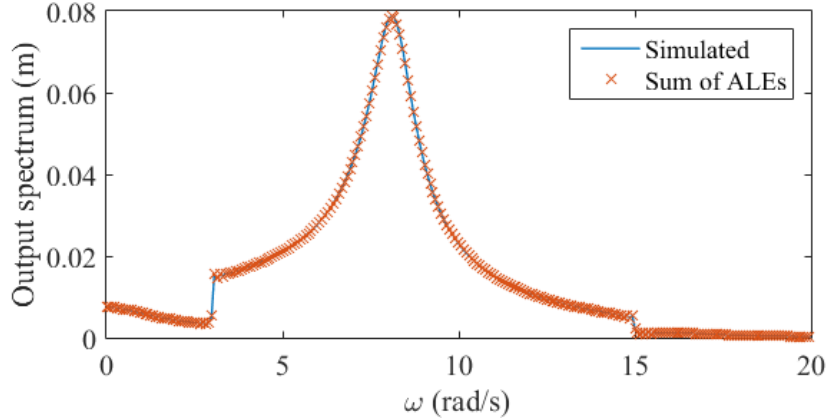


Figure 3.2: The simulated output spectrum of the system and sum of the output spectrum from the ALEs in the frequency domain when  $a_2 = 500$  and  $a_3 = 200$ .

From Figure 3.2, it can be said that the sum of the ALEs results in the frequency domain is also in good accuracy to the simulated results. These results show that ALEs can describe the nonlinear system that possesses a Volterra series representation and gave good estimation of the output signal and output spectrum of the nonlinear system.

### 3.2.4 Determination of OFRF of the SISO nonlinear system using ALEs

#### 3.2.4.1 Algorithm to determine OFRF of the SISO nonlinear system using ALEs

The OFRF of the SISO nonlinear system can be determined using the following algorithm

1. Determine the OFRF representation of the nonlinear system using algorithm in section 3.2.2.1. The OFRF representation can be written as (3.10),

$$\hat{Y}(j\omega) = \sum_{n=1}^{N_{max}} \mathbf{M}_{nf} P_{nf} \quad (3.33)$$

where  $f$  is corresponding to the number of element in  $\mathbf{M}_n$ .

2. Determine the ALEs of the nonlinear system using the algorithm in section 3.2.3.2.

The output spectrum of the nonlinear system can be written as (3.27)

$$\hat{Y}(j\omega) = \sum_{n=1}^{N_{max}} \hat{Y}_n(j\omega) \quad (3.34)$$

3. The number of the set of ALEs simulations needed to determine OFRF is equal to the maximum value of  $j$ . The output spectrums for each simulation can be written as

$$\hat{Y}_v(j\omega) = \sum_{n=1}^{N_{max}} \hat{Y}_{nv}(j\omega) \quad (3.35)$$

where  $v = 1, 2, \dots, j$  are corresponding to the simulation number.

4. The OFRF "coefficients" need to be determined per Nth-order. The solution for the OFRF "coefficients" can be determined using the OFRF representation and the output spectrums from the simulations where

$$\begin{bmatrix} \hat{P}_{n1}(j\omega) \\ \hat{P}_{n2}(j\omega) \\ \vdots \\ \hat{P}_{nv}(j\omega) \end{bmatrix} = \begin{bmatrix} \mathbf{M}_n \text{ for simulation 1} \\ \mathbf{M}_n \text{ for simulation 2} \\ \vdots \\ \mathbf{M}_n \text{ for simulation v} \end{bmatrix}^{-1} \begin{bmatrix} \hat{Y}_{n1}(j\omega) \\ \hat{Y}_{n2}(j\omega) \\ \vdots \\ \hat{Y}_{nv}(j\omega) \end{bmatrix} \quad (3.36)$$

This algorithm allow the process for the determination of OFRF become more simpler and systematic. However, it is needed to ensure the matrix formed using the chosen values of  $\mathbf{M}_n$  for each simulations is not an ill-conditioned matrix. This can be done using the singular values decomposition techniques. Using the OFRF determined, the analysis and design of the nonlinear system can be done.

### 3.2.4.2 Example

Consider the same cubic duffing oscillator system

$$240\ddot{y} + 296\dot{y} + 16000y + a_2y^2 + a_3y^3 = u(t) \quad (3.37)$$

and the results of the analysis in the previous sections, the OFRF representation

$$\hat{Y}(j\omega) = \hat{P}_1(j\omega) + a_2\hat{P}_2(j\omega) + a_2^2\hat{P}_{31}(j\omega) + a_3\hat{P}_{32}(j\omega) + a_2a_3\hat{P}_{41}(j\omega) + a_2^3\hat{P}_{42}(j\omega) \quad (3.38)$$

and the estimation of the output spectrum up to 4th-order

$$\hat{Y}(j\omega) = \hat{Y}_1(j\omega) + \hat{Y}_2(j\omega) + \hat{Y}_3(j\omega) + \hat{Y}_4(j\omega) \quad (3.39)$$

From these results, it can be understood that when using the method of determining OFRF using ALEs for this system, only two sets of ALEs simulations using different combinations of  $a_2$  and  $a_3$  were needed to determine the OFRF of this mechanical system. Table 3.1 shows the combinations of  $a_2$  and  $a_3$  used in the two simulations.

Table 3.1: Value of  $a_2$  and  $a_3$  used in the two simulations

Simulation	$a_2$	$a_3$
1	500	200
2	1000	700

This mean that the number of numerical simulation needed is less than the previous method, the method used in [46] where it need to simulate 8 simulations with different combinations of  $a_2$  and  $a_3$  to get fourth order OFRF of the mechanical system. Then, the two equations below showed the estimation of the output spectrum of the system in the frequency domain for simulation 1 and 2 respectively,

$$\hat{Y}_1(j\omega) = \hat{Y}_{11}(j\omega) + \hat{Y}_{21}(j\omega) + \hat{Y}_{31}(j\omega) + \hat{Y}_{41}(j\omega) \quad (3.40)$$

$$\hat{Y}_2(j\omega) = \hat{Y}_{12}(j\omega) + \hat{Y}_{22}(j\omega) + \hat{Y}_{32}(j\omega) + \hat{Y}_{42}(j\omega) \quad (3.41)$$

Then, the solution for the OFRF "coefficients" can be determined as below

$$\begin{aligned} \hat{P}_{11}(j\omega) &= \hat{Y}_{11}(j\omega) \\ \left[ \hat{P}_{21}(j\omega) \right] &= \left[ a_2 \right]^{-1} \left[ \hat{Y}_{21}(j\omega) \right] \\ \left[ \begin{array}{c} \hat{P}_{31}(j\omega) \\ \hat{P}_{32}(j\omega) \end{array} \right] &= \left[ \begin{array}{cc} a_{2(1)}^2 & a_{3(1)} \\ a_{2(2)}^2 & a_{3(2)} \end{array} \right]^{-1} \left[ \begin{array}{c} \hat{Y}_{31}(j\omega) \\ \hat{Y}_{32}(j\omega) \end{array} \right] \\ \left[ \begin{array}{c} \hat{P}_{41}(j\omega) \\ \hat{P}_{42}(j\omega) \end{array} \right] &= \left[ \begin{array}{cc} a_{2(1)}a_{3(1)} & a_{2(1)}^3 \\ a_{2(2)}a_{3(2)} & a_{2(2)}^3 \end{array} \right]^{-1} \left[ \begin{array}{c} \hat{Y}_{41}(j\omega) \\ \hat{Y}_{42}(j\omega) \end{array} \right] \end{aligned} \quad (3.42)$$

and the OFRF for the mechanical system is determined. Using this new numerical method, the OFRF determined should give good estimation when  $500 \geq a \geq 1000$  and  $200 \geq b \geq 700$ .

To verify the effectiveness of this approach, the OFRF determined was tested with a different set of parameters,  $a_2 = 700$  and  $a_3 = 400$  and compared with the simulated output spectrum. Figure 3.3 shows the comparison of the amplitude of  $Y(j\omega)$  and  $\hat{Y}(j\omega)$  when  $a_2 = 700$  and  $a_3 = 400$ .

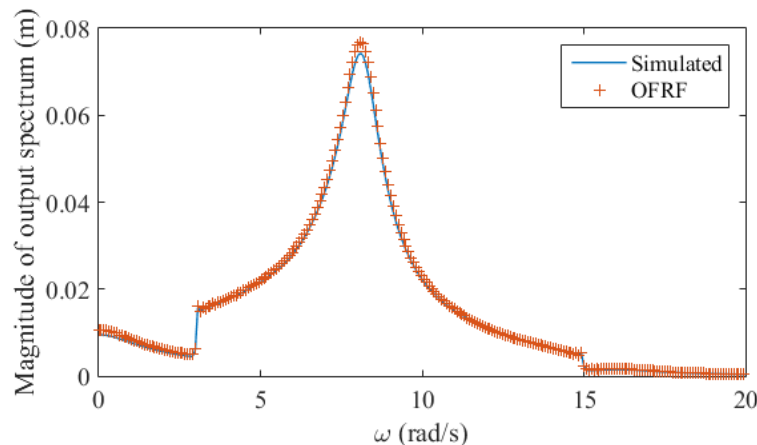


Figure 3.3: Comparison between the simulated output spectrum and the spectrum evaluated using OFRF when  $a_2 = 700$  and  $a_3 = 400$ .

It can be observed that the results from both simulated output spectrum and the spectrum evaluated using OFRF showed excellent agreement. The OFRF determined can estimate the output spectrum for different values of the parameters  $a_2$  and  $a_3$ . Comparing this result with [46], both OFRF determined was fourth order but the number of simulations used to determine OFRF are different. This method only need 2 set of simulations while the method used in [46] need 8 simulations with different combinations of  $a_2$  and  $a_3$  to get fourth order OFRF. This implies that the determination of OFRF using ALEs reduce the number of simulations needed thus make the OFRF determination easier to be carried out. In this research, all the results are from the numerical simulations. On the other hand, if the OFRF determined is compared with the experimental data, the noise in the data need to be considered. The noise needs to be filtered out before the analysis.

### **3.3 The OFRF based analysis and design of a passive engine mount**

#### **3.3.1 Passive engine mount**

Most vibration systems are inherently nonlinear. Therefore a proper design of the system nonlinearity has great significance for achieving desired vibration control performance. In this context, an appropriate design of nonlinear parameters are often needed. Thus, the concept of nonlinear vibration isolation had been studied by the researchers. Traditionally, harmonic balance [69] and averaging methods [34] have been used to analyse the effects of nonlinear parameters on the system vibration responses. Then, the nonlinear parameters are designed based on the results of analysis.

Different optimization techniques had been approached by researchers for the optimization of the vibration isolators. A RMS cost function method had been developed where the damping

and stiffness values for the linear isolator can be optimized [52]. Alkhatib et al. [1] used the RMS method and the generic method to optimize a linear quarter car suspension system. However, the implementation of this techniques to the nonlinear systems are complicated because of the nonlinearities in the model. In 2008, Peng and Lang [59] used the OFRF based analysis where the relationship between the nonlinear parameters and the output frequency of a passive engine mount was determined and facilitated the analysis and design process.

In this section, the new numerical method to determine OFRF using ALEs will be applied to the nonlinear passive engine mount. Passive engine mount is one type of passive isolators that used to isolate the inherently nonlinear vibration systems. Ibrahim [31] made an outstanding review of nonlinear passive vibration isolators. Detailed process of the determination of OFRF will be presented. Using the OFRF determined, the relationship between the nonlinear parameters, the damping and the stiffness of the system and the output can be understood. This result enables the OFRF based design of nonlinear systems especially nonlinear vibration isolators to be more easily implemented so as to significantly facilitate the application of nonlinear designs in engineering practice.

Consider a second order nonlinear passive engine mount discussed in [59] whose motion governing equation is given by

$$m\ddot{y} + (c_1 + c_2y^2)\dot{y} + (k_1 + k_2y^2)y = -mu_1 \quad (3.43)$$

where  $y = x_2 - x_1$  and  $u = \dot{x}_1$ . Figure 3.4 shows the schematic of the nonlinear passive engine mount.

The parameters  $m, c_1$  and  $k_1$  are fixed as

$$m = 20 \times 10^6 \text{ kg} \quad c_1 = 10 \times 10^4 \text{ Ns/m} \quad k_1 = 40 \times 10^6 \text{ N/m} \quad (3.44)$$

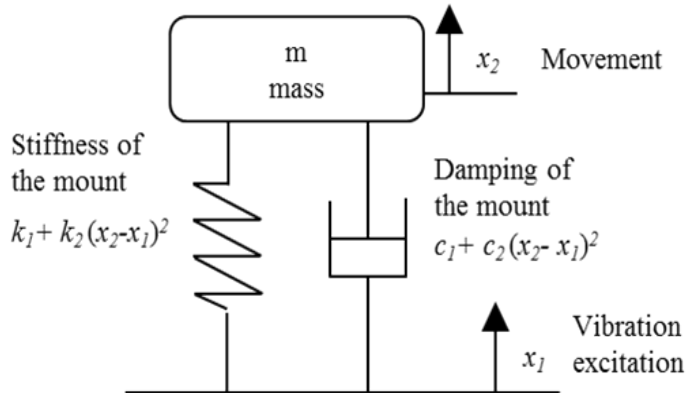


Figure 3.4: Schematic of the nonlinear passive engine mount.

Then, (3.43) can be rewritten as

$$20 \times 10^6 \ddot{y} + (10 \times 10^4 + c_2 y^2) \dot{y} + (40 \times 10^6 + k_2 y^2) y = -20 \times 10^6 \ddot{x}_1 \quad (3.45)$$

and (3.45) is obviously a specific instance of (3.1) with \$c\_{1,0}(2) = 20 \times 10^6\$, \$c\_{1,0}(1) = 10 \times 10^4\$, \$c\_{1,0}(0) = 40 \times 10^6\$, \$c\_{3,0}(0,0,1) = c\_2\$, \$c\_{3,0}(0,0,0) = k\_2\$, and \$c\_{0,1}(2) = -20 \times 10^6\$. In this analysis, the input base excitation, \$u\$ is the specific random signal generated.

### 3.3.2 OFRF representation of the passive engine mount

The OFRF that will be determined in this application is fifth order. First step in this method is to determine the set of monomials involved in the representation of \$\hat{Y}(j\omega)\$ up to 5th-order. Set \$n = 1, 2, \dots, 5\$ and all the monomials involved can be determine using the algorithm presented in section 3.2.2.1. The results of the algorithm are

$$\begin{aligned} \mathbf{M}_1 &= [1] \\ \mathbf{M}_3 &= [c_2, k_2] \\ \mathbf{M}_5 &= [c_2^2, c_2 k_2, k_2^2] \end{aligned} \quad (3.46)$$

and

$$\bar{\mathbf{M}}_5 = \bigcup_{n=1}^5 \mathbf{M}_n = [1, c_2, k_2, c_2^2, c_2 k_2, k_2^2] \quad (3.47)$$

Then, the OFRF representation can be determined where every monomial is paired with an OFRF "coefficient". The OFRF representation of the passive engine mount system is

$$\hat{Y}(j\omega) = \hat{P}_{11}(j\omega) + c_2 \hat{P}_{31}(j\omega) + k_2 \hat{P}_{32}(j\omega) + c_2^2 \hat{P}_{51}(j\omega) + c_2 k_2 \hat{P}_{52}(j\omega) + k_2^2 \hat{P}_{53}(j\omega) \quad (3.48)$$

### 3.3.3 ALEs derivation of the passive engine mount

For the derivation of ALE of the nonlinear system, the non-zero ALEs up to fifth order can be determined using the algorithm discussed in Section 3.2.3.2. First set  $N_{max} = 5$ . Rewritten (3.45) as

$$20 \times 10^6 \sum_{n=1}^{\infty} D^2 y(t) + 10 \times 10^4 \sum_{n=1}^{\infty} D^1 y(t) + 40 \times 10^6 \sum_{n=1}^{\infty} y(t) + \\ c_2 \left( \sum_{n=1}^{\infty} D^1 y(t) \right) \left( \sum_{n=1}^{\infty} y(t) \right)^2 + k_2 \left( \sum_{n=1}^{\infty} y(t) \right)^3 + 20 \times 10^6 D^2 x_1(t) = 0 \quad (3.49)$$

where for  $c_{3,0}(0,0,1) = c_2$  and  $c_{3,0}(0,0,0) = k_2$ .

Then, the ALEs for every nth-order up to any 5th-order can be written as

$$c_{1,0}(2)\ddot{y}_1(t) + c_{1,0}(1)\dot{y}_1(t) + c_{1,0}(0)y_1(t) = c_{0,1}(l_1)D^{l_1}u(t) + J_1 - J_0 \\ c_{1,0}(2)\ddot{y}_3(t) + c_{1,0}(1)\dot{y}_3(t) + c_{1,0}(0)y_3(t) = c_{0,3}(l_1 \dots, l_3) \prod_{i=1}^3 D^{l_i}u(t) + J_3 - J_2 \quad (3.50) \\ c_{1,0}(2)\ddot{y}_5(t) + c_{1,0}(1)\dot{y}_5(t) + c_{1,0}(0)y_5(t) = c_{0,5}(l_1 \dots, l_5) \prod_{i=1}^5 D^{l_i}u(t) + J_5 - J_4$$

where

$$J_0 = J_1 = 0$$

$$c_{0,1}(l_1)D^{l_1}u(t) = 20 \times 10^6 D^2x_1(t)$$

$$c_{0,3}(l_1 \dots, l_3) \prod_{i=1}^3 D^{l_i}u(t) = c_{0,5}(l_1 \dots, l_5) \prod_{i=1}^5 D^{l_i}u(t) = 0$$

Lastly, solving for each  $J_n$ , the ALES for the system up to 5th-order are

$$\begin{aligned} 20 \times 10^6 \ddot{y}_1(t) + 10 \times 10^4 \dot{y}_1(t) + 40 \times 10^6 y_1(t) &= -20 \times 10^6 \ddot{x}_1 \\ 20 \times 10^6 \ddot{y}_3(t) + 10 \times 10^4 \dot{y}_3(t) + 40 \times 10^6 y_3(t) &= -c_2 y_1(t)^2 \dot{y}_1(t) - k_2 y_1(t)^3 \\ 20 \times 10^6 \ddot{y}_5(t) + 10 \times 10^4 \dot{y}_5(t) + 40 \times 10^6 y_5(t) &= \\ &= -c_2(2y_1(t)y_3(t)\dot{y}_1 + y_3(t)^2\dot{y}_1 + y_1(t)^2\dot{y}_3 + 2y_1(t)y_3(t)\dot{y}_3 + y_3(t)^2\dot{y}_3) \\ &\quad -k_2(3y_1(t)^2y_3(t) + 3y_1(t)y_3(t)^2 + y_3(t)^3) \end{aligned} \tag{3.51}$$

The estimation of the output signal of the system in the time domain up to 5th-order is

$$\hat{y}(t) = \hat{y}_1(t) + \hat{y}_3(t) + \hat{y}_5(t) \tag{3.52}$$

while the estimation of the output spectrum for the system up to 5th-order is

$$\hat{Y}(j\omega) = \hat{Y}_1(j\omega) + \hat{Y}_3(j\omega) + \hat{Y}_5(j\omega) \tag{3.53}$$

The estimation of the output signal and the output spectrum of the system are the sum of ALEs in time domain and frequency domain respectively.

### 3.3.4 Determination of OFRF using ALEs

Then, using the algorithm presented in the Section 3.2.4.1, the OFRF of the passive engine mount can be determined. First, rewritten the OFRF representation of the passive engine

mount system, (3.48) that was determined using algorithm derived in Section 3.2.2.1

$$\hat{Y}(j\omega) = \hat{P}_{11}(j\omega) + c_2 \hat{P}_{31}(j\omega) + k_2 \hat{P}_{32}(j\omega) + c_2^2 \hat{P}_{51}(j\omega) + c_2 k_2 \hat{P}_{52}(j\omega) + k_2^2 \hat{P}_{53}(j\omega) \quad (3.54)$$

Then, the ALEs of the passive engine mount was determined using the algorithm in Section 3.2.3.2. The output spectrum of the passive engine mount is

$$\hat{Y}(j\omega) = \hat{Y}_1(j\omega) + \hat{Y}_3(j\omega) + \hat{Y}_5(j\omega) \quad (3.55)$$

Based on algorithm to determine the OFRF using ALEs only three sets of ALEs simulations using different combinations of  $c_2$  and  $k_2$  were needed to determine the OFRF of this passive engine mount system. Table 3.2 shows the combinations of  $c_2$  and  $k_2$  used in the three simulations.

Table 3.2: Value of  $c_2$  and  $k_2$  used in the three simulations

Simulation,v	$c_2$	$k_2$
1	$20 \times 10^3$	$25 \times 10^3$
2	$40 \times 10^3$	$40 \times 10^3$
3	$60 \times 10^3$	$55 \times 10^3$

The estimation of the output spectrum of the system in the frequency domain for simulation  $v = 1, 2$  and  $3$  respectively are

$$\hat{Y}_v(j\omega) = \hat{Y}_{1v}(j\omega) + \hat{Y}_{3v}(j\omega) + \hat{Y}_{5v}(j\omega) \quad (3.56)$$

Figure 3.5 shows the magnitude of the output spectrum in the frequency domain of the system in comparison to the sum of ALEs in the frequency domain for simulation 1 when  $c_2 = 60 \times 10^3$  and  $k_2 = 10 \times 10^3$ . Figure 3.5 shows that the sum of the ALEs in the frequency domain is the same as the magnitude of the output spectrum of the system when  $c_2 = 60 \times 10^3$  and  $k_2 = 10 \times 10^3$ .

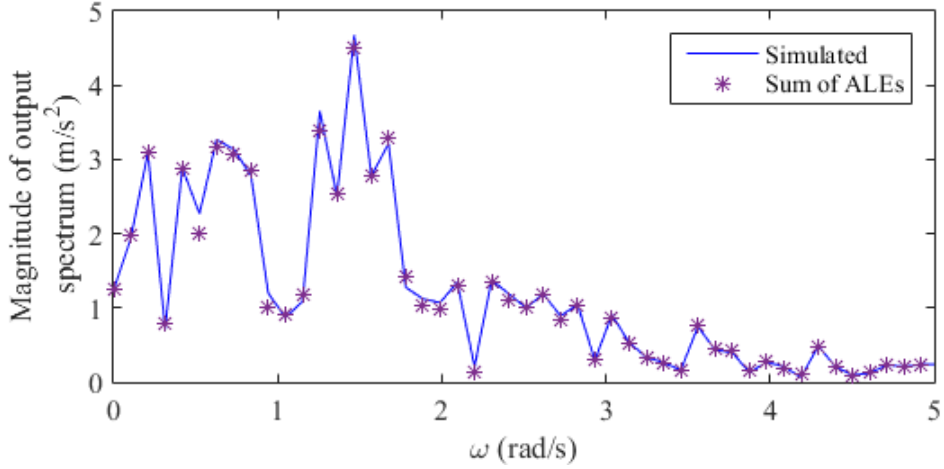


Figure 3.5: Comparison between the simulated output spectrum and the total of ALEs output spectrum when  $c_2 = 60 \times 10^3$  and  $k_2 = 10 \times 10^3$ .

Then, using the three simulations and the OFRF representation that had been determined, the OFRF of the system can be produced.  $\hat{P}_{11}(j\omega)$ ,  $\hat{P}_{31}(j\omega)$ ,  $\hat{P}_{32}(j\omega)$ ,  $\hat{P}_{51}(j\omega)$ ,  $\hat{P}_{52}(j\omega)$ , and  $\hat{P}_{53}(j\omega)$  can be evaluated where

$$\hat{P}_{11}(j\omega) = \hat{Y}_{11}(j\omega) \quad (3.57)$$

$$\begin{bmatrix} \hat{P}_{31}(j\omega) \\ \hat{P}_{32}(j\omega) \end{bmatrix} = \begin{bmatrix} c_{2(1)} & k_{2(1)} \\ c_{2(2)} & k_{2(2)} \end{bmatrix}^{-1} \begin{bmatrix} \hat{Y}_{31}(j\omega) \\ \hat{Y}_{32}(j\omega) \end{bmatrix} \quad (3.58)$$

$$\begin{bmatrix} \hat{P}_{51}(j\omega) \\ \hat{P}_{52}(j\omega) \\ \hat{P}_{53}(j\omega) \end{bmatrix} = \begin{bmatrix} c_{2(1)}^2 & c_{2(1)}k_{2(1)} & k_{2(1)}^2 \\ c_{2(2)}^2 & c_{2(2)}k_{2(2)} & k_{2(2)}^2 \\ c_{2(3)}^2 & c_{2(3)}k_{2(3)} & k_{2(3)}^2 \end{bmatrix}^{-1} \begin{bmatrix} \hat{Y}_{51}(j\omega) \\ \hat{Y}_{52}(j\omega) \\ \hat{Y}_{53}(j\omega) \end{bmatrix} \quad (3.59)$$

### 3.3.5 The results and analysis

To verify the OFRF of the system that had been obtained,  $\hat{Y}(j\omega)$  obtained using OFRF determined was compared with the  $Y(j\omega)$  from the simulated data. Figure 3.6 shows the comparison of the amplitude of  $\hat{Y}(j\omega)$  and  $Y(j\omega)$  when  $c_2 = 30 \times 70^3$  and  $k_2 = 40 \times 10^3$ . The OFRF determined using this new method should give good estimation when  $20 \times 10^3 \geq c_2 \geq 60 \times 10^3$  and  $25 \times 10^3 \geq k_2 \geq 55 \times 10^3$ .

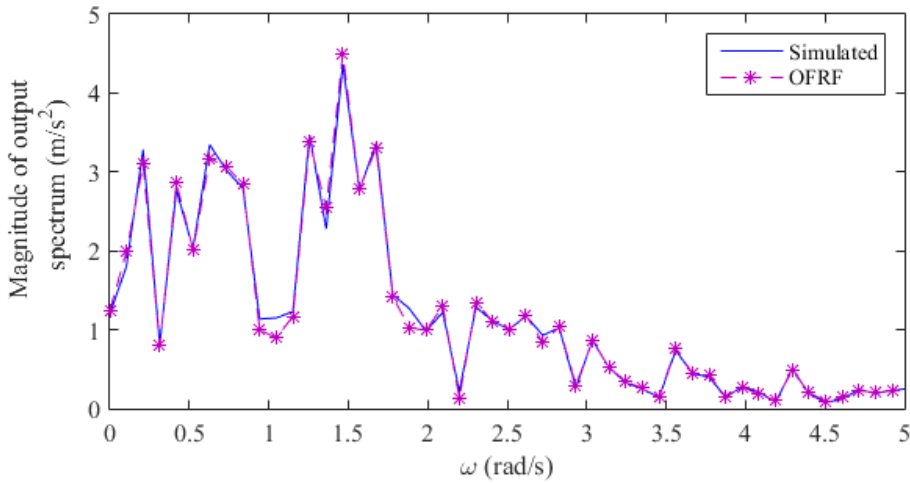


Figure 3.6: Comparison between the simulated output spectrum and the spectrum evaluated using OFRF when  $c_2 = 70 \times 10^3$  and  $k_2 = 40 \times 10^3$  for the passive engine mount system.

From Figure 3.6, the output spectrum evaluated using OFRF is in excellent agreement with the simulated output spectrum although there is small error in the lower frequency. Overall, it can be observed that OFRF provide good estimation of the magnitude of the output spectrum. In addition, this method of determining OFRF using OFRF only need 3 simulations whereas the current literature method [46] need at least 6 simulations. Thus, this proves that the method of determining the OFRF by using ALEs produce an excellent result and increase the efficiency of the process involved.

Using the OFRF determined, the design of the system parameters  $c_2$  and  $k_2$  can be performed efficiently as the OFRF shows the relationship between the nonlinear parameters and the output frequency response function. Figure 3.7 shows the OFRF based relationship between the parameters  $c_2$  and  $k_2$  and magnitude of the output spectrum at 1.466 rad/s frequency.

From Figure 3.7, the relationship between the parameters  $c_2$  and  $k_2$  and magnitude of the output spectrum at 1.466 rad/s frequency can be understood clearly. The magnitude of the output spectrum increases with the increases of damping coefficient,  $c_2$  while it decreases

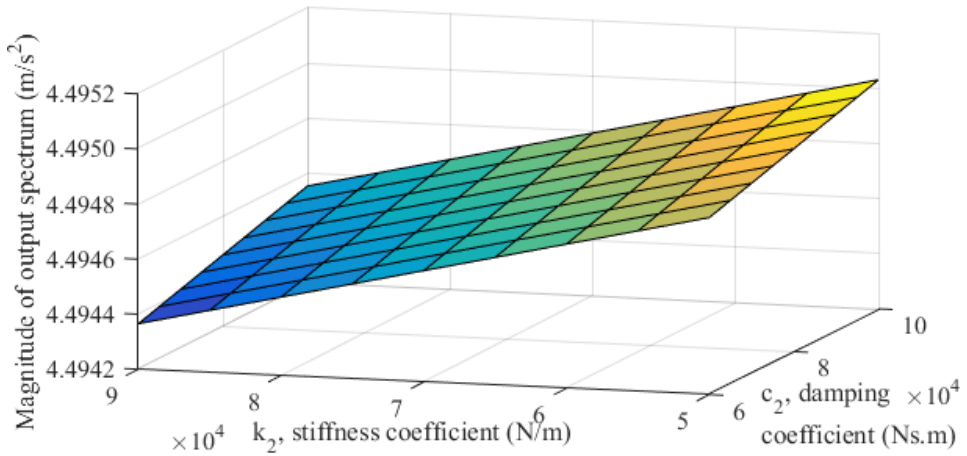


Figure 3.7: The relationship between the parameters  $c_2$  and  $k_2$  and magnitude of the output spectrum at 1.466 rad/s for the passive engine mount system.

with the increases of the stiffness coefficient,  $k_2$ . When comparing with the OFRF determined, which is as follows

$$\hat{Y}(j\omega) = \hat{P}_{11}(j\omega) + c_2 \hat{P}_{31}(j\omega) + k_2 \hat{P}_{32}(j\omega) + c_2^2 \hat{P}_{51}(j\omega) + c_2 k_2 \hat{P}_{52}(j\omega) + k_2^2 \hat{P}_{53}(j\omega) \quad (3.60)$$

it can be understood that the values of OFRF "coefficients",  $\hat{P}_{51}(j\omega)$ ,  $\hat{P}_{52}(j\omega)$  and  $\hat{P}_{53}(j\omega)$  are insignificant compared to the values of OFRF "coefficients",  $\hat{P}_{11}(j\omega)$ ,  $\hat{P}_{31}(j\omega)$  and  $\hat{P}_{32}(j\omega)$ . This shows that the relationship is linear. This relationship will be useful for designing process of the passive engine mount.

## 3.4 Conclusion

In this chapter, the detailed algorithms involved in the new numerical method of determining OFRF for SISO nonlinear system using ALEs were presented. The concept of the OFRF for SISO nonlinear systems is discussed and an algorithm is derived in Section 3.2.2.1 where the OFRF representation of the output spectrum of the system to any inputs can be derived. Then, the algorithm to determine ALEs for nonlinear systems that can be described by the

NDE model are presented in Section 3.2.3.2. Finally, using the relationship between the OFRF representation and the ALEs, the new algorithm to determine the OFRF for the SISO nonlinear system using ALEs was derived as in Section 3.2.4.1.

This new numerical method allows OFRF, which reveals a significant link between the system output frequency response and the parameters that define the system nonlinearity to be determined with a significantly less number of numerical simulations compared to previous works. The OFRF based analysis was applied to a passive engine mount system. Detailed process of the OFRF determination using the new numerical method discussed in this chapter was presented and the analysis and design of the passive engine mount system were done. The OFRF provide an explicit relationship between the output spectrum and the nonlinear parameters of the passive engine mount, the damping coefficient and the stiffness coefficient. This relationship provides an insight on the relationship thus useful for the design process of the nonlinear systems.

As a conclusion, the new numerical method proposed in this chapter is more efficient to determine OFRF for SISO nonlinear systems compared to the currently available method [46, 35] and can be used to the wide area of engineering. It can help in the frequency domain analysis on how the system behaviours affected by the nonlinear parameter and in the design of the parameters to achieve desired system output frequency responses. The numerical method discussed in this chapter only works for a SISO nonlinear system, but its concept will be used as a foundation for the next chapter.

# **Chapter 4**

## **A new numerical method for determination of OFRFs of MIMO nonlinear systems**

### **4.1 Introduction**

In the previous chapter, a new numerical method for the determination of OFRF of single input single output (SISO) nonlinear systems is proposed. The new numerical method allows the determination of output frequency response function (OFRF) to be less tedious compared to the current numerical method, thus makes the design of SISO nonlinear systems to be done more efficiently compared to before. As most of engineering systems are multi input-multi output (MIMO) nonlinear system, it will be great if the new numerical method can be used to determine the OFRF for the MIMO nonlinear systems.

After a thorough analysis, it was found that this new numerical method can be extended and used for the determination of OFRF for the MIMO nonlinear system. This finding was motivated by [60] where it presented the concept of Nonlinear Output Frequency Response

Function(NOFRF) that can be used in the multi input nonlinear systems. This chapter discusses the concept of determination of OFRF of MIMO nonlinear systems which was the extended version of the SISO nonlinear system concept. The new numerical method allowed the idea of OFRF to be used in a more complicated system.

This chapter begins by defining the nonlinear differential equation (NDE) model for MIMO nonlinear system. The new numerical method discussed in this chapter consists of three synergizing algorithms. The first algorithm is about the determination of OFRF representation of the MIMO nonlinear system. The second algorithm is the determination of ALEs for the MIMO nonlinear system where the ALEs can be determined easily up to any nth-order. The last algorithm is focusing on the determination of OFRF using the ALEs. This algorithm uses the relationship between the OFRF representation and the ALEs determined in the first two algorithms. These three algorithms make the determination of OFRF more systematic.

The new numerical method presented in this chapter allowed the concept of OFRF to be applied to a wide range of nonlinear engineering system as most of the engineering systems are nonlinear. The OFRF based design of a building structure vibration isolation system has then be used to demonstrate how the new numerical method discussed in this chapter can be applied to implement a design for application in earthquake engineering. A paper on the implementation of OFRF into the earthquake engineering [54] had been submitted and accepted for the International Conference on Smart Infrastructure and Construction (ICSIC 2016).

## 4.2 A new numerical method for determining the OFRF of a MIMO nonlinear system

### 4.2.1 Nonlinear differential equation (NDE) model for multi input multi output (MIMO)

Consider a r-input and m-output nonlinear system. The dynamics of  $k_i$ th subsystem can be represented by

$$\sum_{n=1}^{N_l} \sum_{p=0}^n \sum_{\alpha_1=1}^m \sum_{\alpha_2=\alpha_1}^m \dots \sum_{\alpha_p=\alpha_{p-1}}^m \sum_{\beta_1=1}^r \sum_{\beta_2=\beta_1}^r \dots \sum_{\beta_q=\beta_{q-1}}^r \sum_{l_1, \dots, l_{p+q}}^L c_{pq}^{\alpha_1, \dots, \alpha_p, \beta_1, \dots, \beta_q} (k_i : l_1, \dots, l_{p+q}) \\ \times \prod_{i=1}^p D^{l_i} y_{\alpha_i}(t) \times \prod_{i=p+1}^{p+q} D^{l_i} u_{\beta_{i-p}}(t) = 0 \quad (4.1)$$

where  $p + q = n$ , L is the order of the maximum derivative and the operator  $D^{l_i}$  is defined as

$$D^{l_i} x(t) = \frac{d^{l_i} x(t)}{dt^{l_i}} \quad (4.2)$$

This equation explains each  $k_i$ th subsystem individually where the parameter  $c_{pq}^{\alpha_1, \dots, \alpha_p, \beta_1, \dots, \beta_q} (k_i : l_1, \dots, l_{p+q})$  is associated with the term  $\prod_{i=1}^p D^{l_i} y_{\alpha_i}(t) \prod_{i=p+1}^{p+q} D^{l_i} u_{\beta_{i-p}}(t) = 0$ .

To illustrate a MIMO-NDE model, consider a quadratic nonlinear system that was described as

$$\begin{aligned} \ddot{y}_1(t) + 20\dot{y}_1(t) + 1010y_1(t) + 140y_2(t) + ay_1^2(t) + 200y_1(t)y_2(t) + by_2^2(t) &= u_1(t) \\ \ddot{y}_2(t) + 20\dot{y}_2(t) + 4010y_2(t) + 72y_1(t) + 100y_1^2(t) + 300y_1(t)y_2(t) + 200y_2^2(t) &= u_2(t) \end{aligned} \quad (4.3)$$

This MIMO-NDE model could be represented in the (4.1) form. The coefficients for the first subsystem are

$$\begin{aligned}
 c_{1,0}^1(1 : 2) &= 1, \\
 c_{1,0}^1(1 : 1) &= 20, \\
 c_{1,0}^1(1 : 0) &= 1010, \\
 c_{1,0}^2(1 : 0) &= 140, \\
 c_{2,0}^{1,1}(1 : 0, 0) &= a, \\
 c_{2,0}^{1,2}(1 : 0, 0) &= 200, \\
 c_{2,0}^{2,2}(1 : 0, 0) &= b, \\
 c_{0,1}^1(1 : 0) &= -1
 \end{aligned} \tag{4.4}$$

and the coefficients for the second subsystem are

$$\begin{aligned}
 c_{1,0}^2(2 : 2) &= 1, \\
 c_{1,0}^2(2 : 1) &= 20, \\
 c_{1,0}^2(2 : 0) &= 4010, \\
 c_{1,0}^1(2 : 0) &= 72, \\
 c_{2,0}^{1,1}(2 : 0, 0) &= 100, \\
 c_{2,0}^{1,2}(2 : 0, 0) &= 300, \\
 c_{2,0}^{2,2}(2 : 0, 0) &= 200, \\
 c_{0,1}^2(2 : 0) &= -1
 \end{aligned} \tag{4.5}$$

## 4.2.2 The Output Frequency Response Function for MIMO nonlinear system

### 4.2.2.1 OFRF representation of the MIMO nonlinear system

It is the same basic concept as stated before, where the explicit analytical relationship between the output frequency response and the model parameters for nonlinear systems exists, if and only if the nonlinear system can be described by model (4.1), and satisfies the following assumptions:

- The system is stable at zero equilibrium
- The systems can equivalently be described by the Volterra series model with  $N \geq M$  over a regime around the equilibrium,

The OFRF of a general MIMO nonlinear system is the extension of the OFRF of a general nonlinear system[46] and can be represented as

$$\begin{aligned}\hat{Y}_{\alpha_i}(j\omega) &= \sum_{(j_1, \dots, j_{S_N}) \in J} \gamma_{(j_1, \dots, j_{S_N})}(\omega) x_1^{j_1} \dots x_{S_N}^{j_{S_N}} \\ &= \sum_{j_1}^{m_1} \sum_{j_2}^{m_2} \dots \sum_{j_{S_N}}^{m_{S_N}} \gamma_{(j_1, \dots, j_{S_N})}(\omega) x_1^{j_1} \dots x_{S_N}^{j_{S_N}}\end{aligned}\quad (4.6)$$

where  $x_i, i = 1, \dots, S_N$  are the parameters which define the system nonlinearity;  $m_i$  is the maximum power of  $x_i, i = 1, \dots, S_N$ .  $x_1^{j_1} \dots x_{S_N}^{j_{S_N}}$  represent the coefficients of the term  $\gamma_{(j_1, \dots, j_{S_N})}(\omega)$  which is a set of all monomials involved in the representation of  $\hat{Y}_{\alpha_i}(j\omega)$ .

In order to determine the OFRF representation of the MIMO nonlinear system, the set of the monomials involved in the representation of  $\hat{Y}(j\omega)$  up to  $N_{max}$ th-order, denote as  $\mathbf{M}_{N_{max}}$  need to be determined first. Then using the  $\mathbf{M}_{N_{max}}$  determined, the OFRF representation of the MIMO nonlinear system can be derived.

The OFRF representation of a MIMO nonlinear system can be determined by the following algorithm,

1. Set  $N_{max} > 0$  and  $n = 1, 2, \dots, N_{max}$ .
2.  $\mathbf{M}_1 = [1]$ . Calculate  $\mathbf{M}_n$  by using

$$\begin{aligned} \mathbf{M}_n = & \left[ \bigcup_{l_1, \dots, l_n=0}^L [c_{0n}^{\alpha_1, \dots, \alpha_p, \beta_1, \dots, \beta_q}(k_i : l_1, \dots, l_p)] \right] \\ & \cup \left[ \bigcup_{q=1}^{n-1} \bigcup_{p=1}^{n-q} \bigcup_{l_1, \dots, l_n=0}^L [c_{0n}^{\alpha_1, \dots, \alpha_p, \beta_1, \dots, \beta_q}(k_i : l_1, \dots, l_p) \otimes \mathbf{M}_{n-q,p}] \right] \\ & \cup \left[ \bigcup_{p=2}^n \bigcup_{l_1, \dots, l_p=0}^L [c_{p0}^{\alpha_1, \dots, \alpha_p, \beta_1, \dots, \beta_q}(k_i : l_1, \dots, l_p) \otimes \mathbf{M}_{np}] \right] \end{aligned} \quad (4.7)$$

where  $\otimes$  is the Kronecker product, and

$$\mathbf{M}_{np} = \bigcup_{i=1}^{n-p+1} (\mathbf{M}_i \otimes \mathbf{M}_{n-i,p-1}) \quad \text{and} \quad \mathbf{M}_{n1} = \mathbf{M}_n \quad (4.8)$$

3. Then, the set of the parametric characteristics of the system in (4.6) can be expressed as

$$\bar{\mathbf{M}}_{N_{max}} = \bigcup_{n=1}^{N_{max}} \mathbf{M}_n \quad (4.9)$$

4. Lastly, the OFRF representation of each outputs of the MIMO nonlinear system can be written as

$$\hat{Y}_{\alpha_i}(j\omega) = \sum_{n=1}^{N_{max}} \mathbf{M}_{nf} P_{nf} \quad (4.10)$$

where  $f$  is corresponding to the number of element in  $\mathbf{M}_n$  and  $\alpha_i$  is corresponding to the output.

The OFRF representation is the same for each output but the value of the OFRF "coefficients" are different. This algorithm is an extended version of the algorithm discussed in the Section 3.2.2.1 and it works for MIMO nonlinear systems that have subsystems.

#### 4.2.2.2 Example

In order to understand this algorithm more, considering the quadratic nonlinear system that was discussed before, the OFRF representation of the first subsystem up to fourth order can be determined priori using the algorithm that has been discussed. Firstly, set  $N_{max} = 4$ ,  $n = 1, 2, 3, 4$  and the monomial for the first order,  $\mathbf{M}_1 = [1]$ . Then, calculate each  $\mathbf{M}_n$  using (4.7) for quadratic nonlinear system. The outcomes of the calculation are

$$\begin{aligned}\mathbf{M}_2 &= [a, b] \\ \mathbf{M}_3 &= [a^2, ab, b^2] \\ \mathbf{M}_4 &= [a^3, a^2b, ab^2, b^3]\end{aligned}\tag{4.11}$$

Lastly, the set of the parametric characteristics for cubic duffing oscillator system up to 4-th order can be expressed as

$$\bar{\mathbf{M}}_4 = \bigcup_{n=1}^4 \mathbf{M}_n = [1, a, b, a^2, ab, b^2, a^3, a^2b, ab^2, b^3]\tag{4.12}$$

and using this results, the OFRF representation of the two outputs of the quadratic nonlinear system can be written as

$$\begin{aligned}\hat{Y}_1(j\omega) &= \hat{P}_{11}(j\omega) + a\hat{P}_{21}(j\omega) + b\hat{P}_{22}(j\omega) + a^2\hat{P}_{31}(j\omega) + ab\hat{P}_{32}(j\omega) \\ &\quad + b^2\hat{P}_{33}(j\omega) + a^3\hat{P}_{41}(j\omega) + a^2b\hat{P}_{42}(j\omega) + ab^2\hat{P}_{43}(j\omega) + b^3\hat{P}_{44}(j\omega) \\ \hat{Y}_2(j\omega) &= \hat{P}_{11}(j\omega) + a\hat{P}_{21}(j\omega) + b\hat{P}_{22}(j\omega) + a^2\hat{P}_{31}(j\omega) + ab\hat{P}_{32}(j\omega) \\ &\quad + b^2\hat{P}_{33}(j\omega) + a^3\hat{P}_{41}(j\omega) + a^2b\hat{P}_{42}(j\omega) + ab^2\hat{P}_{43}(j\omega) + b^3\hat{P}_{44}(j\omega)\end{aligned}\tag{4.13}$$

From (4.13), it can bee seen that for both outputs, the OFRF representations are the same. Although the OFRF representations are the same, the OFRF "coefficients" are different.

### 4.2.3 Derivation of ALEs for MIMO nonlinear systems

#### 4.2.3.1 ALEs for MIMO nonlinear system

Similarly to the SISO nonlinear system, MIMO nonlinear systems also can be described by a series of ALEs as any system that possesses a Volterra series representation can be described by a series of associated linear equations (ALEs) [86] [85]. To derive ALEs for MIMO-NDE systems, consider MIMO nonlinear systems that have the input and the output terms independent and not related to each other

$$\begin{aligned} & \sum_{\alpha_1=1}^m \sum_{\alpha_2=\alpha_1}^m \dots \sum_{\alpha_p=\alpha_{p-1}}^m \sum_{p=1}^P \sum_{l_1, \dots, l_p}^L c_{p0}(k_i : l_1, \dots, l_p) \prod_{i=1}^p D^{l_i} y_{\alpha_i}(t) \\ & + \sum_{\beta_1=1}^r \sum_{\beta_2=\beta_1}^r \dots \sum_{\beta_q=\beta_{q-1}}^r \sum_{q=1}^Q \sum_{l_1, \dots, l_q}^L c_{0q}(k_i : l_1, \dots, l_q) \prod_{i=1}^q D^{l_i} u_{\beta_i}(t) = 0 \end{aligned} \quad (4.14)$$

Then separating the NDE to two different parts for the output, linear and nonlinear parts generates

$$\begin{aligned} & \sum_{\alpha_1=1}^m \sum_{\alpha_2=\alpha_1}^m \dots \sum_{\alpha_p=\alpha_{p-1}}^m \sum_{l_1=0}^L c_{10}(k_i : l_1) D^{l_1} y_{\alpha_i}(t) \\ & + \sum_{\alpha_1=1}^m \sum_{\alpha_2=\alpha_1}^m \dots \sum_{\alpha_p=\alpha_{p-1}}^m \sum_{p=2}^P \sum_{l_1, \dots, l_p}^L c_{p0}(k_i : l_1, \dots, l_p) \prod_{i=1}^p D^{l_i} y_{\alpha_i}(t) \\ & + \sum_{\beta_1=1}^r \sum_{\beta_2=\beta_1}^r \dots \sum_{\beta_q=\beta_{q-1}}^r \sum_{q=1}^Q \sum_{l_1, \dots, l_q}^L c_{0q}(k_i : l_1, \dots, l_q) \prod_{i=1}^q D^{l_i} u_{\beta_i}(t) = 0 \end{aligned} \quad (4.15)$$

Using the knowledge that the NDE model possesses a Volterra representation, substitution of

$$y_{\alpha_i}(t) = \sum_{n=1}^{\infty} y_{\alpha_i, n}(t) \quad (4.16)$$

into equation (4.15) results in

$$\begin{aligned} & \sum_{\alpha_1=1}^m \sum_{\alpha_2=\alpha_1}^m \dots \sum_{\alpha_p=\alpha_{p-1}}^m \sum_{l_1=0}^L c_{10}(k_i : l_1) \sum_{n=1}^{\infty} D^{l_1} y_{\alpha_i, n}(t) \\ & + \sum_{\alpha_1=1}^m \sum_{\alpha_2=\alpha_1}^m \dots \sum_{\alpha_p=\alpha_{p-1}}^m \sum_{p=2}^P \sum_{l_1, \dots, l_p}^L c_{p0}(k_i : l_1, \dots, l_p) \prod_{i=1}^p \sum_{n=1}^{\infty} D^{l_i} y_{\alpha_i, n}(t) \\ & + \sum_{\beta_1=1}^r \sum_{\beta_2=\beta_1}^r \dots \sum_{\beta_q=\beta_{q-1}}^r \sum_{q=1}^Q \sum_{l_1, \dots, l_q}^L c_{0q}(k_i : l_1, \dots, l_q) \prod_{i=1}^q D^{l_i} u_{\beta_i}(t) = 0 \quad (4.17) \end{aligned}$$

Then, rearrangement of the nonlinear part of the equation (4.17) is made as

$$\begin{aligned} & \sum_{\alpha_1=1}^m \sum_{\alpha_2=\alpha_1}^m \dots \sum_{\alpha_p=\alpha_{p-1}}^m \sum_{l_1=0}^L c_{10}(k_i : l_1) \sum_{n=1}^{\infty} D^{l_1} y_{\alpha_i, n}(t) + \sum_{\alpha_1=1}^m \sum_{\alpha_2=\alpha_1}^m \dots \sum_{\alpha_p=\alpha_{p-1}}^m \sum_{p=2}^P \sum_{l_1, \dots, l_p}^L \\ & c_{p0}(k_i : l_1, \dots, l_p) \left( \sum_{n=1}^{\infty} D^0 y_{\alpha_i, n}(t) \right)^{p_0} \left( \sum_{n=1}^{\infty} D^1 y_{\alpha_i, n}(t) \right)^{p_1} \dots \left( \sum_{n=1}^{\infty} D^s y_{\alpha_i, n}(t) \right)^{p_s} \\ & + \sum_{\beta_1=1}^r \sum_{\beta_2=\beta_1}^r \dots \sum_{\beta_q=\beta_{q-1}}^r \sum_{q=1}^Q \sum_{l_1, \dots, l_q}^L c_{0q}(k_i : l_1, \dots, l_q) \prod_{i=1}^q D^{l_i} u_{\beta_i}(t) = 0 \quad (4.18) \end{aligned}$$

where  $p_0 + p_1 + \dots + p_s = p$ .

Then, leaving on the LHS of the equation only the linear elements, (4.18) will be

$$\begin{aligned} & \sum_{\alpha_1=1}^m \sum_{\alpha_2=\alpha_1}^m \dots \sum_{\alpha_p=\alpha_{p-1}}^m \sum_{l_1=0}^L c_{10}(k_i : l_1) \sum_{n=1}^{\infty} D^{l_1} y_{\alpha_i, n}(t) = - \sum_{\alpha_1=1}^m \sum_{\alpha_2=\alpha_1}^m \dots \sum_{\alpha_p=\alpha_{p-1}}^m \sum_{p=2}^P \sum_{l_1, \dots, l_p}^L \\ & c_{p0}(k_i : l_1, \dots, l_p) \left( \sum_{n=1}^{\infty} D^0 y_{\alpha_i, n}(t) \right)^{p_0} \left( \sum_{n=1}^{\infty} D^1 y_{\alpha_i, n}(t) \right)^{p_1} \dots \left( \sum_{n=1}^{\infty} D^s y_{\alpha_i, n}(t) \right)^{p_s} \\ & - \sum_{\beta_1=1}^r \sum_{\beta_2=\beta_1}^r \dots \sum_{\beta_q=\beta_{q-1}}^r \sum_{q=1}^Q \sum_{l_1, \dots, l_q}^L c_{0q}(k_i : l_1, \dots, l_q) \prod_{i=1}^q D^{l_i} u_{\beta_i}(t) = 0 \quad (4.19) \end{aligned}$$

For the determination of OFRF using ALEs derivation, the systems will be assessed up to  $N_{max}$  order, thus (4.19) can be written as

$$\begin{aligned} \sum_{\alpha_1=1}^m \sum_{\alpha_2=\alpha_1}^m \dots \sum_{\alpha_p=\alpha_{p-1}}^m \sum_{l_1=0}^L c_{10}(k_i : l_1) \sum_{n=1}^{N_{max}} D^{l_1} y_{\alpha_i, n}(t) &= - \sum_{\alpha_1=1}^m \sum_{\alpha_2=\alpha_1}^m \dots \sum_{\alpha_p=\alpha_{p-1}}^m \sum_{p=2}^P \sum_{l_1, \dots, l_p} \\ c_{p0}(k_i : l_1, \dots, l_p) \left( \sum_{n=1}^{N_{max}} D^0 y_{\alpha_i, n}(t) \right)^{p_0} \left( \sum_{n=1}^{N_{max}} D^1 y_{\alpha_i, n}(t) \right)^{p_1} \dots \left( \sum_{n=1}^{N_{max}} D^s y_{\alpha_i, n}(t) \right)^{p_s} \\ - \sum_{\beta_1=1}^r \sum_{\beta_2=\beta_1}^r \dots \sum_{\beta_q=\beta_{q-1}}^r \sum_{q=1}^Q \sum_{l_1, \dots, l_q}^L c_{0q}(k_i : l_1, \dots, l_q) \prod_{i=1}^q D^{l_i} u_{\beta_i}(t) &= 0 \end{aligned} \quad (4.20)$$

and (4.20) can be simplified as

$$\begin{aligned} \sum_{\alpha_1=1}^m \sum_{\alpha_2=\alpha_1}^m \dots \sum_{\alpha_p=\alpha_{p-1}}^m \sum_{l_1=0}^L c_{10}(k_i : l_1) \sum_{n=1}^{N_{max}} D^{l_1} y_{\alpha_i, n}(t) \\ = - \sum_{\alpha_1=1}^m \sum_{\alpha_2=\alpha_1}^m \dots \sum_{\alpha_p=\alpha_{p-1}}^m \sum_{p=2}^P \sum_{l_1, \dots, l_p}^L c_{p0}(k_i : l_1, \dots, l_p) \left( \prod_{s=0}^S \left( \sum_{n=1}^{N_{max}} D^s y_{\alpha_i, n}(t) \right)^{p_s} \right) \\ - \sum_{\beta_1=1}^r \sum_{\beta_2=\beta_1}^r \dots \sum_{\beta_q=\beta_{q-1}}^r \sum_{q=1}^Q \sum_{l_1, \dots, l_q}^L c_{0q}(k_i : l_1, \dots, l_q) \prod_{i=1}^q D^{l_i} u_{\beta_i}(t) \end{aligned} \quad (4.21)$$

where  $S$  is the maximum power of the nonlinear terms for each nonlinear output terms. From equation (4.21), it can be seen the relationship between the input and the outputs; linear and nonlinear.

For the determination of OFRF using ALEs in MIMO-NDE system, the analysis of the output of the nonlinear system is done order by order for the set of MIMO-NDE system, where the linear terms on the left hand side is solved by using nonlinear terms that is one order lower on the right hand side. Then, the response of the nonlinear system is the total of all the response from the ALEs. The algorithm to determine ALE for the MIMO-NDE model is discussed in the next subsection.

#### 4.2.3.2 Algorithm to determine ALE for MIMO-NDE model

The following algorithm can be used to determine the ALEs for every Nth-order up to any  $N_{max}$ th-order for the MIMO-NDE model. Note that determination of the total response will be the summation of all the responses in ALEs. This algorithm is for a MIMO-NDE model, where the linear and nonlinear parts of the outputs had been separated, and the input and the output terms are independent and not related to each other

$$\sum_{l_1=0}^L c_{10}(k_i : l_1) \sum_{n=1}^{N_{max}} D^{l_1} y_{\alpha_i, n}(t) = - \sum_{p=2}^P \sum_{l_1, \dots, l_p} c_{p0}(k_i : l_1, \dots, l_p) \left( \prod_{s=0}^S \left( \sum_{n=1}^{N_{max}} D^s y_{\alpha_i, n}(t) \right)^{p_s} \right) - \sum_{q=1}^Q \sum_{l_1, \dots, l_q} c_{0q}(k_i : l_1, \dots, l_q) \prod_{i=1}^q D^{l_i} u_{\beta_i}(t) \quad (4.22)$$

where P is maximum degree of nonlinearity in terms of  $y(t)$ , Q is maximum degree of nonlinearity in terms of  $u(t)$ , L is the maximum order of differential function, S is the maximum power of the nonlinear terms for each nonlinear output terms and the operator  $D$  is defined by

$$D^l x(t) = \frac{d^l x(t)}{dt^l} \quad (4.23)$$

The ALEs for every nth-order up to any  $N_{max}$ th-order can be determined using the steps below

1. Set  $n = 1, 2, \dots, N_{max}$  where  $N_{max} > 0$ .
2.  $J_{n,0} = J_{n,1} = 0$ . The ALEs for every nth-order can be written as

$$\sum_{l_1=0}^L c_{10}(k_i : l_1) D^{l_1} y_{\alpha_i, n}(t) = \sum_{l_1, \dots, l_n} c_{0n}(k_i : l_1, \dots, l_n) \prod_{i=1}^n D^{l_i} u_{\beta_i}(t) + J_{\alpha_i, n} - J_{\alpha_i, n-1} \quad (4.24)$$

where

$$J_{\alpha_i, n} = - \sum_{p=2}^P \sum_{l_1, \dots, l_p} c_{p0}(k_i : l_1, \dots, l_p) \left( \prod_{s=0}^S \left( \sum_{n=1}^{n-1} D^s y_{\alpha_i, n}(t) \right)^{p_s} \right) \quad (4.25)$$

3. The estimation of the output signal and the output spectrum for each outputs of the system up to  $N_{max}$ th-order thus can be written as

$$\hat{y}_{\alpha_i}(t) = \sum_{n=1}^{N_{max}} \hat{y}_{\alpha_i,n}(t) \quad (4.26)$$

and

$$\hat{Y}_{\alpha_i}(j\omega) = \sum_{n=1}^{N_{max}} \hat{Y}_{\alpha_i,n}(j\omega) \quad (4.27)$$

where  $\alpha_i$  is corresponding to the ouput and  $n$  is the order of the ALE.

This algorithm makes the ALEs for every Nth-order up to any  $N_{max}$ th-order can be determined easily for each set of MIMO-NDE model.

#### 4.2.3.3 Example

To show the effectiveness of this algorithm, the ALEs for quadratic nonlinear system up to 4th-order is determined using the steps in the algorithm. Take a look again at the NDE form of the quadratic nonlinear system as in (4.3)

$$\begin{aligned} \ddot{y}_1(t) + 20\dot{y}_1(t) + 1010y_1(t) + 140y_2(t) + ay_1^2(t) + 200y_1(t)y_2(t) + by_2^2(t) &= u_1(t) \\ \ddot{y}_2(t) + 20\dot{y}_2(t) + 4010y_2(t) + 72y_1(t) + 100y_1^2(t) + 300y_1(t)y_2(t) + 200y_2^2(t) &= u_2(t) \end{aligned}$$

In order to use the algorithm, rewrite (4.3) in the different form as

$$\begin{aligned} D^2y_1(t) + 20D^1y_1(t) + 1010y_1(t) + 140y_2(t) \\ + ay_1(t)^2 + 200y_1(t)y_2(t) + by_2(t)^2 &= u_1(t) \\ D^2y_2(t) + 20D^1y_2(t) + 4010y_2(t) + 72y_1(t) \\ + 100y_1(t)^2 + 300y_1(t)y_2(t) + 200y_2(t)^2 &= u_2(t) \end{aligned} \quad (4.28)$$

Using the steps in the algorithm, set  $N_{max} = 4$ ,  $n = 1, 2, 3, 4$ . Then, the general ALEs for every order up to 4th-order can be written as

$$\begin{aligned}
 & c_{1,0}^1(1:2)D^2y_{1,1}(t) + c_{1,0}^1(1:1)D^1y_{1,1}(t)) + c_{1,0}^2(1:0)y_{2,1}(t) + c_{1,0}^1(1:0)y_{1,1}(t) \\
 &= c_{0,1}^1(1:l_1)D^{l_1}u_1(t) + J_{1,1} - J_{1,0} \\
 & c_{1,0}^2(2:2)D^2y_{2,1}(t) + c_{1,0}^2(2:1)D^1y_{2,1}(t)) + c_{1,0}^2(2:0)y_{2,1}(t) + c_{1,0}^1(2:0)y_{1,1}(t) \\
 &= c_{0,1}^2(2:l_1)D^{l_1}u_2(t) + J_{2,1} - J_{2,0} \\
 \\ 
 & c_{1,0}^1(1:2)D^2y_{1,2}(t) + c_{1,0}^1(1:1)D^1y_{1,2}(t)) + c_{1,0}^1(1:0)y_{1,2}(t) + c_{1,0}^2(1:0)y_{2,2}(t) \\
 &= c_{0,2}^{1,1}(1:l_1, l_2)D^{l_1}u_1(t)D^{l_2}u_1(t) + J_{1,2} - J_{1,1} \\
 & c_{1,0}^2(2:2)D^2y_{2,2}(t) + c_{1,0}^2(2:1)D^1y_{2,2}(t)) + c_{1,0}^2(2:0)y_{2,2}(t) + c_{1,0}^1(2:0)y_{1,2}(t) \\
 &= c_{0,2}^{2,2}(2:l_1, l_2)D^{l_1}u_2(t)D^{l_2}u_2(t) + J_{2,2} - J_{2,1} \\
 & \quad (4.29) \\
 & c_{1,0}^1(1:2)D^2y_{1,3}(t) + c_{1,0}^1(1:1)D^1y_{1,3}(t)) + c_{1,0}^1(1:0)y_{1,3}(t) + c_{1,0}^2(1:0)y_{2,3}(t) \\
 &= c_{0,3}^{1,1,1}(1:l_1, l_2, l_3)D^{l_1}u_1(t)D^{l_2}u_1(t)D^{l_3}u_1(t) + J_{1,3} - J_{1,2} \\
 & c_{1,0}^2(2:2)D^2y_{1,3}(t) + c_{1,0}^2(2:1)D^1y_{1,3}(t)) + c_{1,0}^2(2:0)y_{2,3}(t) + c_{1,0}^1(2:0)y_{1,3}(t) \\
 &= c_{0,3}^{2,2,2}(2:l_1, l_2, l_3)D^{l_1}u_2(t)D^{l_2}u_2(t)D^{l_3}u_2(t) + J_{2,3} - J_{2,2} \\
 \\ 
 & c_{1,0}^1(1:2)D^2y_{1,4}(t) + c_{1,0}^1(1:1)D^1y_{1,4}(t)) + c_{1,0}^1(1:0)y_{1,4}(t) + c_{1,0}^2(1:0)y_{2,4}(t) \\
 &= c_{0,4}^{1,1,1,1}(1:l_1, l_2, l_3, l_4)D^{l_1}u_1(t)D^{l_2}u_1(t)D^{l_3}u_1(t)D^{l_4}u_1(t) + J_{1,4} - J_{1,3} \\
 & c_{1,0}^2(2:2)D^2y_{1,4}(t) + c_{1,0}^2(2:1)D^1y_{1,4}(t)) + c_{1,0}^2(2:0)y_{2,4}(t) + c_{1,0}^1(2:0)y_{1,4}(t) \\
 &= c_{0,4}^{2,2,2,2}(2:l_1, l_2, l_3, l_4)D^{l_1}u_2(t)D^{l_2}u_2(t)D^{l_3}u_2(t)D^{l_4}u_2(t) + J_{2,4} - J_{2,3} \\
 \end{aligned}$$

where  $J_0 = J_1 = 0$ ,  $c_{0,1}^1(1:l_1)D^{l_1}u_1(t) = u_1(t)$ ,  $c_{0,1}^2(2:l_1)D^{l_1}u_2(t) = u_2(t)$  and  $c_{0,2}^1(1:l_1, l_2) = c_{0,2}^2(2:l_1, l_2) = c_{0,3}^1(1:l_1, l_2, l_3) = c_{0,3}^2(2:l_1, l_2, l_3) = c_{0,4}^1(1:l_1, l_2, l_3, l_4) = c_{0,4}^2(2:l_1, l_2, l_3, l_4) = 0$ .

After solving  $J_{1,n}$  and  $J_{2,n}$ , the ALEs for the system up to 4th-order can be written as

$$D^2y_{1,1}(t) + 20D^1y_{1,1}(t)) + 1010y_{1,1}(t) + 140y_{2,1}(t) = u_1(t)$$

$$D^2y_{1,1}(t) + 20D^1y_{1,1}(t)) + 4010y_{2,1}(t) + 72y_{1,1}(t) = u_2(t)$$

$$D^2y_{1,2}(t) + 20D^1y_{1,2}(t)) + 1010y_{1,2}(t) + 140y_{2,2}(t)$$

$$= -a(y_{1,1}(t))^2 - 200y_{1,1}(t)y_{2,1}(t) - b(y_{2,1}(t))^2$$

$$D^2y_{1(2)}(t) + 20D^1y_{1(2)}(t)) + 4010y_{2(2)}(t) + 72y_{1(2)}(t)$$

$$= -100(y_{1,1}(t))^2 - 300y_{1,1}(t)y_{2,1}(t) - 200(y_{2,1}(t))^2$$

$$D^2y_{1,3}(t) + 20D^1y_{1,3}(t)) + 1010y_{1,3}(t) + 140y_{2,3}(t) = -a[(y_{1,2}(t))^2 + 2y_{1,1}(t)y_{1,2}(t)]$$

$$- 200[y_{1,1}(t)y_{2,2}(t) + y_{1,2}(t)y_{2,1}(t) + y_{1,2}(t)y_{2,2}(t)] - b[(y_{2,2}(t))^2 + 2y_{2,1}(t)y_{2,2}(t)]$$

$$D^2y_{1,3}(t) + 20D^1y_{1,3}(t)) + 4010y_{2,3}(t) + 72y_{1,3}(t) = -100[(y_{1,2}(t))^2 + 2y_{1,1}(t)y_{1,2}(t)]$$

$$- 300[y_{1,1}(t)y_{2,2}(t) + y_{1,2}(t)y_{2,1}(t) + y_{1,2}(t)y_{2,2}(t)] - 200[(y_{2,2}(t))^2 + 2y_{2,1}(t)y_{2,2}(t)]$$

$$D^2y_{1,2}(t) + 20D^1y_{1,4}(t)) + 1010y_{1,4}(t) + 140y_{2,4}(t)$$

$$= -a[(y_{1,3}(t))^2 + 2y_{1,1}(t)y_{1,3}(t) + 2y_{1,2}(t)y_{1,3}(t)] - 200[y_{1,1}(t)y_{2,3}(t)$$

$$+ y_{1,2}(t)y_{2,3}(t) + y_{1,3}(t)y_{2,1}(t) + y_{1,3}(t)y_{2,2}(t) + y_{1,3}(t)y_{2,3}(t)] - b[(y_{1,3}(t))^2$$

$$+ 2y_{2,1}(t)y_{2,3}(t) + 2y_{2,2}(t)y_{2,3}(t)]$$

$$D^2y_{1,4}(t) + 20D^1y_{1,4}(t)) + 4010y_{2,4}(t) + 72y_{1,4}(t)$$

$$= -100[(y_{1,3}(t))^2 + 2y_{1,1}(t)y_{1,3}(t) + 2y_{1,2}(t)y_{1,3}(t)] - 300[y_{1,1}(t)y_{2,3}(t)$$

$$+ y_{1,2}(t)y_{2,3}(t) + y_{1,3}(t)y_{2,1}(t) + y_{1,3}(t)y_{2,2}(t) + y_{1,3}(t)y_{2,3}(t)] - 200[(y_{1,3}(t))^2$$

$$+ 2y_{2,1}(t)y_{2,3}(t) + 2y_{2,2}(t)y_{2,3}(t)]$$

(4.30)

Lastly, the estimation of the outputs signal and the outputs spectrum for the system up to 4th-order for both outputs thus can be written as

$$\begin{aligned}\hat{y}_1(t) &= \hat{y}_{1,1}(t) + \hat{y}_{1,2}(t) + \hat{y}_{1,3}(t) + \hat{y}_{1,4}(t) \\ \hat{y}_2(t) &= \hat{y}_{2,1}(t) + \hat{y}_{2,2}(t) + \hat{y}_{2,3}(t) + \hat{y}_{2,4}(t)\end{aligned}\quad (4.31)$$

and

$$\begin{aligned}\hat{Y}_1(j\omega) &= \hat{Y}_{1,1}(j\omega) + \hat{Y}_{1,2}(j\omega) + \hat{Y}_{1,3}(j\omega) + \hat{Y}_{1,4}(j\omega) \\ \hat{Y}_2(j\omega) &= \hat{Y}_{2,1}(j\omega) + \hat{Y}_{2,2}(j\omega) + \hat{Y}_{2,3}(j\omega) + \hat{Y}_{2,4}(j\omega)\end{aligned}\quad (4.32)$$

Comparing with the previous chapter, Section 3.2.3.2, the estimation of the output signal and the output spectrum look the same as estimation for the SISO nonlinear system. However, for MIMO-NDE model, the estimation is independent for all outputs produced. The estimation of the output signal is the total of all ALEs responses for each outputs. Figure 4.1 shows the comparison of the simulated results and the sum of the ALEs results in the time domain to indicate the significant of (4.31).

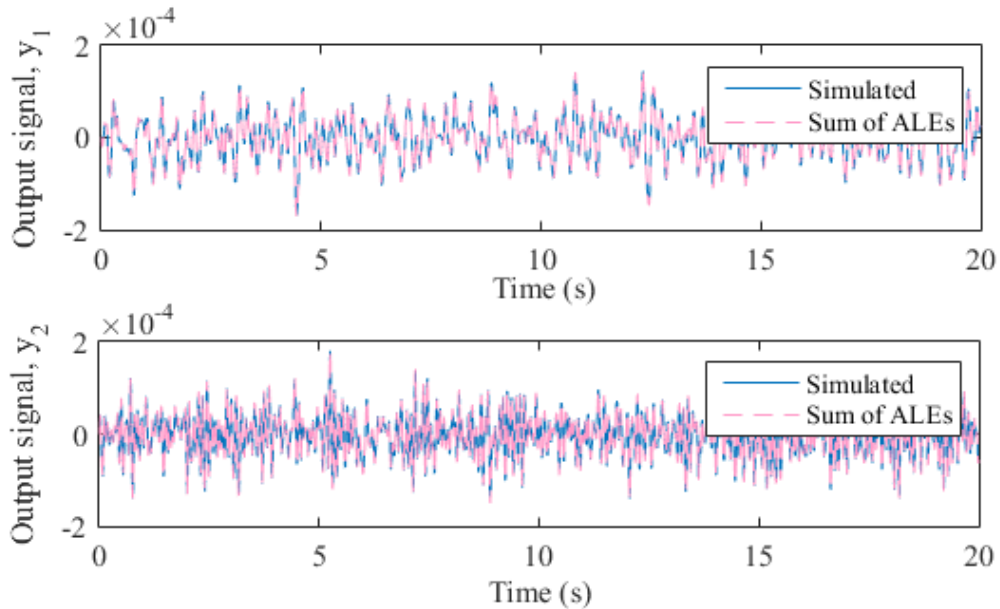


Figure 4.1: The simulated output signals for both  $y_1$  and  $y_2$  of the system and sum of the signals from the ALEs in the time domain when  $a = 50$  and  $b = 150$ .

Then, from (4.38), which is the result of Fourier transform of (4.31), it is understandable that the ouput spectrum for each output can be approximated by the sum of the each outputs solutions of the ALE in the frequency domain. Figure 4.2 shows the comparison of the simulated output spectrum and the sum of the solutions of the ALE in the frequency domain for each outputs,  $y_1$  and  $y_2$ .

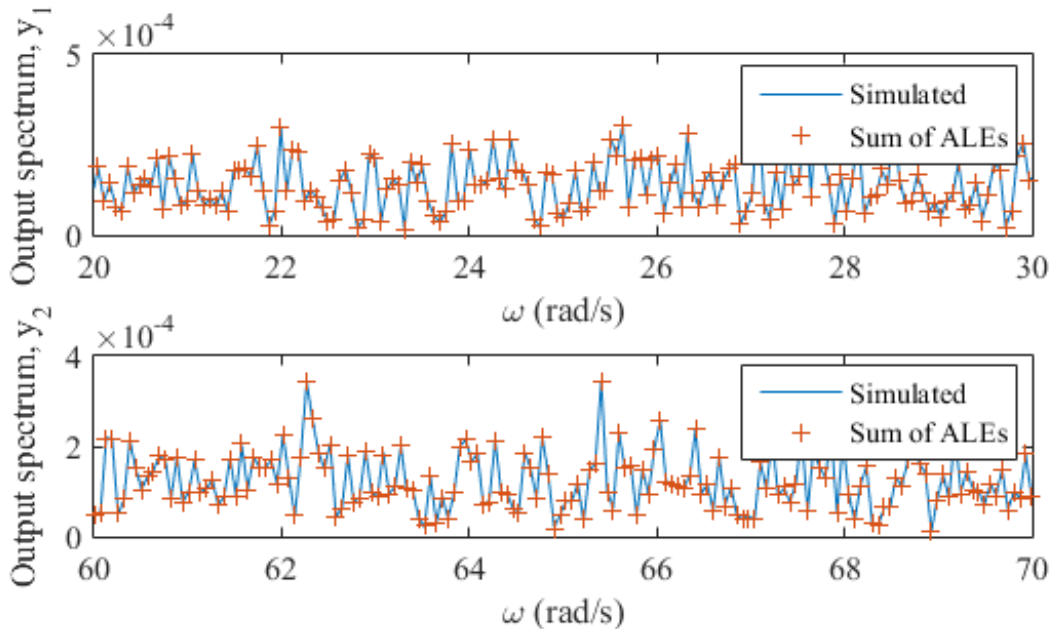


Figure 4.2: The simulated output spectrum of the system and sum of the output spectrum from the ALEs in the frequency domain when  $a = 50$  and  $b = 150$  for both  $y_1$  and  $y_2$ .

From both Figure 4.1 and Figure 4.2, it can be said that the sum of the ALEs results in both the time and frequency domain is in good accuracy to the simulated results for all the outputs in the system.

#### 4.2.4 Determination of OFRF using ALEs for MIMO nonlinear system

##### 4.2.4.1 Algorithm to determine OFRF using ALEs for MIMO nonlinear system

The OFRF of the MIMO nonlinear system can be determined using the following algorithm

1. Determine the OFRF representation of the nonlinear system using algorithm in section 4.2.2.1. The OFRF representation can be written as (4.10),

$$\hat{Y}_{\alpha_i}(j\omega) = \sum_{n=1}^{N_{max}} \mathbf{M}_{nf} P_{nf} \quad (4.33)$$

where  $f$  is corresponding to the number of element in  $\mathbf{M}_n$  and  $\alpha_i$  is corresponding to the output.

2. Determine the ALEs of the nonlinear system using the algorithm in section 4.2.3.2.

The output spectrum of the nonlinear system can be written as (4.27)

$$\hat{Y}_{\alpha_i}(j\omega) = \sum_{n=1}^{N_{max}} \hat{Y}_{\alpha_i,n}(j\omega) \quad (4.34)$$

where  $\alpha_i$  is corresponding to the ouput and  $n$  is the order of the ALE.

3. The number of the set of ALEs simulations needed to determine OFRF is equal to the maximum value of  $f$ . The output spectrums of the MIMO nonlinear system for each simulation can be written as

$$\hat{Y}_{\alpha_i}^v(j\omega) = \sum_{n=1}^{N_{max}} \hat{Y}_{\alpha_i,n}^v(j\omega) \quad (4.35)$$

where  $v$  is corresponding to the simulation number,  $\alpha_i$  is corresponding to the output and  $n$  is the order of the ALE.

4. The OFRF "coefficients" for each outputs need to be determined per nth-order. The solution for the OFRF "coefficients" for each output can be determined using the OFRF representation and the output spectrums from the simulations where

$$\begin{bmatrix} \hat{P}_{n1}(j\omega) \\ \hat{P}_{n2}(j\omega) \\ \vdots \\ \hat{P}_{nv}(j\omega) \end{bmatrix} = \begin{bmatrix} \mathbf{M}_n \text{ for simulation 1} \\ \mathbf{M}_n \text{ for simulation 2} \\ \vdots \\ \mathbf{M}_n \text{ for simulation v} \end{bmatrix}^{-1} \begin{bmatrix} \hat{Y}_{n1}(j\omega) \\ \hat{Y}_{n2}(j\omega) \\ \vdots \\ \hat{Y}_{nv}(j\omega) \end{bmatrix} \quad (4.36)$$

This algorithm allow the process for the determination of OFRF become more simpler and systematic. Using the OFRF determined, the analysis and design of the nonlinear system can be done.

#### 4.2.4.2 Example

In the previous chapter, the OFRF "coefficients" need to be determined per Nth-order in order to determine the OFRF of the nonlinear system. It will be the same for the MIMO-NDE models that had been discussed throughout this chapter. However, the OFRF "coefficients" for each outputs need to be calculated independently.

The OFRF representations for both outputs,  $y_1$  and  $y_2$  for the quadratic nonlinear systems are

$$\begin{aligned} \hat{Y}_1(j\omega) &= \hat{P}_1(j\omega) + a\hat{P}_{21}(j\omega) + b\hat{P}_{22}(j\omega) + a^2\hat{P}_{31}(j\omega) + ab\hat{P}_{32}(j\omega) \\ &\quad + b^2\hat{P}_{33}(j\omega) + a^3\hat{P}_{41}(j\omega) + a^2b\hat{P}_{42}(j\omega) + ab^2\hat{P}_{43}(j\omega) + b^3\hat{P}_{44}(j\omega) \\ \hat{Y}_2(j\omega) &= \hat{P}_1(j\omega) + a\hat{P}_{21}(j\omega) + b\hat{P}_{22}(j\omega) + a^2\hat{P}_{31}(j\omega) + ab\hat{P}_{32}(j\omega) \\ &\quad + b^2\hat{P}_{33}(j\omega) + a^3\hat{P}_{41}(j\omega) + a^2b\hat{P}_{42}(j\omega) + ab^2\hat{P}_{43}(j\omega) + b^3\hat{P}_{44}(j\omega) \end{aligned} \quad (4.37)$$

and the estimation of the output spectrum up to 4th-order for both outputs,  $y_1$  and  $y_2$  are

$$\begin{aligned} \hat{Y}_1(j\omega) &= \hat{Y}_{1,1}(j\omega) + \hat{Y}_{1,2}(j\omega) + \hat{Y}_{1,3}(j\omega) + \hat{Y}_{1,4}(j\omega) \\ \hat{Y}_2(j\omega) &= \hat{Y}_{2,1}(j\omega) + \hat{Y}_{2,2}(j\omega) + \hat{Y}_{2,3}(j\omega) + \hat{Y}_{2,4}(j\omega) \end{aligned} \quad (4.38)$$

From these results, it can be understood that in using the method of determining OFRF using ALEs for this system, four sets of ALEs simulations using different combinations of  $a$

and  $b$  were needed to determine the OFRF of this mechanical system. Table 4.1 shows the combinations of  $a$  and  $b$  used in the four simulations.

Table 4.1: Value of  $a$  and  $b$  used in the four simulations

Simulation, v	$a_v$	$b_v$
1	50	150
2	75	200
3	100	250
4	125	300

From the four sets of simulations, as already mentioned previously, the estimation of the output spectrum of the system in the frequency domain is the total of the ALEs responses. Equation (4.39) shows the estimation of the output spectrum of the system in the frequency domain for 4 simulations for both  $y_1$  and  $y_2$  outputs

$$\begin{aligned}
 \hat{Y}_1^1(j\omega) &= \hat{Y}_{1,1}^1(j\omega) + \hat{Y}_{1,2}^1(j\omega) + \hat{Y}_{1,3}^1(j\omega) + \hat{Y}_{1,4}^1(j\omega) \\
 \hat{Y}_2^1(j\omega) &= \hat{Y}_{2,1}^1(j\omega) + \hat{Y}_{2,2}^1(j\omega) + \hat{Y}_{2,3}^1(j\omega) + \hat{Y}_{2,4}^1(j\omega) \\
 \\ 
 \hat{Y}_1^2(j\omega) &= \hat{Y}_{1,1}^2(j\omega) + \hat{Y}_{1,2}^2(j\omega) + \hat{Y}_{1,3}^2(j\omega) + \hat{Y}_{1,4}^2(j\omega) \\
 \hat{Y}_2^2(j\omega) &= \hat{Y}_{2,1}^2(j\omega) + \hat{Y}_{2,2}^2(j\omega) + \hat{Y}_{2,3}^2(j\omega) + \hat{Y}_{2,4}^2(j\omega) \\
 \\ 
 \hat{Y}_1^3(j\omega) &= \hat{Y}_{1,1}^3(j\omega) + \hat{Y}_{1,2}^3(j\omega) + \hat{Y}_{1,3}^3(j\omega) + \hat{Y}_{1,4}^3(j\omega) \\
 \hat{Y}_2^3(j\omega) &= \hat{Y}_{2,1}^3(j\omega) + \hat{Y}_{2,2}^3(j\omega) + \hat{Y}_{2,3}^3(j\omega) + \hat{Y}_{2,4}^3(j\omega) \\
 \\ 
 \hat{Y}_1^4(j\omega) &= \hat{Y}_{1,1}^4(j\omega) + \hat{Y}_{1,2}^4(j\omega) + \hat{Y}_{1,3}^4(j\omega) + \hat{Y}_{1,4}^4(j\omega) \\
 \hat{Y}_2^4(j\omega) &= \hat{Y}_{2,1}^4(j\omega) + \hat{Y}_{2,2}^4(j\omega) + \hat{Y}_{2,3}^4(j\omega) + \hat{Y}_{2,4}^4(j\omega)
 \end{aligned} \tag{4.39}$$

It is best to note that the value of OFRF "coefficients" are different for each outputs although the OFRF representation for the outputs are the same.

Then, the solution for the OFRF "coefficients" for output  $y_1$  can be determined as

$$\begin{aligned}
 \hat{P}_1(j\omega) &= \hat{Y}_{1,1}^1(j\omega) \\
 \begin{bmatrix} \hat{P}_{21}(j\omega) \\ \hat{P}_{22}(j\omega) \end{bmatrix} &= \begin{bmatrix} a_1 & b_1 \\ a_2 & b_2 \end{bmatrix}^{-1} \begin{bmatrix} \hat{Y}_{1,2}^1(j\omega) \\ \hat{Y}_{1,2}^2(j\omega) \end{bmatrix} \\
 \begin{bmatrix} \hat{P}_{31}(j\omega) \\ \hat{P}_{32}(j\omega) \\ \hat{P}_{33}(j\omega) \end{bmatrix} &= \begin{bmatrix} a_1^2 & a_1 b_1 & b_1^2 \\ a_2^2 & a_2 b_2 & b_2^2 \\ a_3^2 & a_3 b_3 & b_3^2 \end{bmatrix}^{-1} \begin{bmatrix} \hat{Y}_{1,3}^1(j\omega) \\ \hat{Y}_{1,3}^2(j\omega) \\ \hat{Y}_{1,3}^3(j\omega) \end{bmatrix} \\
 \begin{bmatrix} \hat{P}_{41}(j\omega) \\ \hat{P}_{42}(j\omega) \\ \hat{P}_{43}(j\omega) \\ \hat{P}_{43}(j\omega) \end{bmatrix} &= \begin{bmatrix} a_1^3 & a_1^2 b_1 & a_1 b_1^2 & b_1^3 \\ a_2^3 & a_2^2 b_2 & a_2 b_2^2 & b_2^3 \\ a_3^3 & a_3^2 b_3 & a_3 b_3^2 & b_3^3 \\ a_4^3 & a_4^2 b_4 & a_4 b_4^2 & b_4^3 \end{bmatrix}^{-1} \begin{bmatrix} \hat{Y}_{1,4}^1(j\omega) \\ \hat{Y}_{1,4}^2(j\omega) \\ \hat{Y}_{1,4}^3(j\omega) \\ \hat{Y}_{1,4}^4(j\omega) \end{bmatrix}
 \end{aligned} \tag{4.40}$$

whereas output  $y_2$  can be determined as

$$\begin{aligned}
 \hat{P}_1(j\omega) &= \hat{Y}_{2,1}^1(j\omega) \\
 \begin{bmatrix} \hat{P}_{21}(j\omega) \\ \hat{P}_{22}(j\omega) \end{bmatrix} &= \begin{bmatrix} a_1 & b_1 \\ a_2 & b_2 \end{bmatrix}^{-1} \begin{bmatrix} \hat{Y}_{2,2}^1(j\omega) \\ \hat{Y}_{2,2}^2(j\omega) \end{bmatrix} \\
 \begin{bmatrix} \hat{P}_{31}(j\omega) \\ \hat{P}_{32}(j\omega) \\ \hat{P}_{33}(j\omega) \end{bmatrix} &= \begin{bmatrix} a_1^2 & a_1 b_1 & b_1^2 \\ a_2^2 & a_2 b_2 & b_2^2 \\ a_3^2 & a_3 b_3 & b_3^2 \end{bmatrix}^{-1} \begin{bmatrix} \hat{Y}_{2,3}^1(j\omega) \\ \hat{Y}_{2,3}^2(j\omega) \\ \hat{Y}_{2,3}^3(j\omega) \end{bmatrix} \\
 \begin{bmatrix} \hat{P}_{41}(j\omega) \\ \hat{P}_{42}(j\omega) \\ \hat{P}_{43}(j\omega) \\ \hat{P}_{43}(j\omega) \end{bmatrix} &= \begin{bmatrix} a_1^3 & a_1^2 b_1 & a_1 b_1^2 & b_1^3 \\ a_2^3 & a_2^2 b_2 & a_2 b_2^2 & b_2^3 \\ a_3^3 & a_3^2 b_3 & a_3 b_3^2 & b_3^3 \\ a_4^3 & a_4^2 b_4 & a_4 b_4^2 & b_4^3 \end{bmatrix}^{-1} \begin{bmatrix} \hat{Y}_{2,4}^1(j\omega) \\ \hat{Y}_{2,4}^2(j\omega) \\ \hat{Y}_{2,4}^3(j\omega) \\ \hat{Y}_{2,4}^4(j\omega) \end{bmatrix}
 \end{aligned} \tag{4.41}$$

Using this new numerical method, the OFRF determined should give good estimation when  $50 \geq a \geq 125$  and  $150 \geq b \geq 300$ .

To prove the effectiveness of this approach, the OFRF determined was compared with the simulated output spectrum when  $a = 90$  and  $b = 240$ . Figure 4.3 shows the comparison of the amplitude of  $Y_1(j\omega)$  and  $\hat{Y}_1(j\omega)$  when  $a = 90$  and  $b = 240$  whereas Figure 4.4 shows the comparison of the amplitude of  $Y_2(j\omega)$  and  $\hat{Y}_2(j\omega)$  when  $a = 90$  and  $b = 240$ .

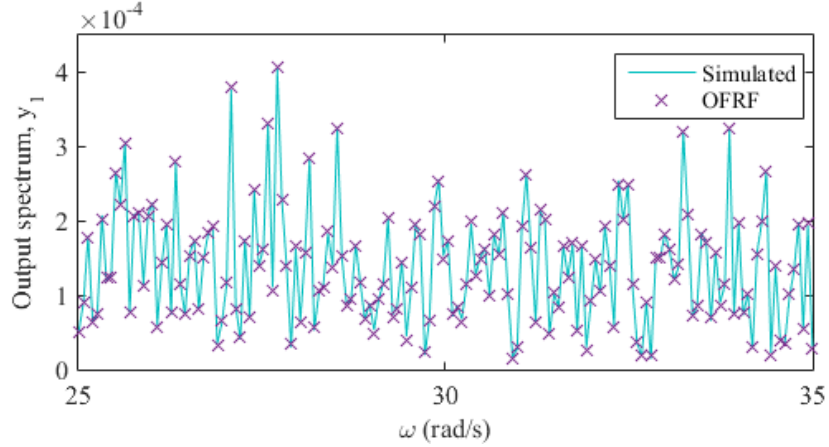


Figure 4.3: Comparison between the simulated output spectrum and the spectrum evaluated using OFRF for output  $y_1$  when  $a = 90$  and  $b = 240$ .

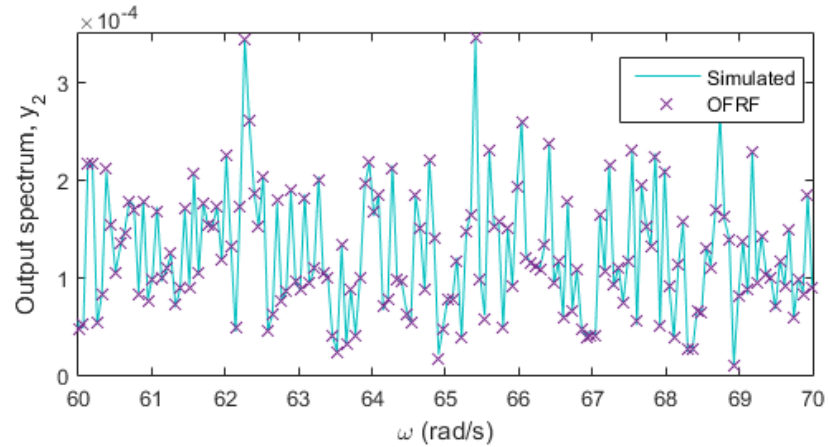


Figure 4.4: Comparison between the simulated output spectrum and the spectrum evaluated using OFRF for output  $y_2$  when  $a = 90$  and  $b = 240$ .

Comparing the two results from both simulated output spectrum and the spectrum evaluated using OFRF for the two outputs, it can be said that the output spectrum evaluated using OFRF is in excellent agreement to the simulated output spectrum. These results indicate that the new numerical method and algorithms discussed can be used to determine the OFRF of

the MIMO-NDE system correctly and efficiently. This will help in the analysis and design process of MIMO-NDE system too.

## 4.3 Application study in earthquake engineering

Nonlinear isolators can effectively protect buildings and bridges against the earthquakes [31]. In this subsection, how OFRF can be used in the earthquake engineering will be discussed. A building with a nonlinear building isolation system will be analysed. It will demonstrate the effectiveness of the new numerical method and how the OFRF based analysis can be applied to implement a design for application in earthquake engineering.

It will first present how to determine OFRF using the new numerical method for the determination of OFRF of MIMO nonlinear system. Then, using the OFRF determined, the relationship between the nonlinear parameters and the output frequency response will be presented to show how the results from the OFRF determination can be used in the design process.

### 4.3.1 The model of Sosokan building

The building that will be analyzed in this subsection is the Sosokan building, a nine-story university building at Keio University [22]. The building has nine level with seven floors above the ground and two basement floors. Figure 4.5 shows the picture of the Sosokan building.

For the OFRF based analysis, consider the equation of motion of the building system of the building at the Keio University [22] where it is given as

$$\mathbf{M}\ddot{\mathbf{x}} + \mathbf{C}\dot{\mathbf{x}} + \mathbf{K}\mathbf{x} = \mathbf{E}\mathbf{u} + \mathbf{F}\ddot{\mathbf{z}} \quad (4.42)$$



Figure 4.5: The picture of Sosokan bulding.

with

$$\mathbf{x} = [x_1 \quad x_2 \quad \dots \quad x_{10}]^T$$

$$\mathbf{M} = \text{diag}(m_1 \quad m_2 \quad \dots \quad m_{10})$$

$$\mathbf{C} = \begin{bmatrix} c_1 + c_2 & -c_2 & \cdots & 0 & 0 \\ -c_2 & c_2 + c_3 & \cdots & \cdots & 0 \\ \vdots & \vdots & \ddots & \vdots & \vdots \\ 0 & \cdots & \cdots & c_9 + c_{10} & -c_{10} \\ 0 & 0 & \cdots & -c_{10} & c_{10} \\ k_1 + k_2 & -k_2 & \cdots & 0 & 0 \\ -k_2 & k_2 + k_3 & \cdots & \cdots & 0 \\ \vdots & \vdots & \ddots & \vdots & \vdots \\ 0 & \cdots & \cdots & k_9 + k_{10} & -k_{10} \\ 0 & 0 & \cdots & -k_{10} & k_{10} \end{bmatrix} \quad (4.43)$$

$$\mathbf{E} = [1 \quad 0 \quad \dots \quad 0]^T$$

$$\mathbf{F} = [-m_1 \quad -m_2 \quad \dots \quad -m_{10}]^T$$

where **M**, **C**, and **K** are the mass, damping and stiffness matrices for the building systems respectively, and **x**, **u**, and  $\ddot{z}$  are the displacement vector, control force and ground acceleration, respectively.

The input, which is the ground acceleration used for this analysis is the data from the wave of the main shock of the 2011 Great East Japan Earthquake [22]. Figure 4.6 shows the input wave of the main shock. Only the data from  $t = 0\text{s}$  to  $t = 60\text{s}$  will be use in this analysis.

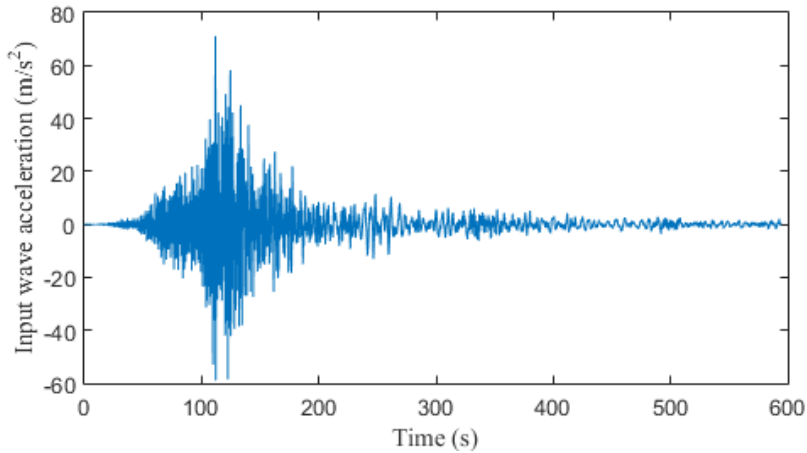


Figure 4.6: The main shock of the 2011 Great East Japan Earthquake.

This system is a single input multi output NDE system where the nonlinearity is in the control force which will be introduced later and it uses one input, the ground acceleration and generates ten outputs. For this analysis, the control force of the system is described as

$$u = (C_1 + C_2 x_1^2) \dot{x}_1 + (K_1 + K_2 x_1^2) x_1 \quad (4.44)$$

which was the damping and stiffness functions of the nonlinear passive isolators.  $C_1$  and  $K_1$  are constants whereas  $C_2$  and  $K_2$  are the parameters that will be investigated in this analysis. The value of  $C_1$  and  $K_1$  are define in the table 4.2 below.

Table 4.2: Value of  $C_1$  and  $K_1$  used in the analysis.

Parameters	Value
$C_1$	$10 \times 10^3$
$K_1$	$10 \times 10^3$

Table 4.3 shows the structural parameters value of the building systems.

Table 4.3: Structural parameters of the building at the Keio University

Floor	Mass $\times 10^6$ kg	Stiffness $\times 10^6$ N/m	Damping $\times 10^6$ Ns/m
RF	2.4999	999.6	8.0487
7F	2.0664	1156.4	9.3110
6F	2.0371	1381.8	11.126
5F	2.0369	1568.0	12.625
4F	2.0500	1813.0	14.598
3F	2.0331	1803.2	14.520
2F	1.8264	1979.6	15.940
1F	2.4906	2763.6	22.252
B1F	3.4382	2273.6	18.306
B2F	4.9814	66.836	0

The nonlinearity of this system is from the nonlinear building isolation system that was installed at the lowest level. Figure 4.7 shows the schematic of the nine levels building at the Keio University with the nonlinear building isolation system installed at the lowest level.

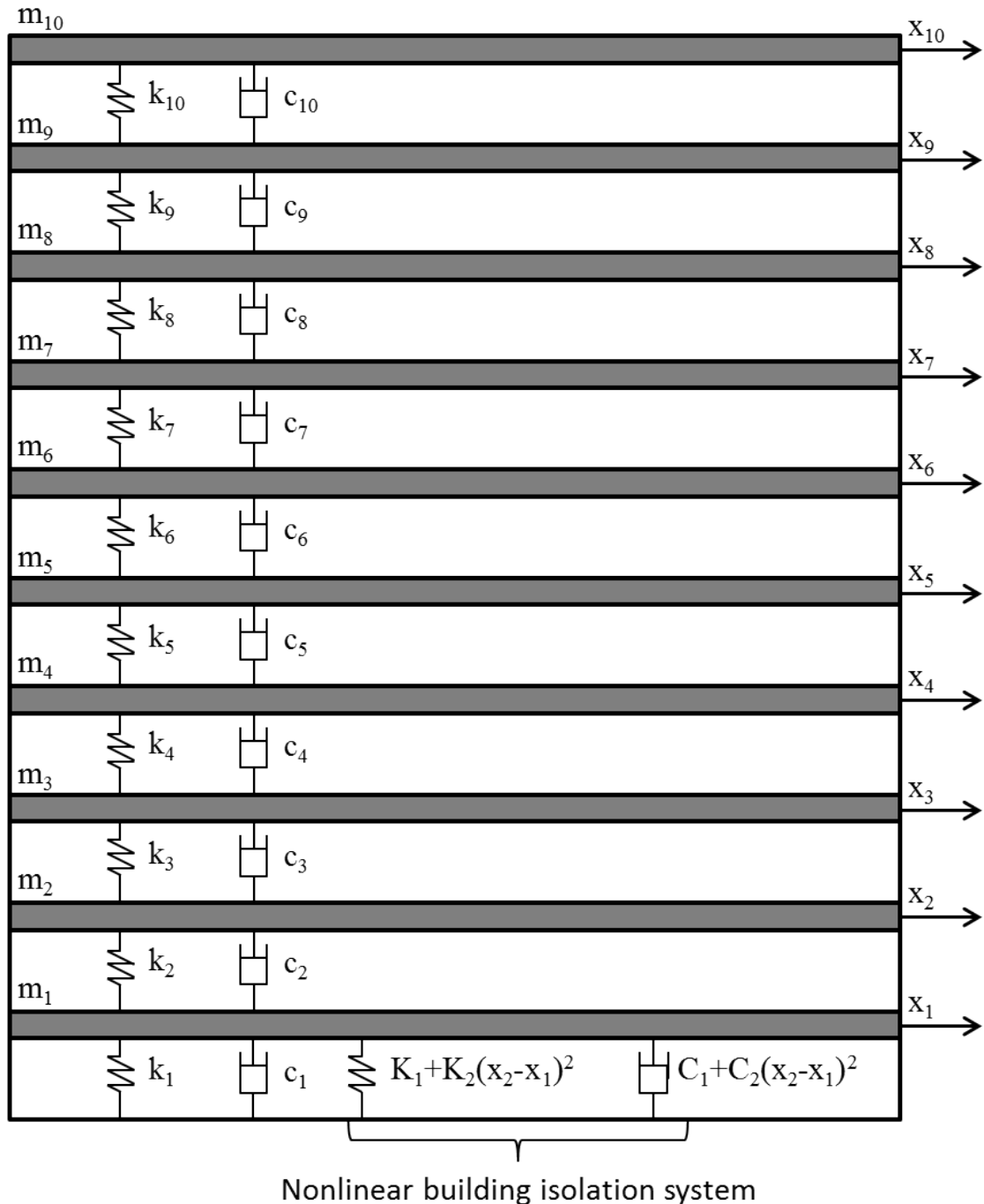


Figure 4.7: The schematic of the building with the nonlinear building isolation system.

### 4.3.2 OFRF representation of the Sosokan building

To determine the OFRF representation, the characteristic parameter vector of the system up to the fifth order can be determined by using the parametric characteristics analysis, where

$$\begin{aligned}\mathbf{M}_1 &= [1] \\ \mathbf{M}_2 &= \text{null} \\ \mathbf{M}_3 &= [C_2, K_2] \\ \mathbf{M}_4 &= \text{null} \\ \mathbf{M}_5 &= [C_2^2, C_2K_2, K_2^2]\end{aligned}\tag{4.45}$$

The second order and fourth order characteristic parameter vector are null because there is no even order monomials in this system. Then, using the result from the parametric characteristic analysis, the OFRF representation of the system for each outputs  $i$ , where  $i = 1, 2, \dots, 10$  can be written as

$$\hat{Y}_i(j\omega) = \hat{P}_1(j\omega) + C_2 \hat{P}_{31}(j\omega) + K_2 \hat{P}_{32}(j\omega) + C_2^2 \hat{P}_{51}(j\omega) + C_2 K_2 \hat{P}_{52}(j\omega) + K_2^2 \hat{P}_{53}(j\omega)\tag{4.46}$$

The OFRF representation is the same for all outputs but the value of the OFRF "coefficients" are independent to the outputs.

### 4.3.3 ALEs derivation of the Sosokan building

The derivation of ALEs for this system is described in Appendix A. From the ALEs determined, the estimation of the outputs signal and the outputs spectrum for the system up to 5th-order for each outputs  $i, i = 1, 2, \dots, 10$  thus can be written as

$$\hat{y}_i(t) = \hat{y}_{i,1}(t) + \hat{y}_{i,3}(t) + \hat{y}_{i,5}(t)\tag{4.47}$$

and

$$\hat{Y}_i(j\omega) = \hat{Y}_{i,1}(j\omega) + \hat{Y}_{i,3}(j\omega) + \hat{Y}_{i,5}(j\omega) \quad (4.48)$$

#### 4.3.4 Determination of OFRF using ALEs

From equation (4.47) - (4.48) analysis, it can be understood that only three sets of ALEs simulations using different combinations of  $C_2$  and  $K_2$  were needed to determine the OFRF of this system. Table 4.4 shows the combinations of  $C_2$  and  $K_2$  used in the three simulations. From the three simulations, the solution for the OFRF "coefficients" for each outputs,  $y_i$

Table 4.4: Value of  $C_2$  and  $K_2$  used in the two simulations

Simulation, v	$C_2$	$K_2$
1	$5 \times 10^6$	$4 \times 10^6$
2	$7 \times 10^6$	$8 \times 10^6$
3	$9 \times 10^6$	$12 \times 10^6$

where  $i = 1, 2, \dots, 10$  which corresponds to each floor can be determined as

$$\begin{aligned} \hat{P}_1(j\omega) &= \hat{Y}_{i,1}^1(j\omega) \\ \begin{bmatrix} \hat{P}_{31}(j\omega) \\ \hat{P}_{32}(j\omega) \end{bmatrix} &= \begin{bmatrix} C_{2,1} & K_{2,1} \\ C_{2,2} & K_{2,2} \end{bmatrix}^{-1} \begin{bmatrix} \hat{Y}_{i,2}^1(j\omega) \\ \hat{Y}_{i,2}^2(j\omega) \end{bmatrix} \\ \begin{bmatrix} \hat{P}_{51}(j\omega) \\ \hat{P}_{52}(j\omega) \\ \hat{P}_{53}(j\omega) \end{bmatrix} &= \begin{bmatrix} C_{2,1}^2 & C_{2,1}K_{2,1} & K_{2,1}^2 \\ C_{2,2}^2 & C_{2,2}K_{2,2} & K_{2,2}^2 \\ C_{2,3}^2 & C_{2,3}K_{2,3} & K_{2,3}^2 \end{bmatrix}^{-1} \begin{bmatrix} \hat{Y}_{i,3}^1(j\omega) \\ \hat{Y}_{i,3}^2(j\omega) \\ \hat{Y}_{i,3}^3(j\omega) \end{bmatrix} \end{aligned} \quad (4.49)$$

It is best to note that the value of OFRF "coefficients" are different for each outputs although the OFRF representation for the outputs are the same. For a better understanding, the OFRF

of the system for each outputs can be written using (4.46) as

$$\begin{aligned}
 \hat{Y}_1(j\omega) &= \hat{P}_1(j\omega) + C_2 \hat{P}_{31}(j\omega) + K_2 \hat{P}_{32}(j\omega) + C_2^2 \hat{P}_{51}(j\omega) + C_2 K_2 \hat{P}_{52}(j\omega) + K_2^2 \hat{P}_{53}(j\omega) \\
 \hat{Y}_2(j\omega) &= \hat{P}_1(j\omega) + C_2 \hat{P}_{31}(j\omega) + K_2 \hat{P}_{32}(j\omega) + C_2^2 \hat{P}_{51}(j\omega) + C_2 K_2 \hat{P}_{52}(j\omega) + K_2^2 \hat{P}_{53}(j\omega) \\
 \hat{Y}_3(j\omega) &= \hat{P}_1(j\omega) + C_2 \hat{P}_{31}(j\omega) + K_2 \hat{P}_{32}(j\omega) + C_2^2 \hat{P}_{51}(j\omega) + C_2 K_2 \hat{P}_{52}(j\omega) + K_2^2 \hat{P}_{53}(j\omega) \\
 &\vdots \\
 \hat{Y}_9(j\omega) &= \hat{P}_1(j\omega) + C_2 \hat{P}_{31}(j\omega) + K_2 \hat{P}_{32}(j\omega) + C_2^2 \hat{P}_{51}(j\omega) + C_2 K_2 \hat{P}_{52}(j\omega) + K_2^2 \hat{P}_{53}(j\omega) \\
 \hat{Y}_{10}(j\omega) &= \hat{P}_1(j\omega) + C_2 \hat{P}_{31}(j\omega) + K_2 \hat{P}_{32}(j\omega) + C_2^2 \hat{P}_{51}(j\omega) + C_2 K_2 \hat{P}_{52}(j\omega) + K_2^2 \hat{P}_{53}(j\omega)
 \end{aligned} \tag{4.50}$$

where the value of OFRF "coefficients",  $\hat{P}_1(j\omega)$ ,  $\hat{P}_{31}(j\omega)$ ,  $\hat{P}_{32}(j\omega)$ ,  $\hat{P}_{51}(j\omega)$ ,  $\hat{P}_{52}(j\omega)$  and  $\hat{P}_{53}(j\omega)$  are different for each outputs and  $\hat{Y}_1(j\omega)$  refers to the outputs for floor B2F and  $\hat{Y}_{10}(j\omega)$  refers to the outputs for floor RF.

#### 4.3.5 The results and analysis

Then using the OFRF determined, different values of  $C_2$  and  $K_2$  had been tested with the OFRF determined and the results were compared with the simulated output spectrum. Figure 4.8 shows the comparison of the amplitude of  $Y_1(j\omega)$  and  $\hat{Y}_1(j\omega)$  when  $C_2 = 120 \times 10^5$  and  $K_2 = 40 \times 10^5$  for odd floors. The comparison for the even floors between the amplitude of  $Y_1(j\omega)$  and  $\hat{Y}_1(j\omega)$  when  $C_2 = 120 \times 10^5$  and  $K_2 = 40 \times 10^5$  are in the Appendix B.

Comparing the results from both simulated output spectrum and the spectrum evaluated using OFRF in 4.8 for each outputs of the odd floors, it can be said that the output spectrums evaluated using OFRF are in excellent agreement to the simulated output spectrum. These results indicate that the new numerical method and algorithms discussed can be used to determine the OFRF of the MIMO-NDE system correctly and efficiently.

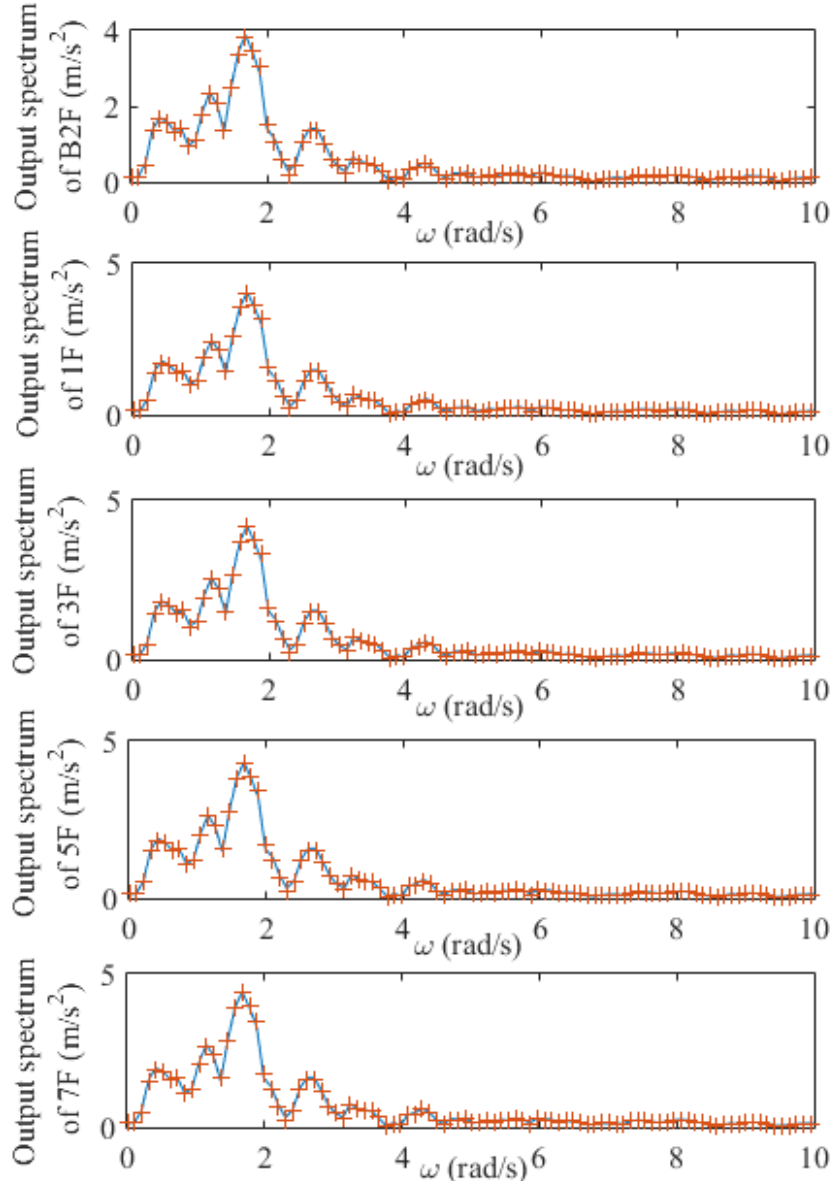


Figure 4.8: Comparison between the simulated output spectrum and the spectrum evaluated using OFRF for the odd floors when  $C_2 = 120 \times 10^5$  and  $K_2 = 40 \times 10^5$ .

From the OFRF determined, the design of the system parameters  $C_2$  and  $K_2$  can be performed efficiently as the OFRF shows the relationship between the nonlinear parameters and the output frequency response. Figure 4.9 shows the OFRF based relationship between the parameters  $C_2$  and  $K_2$  and magnitude of the output spectrum at 1.6755 rad/s frequency for the 5F Floor.

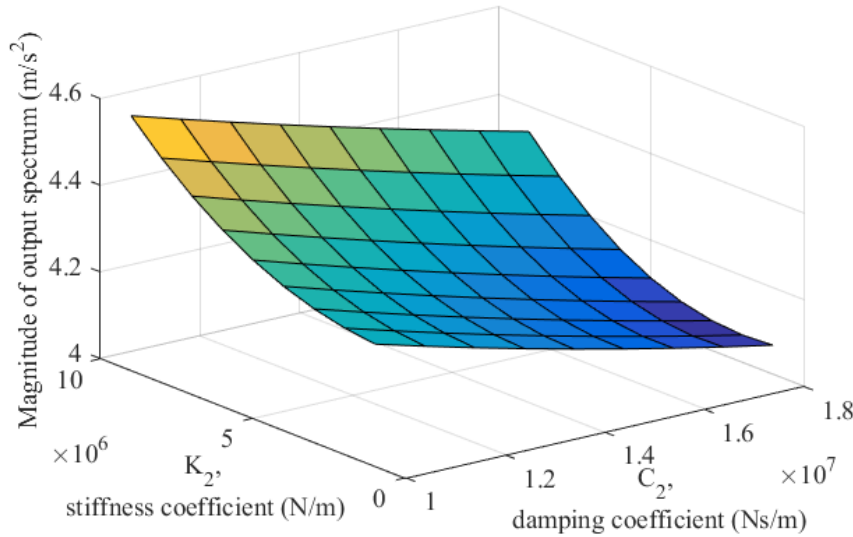


Figure 4.9: The relationship between the parameters,  $C_2$  and  $K_2$  and magnitude of the output spectrum at 1.6755 rad/s frequency for the 5F floor.

Figure 4.9 shows that the relationship is nonlinear. When comparing with the OFRF determined for the 5F floor, which is as follows

$$\hat{Y}_7(j\omega) = \hat{P}_1(j\omega) + C_2 \hat{P}_{31}(j\omega) + K_2 \hat{P}_{32}(j\omega) + C_2^2 \hat{P}_{51}(j\omega) + C_2 K_2 \hat{P}_{52}(j\omega) + K_2^2 \hat{P}_{53}(j\omega) \quad (4.51)$$

it shows that as the relationship is nonlinear, the value of OFRF "coefficients",  $\hat{P}_{51}(j\omega)$ ,  $\hat{P}_{52}(j\omega)$  and  $\hat{P}_{53}(j\omega)$  are significant unlike the case studied in previous chapter. The relationship shown on Figure 4.9 is useful for designing process of the nonlinear building isolation system. In addition, the relationship between the nonlinear parameters and the output frequency response for other floors can be done using the OFRF determined.

## 4.4 Conclusion

In this chapter, the full process of determining OFRF for MIMO nonlinear system using ALEs was presented. This allows OFRF, which reveals a significant link between the system output frequency response and the parameters that define the system nonlinearity to be

determined in more efficiently in a MIMO-NDE engineering system. The concepts in the new numerical method discussed in the previous chapter are extended in this chapter for the MIMO nonlinear system. Three algorithms were derived and developed using the same concept and techniques as in the previous chapter.

The first algorithm to derive the OFRF representation of the output spectrum of the system to any inputs were derived for MIMO nonlinear system in presented in Section 4.2.2.1. Next, the algorithm to determine ALEs for SISO nonlinear systems that can be described by the NDE model are extended to the MIMO system using the same techniques as in previous chapter, Section 3.2.3.2. Then, the relationship between the OFRF representation and the ALEs is used for the determination of OFRF for the MIMO-NDE system. An algorithm to determine the OFRF using the ALEs were presented in Section 4.2.4.1. Using the OFRF determined, the analysis and design of nonlinear systems can be done efficiently.

As a conclusion, the new numerical method introduced in this chapter provides a better way for the analysis of MIMO nonlinear system and can be used to a wide area of engineering. It can help in the frequency domain analysis on how the system behaviours affected by the nonlinear parameter and in the design of the parameters to achieve desired system output frequency responses. The new numerical method presented in this chapter will be used in the analysis of non-isothermal Continuous Stirred Tank Reactor (CSTR) in the next chapter.

# **Chapter 5**

## **Application of OFRF in non-isothermal Continuous Stirred Tank Reactor (CSTR)**

### **5.1 Introduction**

Application of the OFRF can be used in many engineering fields. In this chapter, an application of OFRF in chemical engineering will be discussed to show how this new numerical method in determining OFRF is useful in the chemical engineering area. It will be focusing on the periodic operation of a nonlinear non-isothermal continuous stirred tank reactor (CSTR). CSTR is one of the main types of reactors in chemical process engineering. The CSTR in this analysis will be tested with periodic modulation input. The advantage of periodic modulation of one or more inputs compared to the optimal steady-state operation is it can give better average performance thus improved selectivity and increased conversion of the reactant.

As this new numerical method needs to have the nonlinear model to be defined by the NDE,

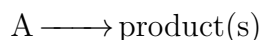
the first step to determine the OFRF of the nonlinear system is to define the mathematical model of the nonlinear non-isothermal CSTR. Then, the new numerical method discussed in the previous chapter is implemented into the non-isothermal CSTR system, and OFRF of the system can be determined. The effectiveness of the new numerical method in determining the OFRF using ALEs is proved with numerical simulations. From the OFRF determined with the new numerical method, a relationship between the parameters that define the system nonlinearity and the output frequency response is revealed.

In this analysis, the OFRF based analysis was done. Using the output spectrums generated from the OFRF determined, the average value of the output spectrum was determined. Then, the mean value of both outputs of the systems; outlet concentration of the reactant and the temperature of the reactor was compared with the numerical simulation results. The results also proved that periodic modulation input provides a better average performance compared to the steady-state operation. Also, this OFRF based analysis provide a new insight and understanding to the nonlinear chemical control because the current literature method only reveals the relationship between the input and output of the nonlinear system.

## 5.2 Implementation of the OFRF into the nonlinear non-isothermal CSTR

### 5.2.1 Mathematical model of a nonlinear non-isothermal CSTR

In this subsection, the mathematical model of a nonlinear non-isothermal CSTR with periodically operated input and homogeneous nth order reaction is modelled. Consider a simple reaction



where a homogeneous n-th order reaction takes place [55]. The rate law is

$$r = k_0 e^{\frac{E_A}{RT}} c_A^n \quad (5.1)$$

where  $c_A$  is the reactant concentration,  $T$  is the temperature,  $E_A$  is the activation energy,  $k_0$  is the preexponential factor in the Arrhenius equation and  $R$  is the universal gas constant.

For the analysis of the nonlinear nonisothermal CSTR, the material balance for the reactant A can be written as

$$V \frac{dc_A}{dt} = F c_{A,in} - F c_A - k_0 e^{-\frac{E_A}{RT}} c_A^n V \quad (5.2)$$

and the energy balance can be written as

$$V \rho c_p \frac{dT}{dt} = F \rho c_p T_{in} - F \rho c_p T + (-\Delta H_R) k_0 e^{-\frac{E_A}{RT}} c_A^n V - U A_w (T - T_j) \quad (5.3)$$

where  $t$  is the time,  $F$  is the volumetric flow rate of the reaction stream,  $V$  is the volume of the CSTR reactor,  $\Delta H_R$  is the heat of reaction,  $A_w$  is the surface area of the heat exchanger,  $U$  is the overall heat transfer coefficient,  $\rho$  is the density and  $c_p$  is the specific heat capacity. There are two subscripts used in the equation, the subscript *in* is for the inlet and the subscript *j* is for the heating/cooling fluid in the reactor jacket.

There are several assumptions made in this analysis:

1. The CSTR reactor is well mixed and is at steady state.
2. The volume,  $V$  is constant where the inlet and outlet flow rates are equal.
3. All physical and chemical properties are independent of temperature.

As the CSTR reactor is considered to be at steady state, the material and energy balances are given with the following expressions:

$$\frac{c_{Ain,s}}{c_{A,s}} = 1 + k_0 e^{-\frac{E_A}{RT_s}} c_{A,s}^{n-1} \frac{V}{F_s} \quad (5.4)$$

$$\frac{T_{in,s}}{T_s} = 1 - \frac{(-\Delta H_R) k_0 e^{-\frac{E_A}{RT_s}} c_{A,s}^n V}{\rho c_p T_s} \frac{V}{F_s} + \frac{U A_w}{\rho c_p} - \frac{U A_w T_{j,s}}{\rho c_p T_s} \quad (5.5)$$

For simplification, the following parameters which is in functions of the physical parameters of the reactor and steady state will be introduced:

$$\begin{aligned} \alpha &= k_0 e^{-\frac{E_A}{RT_s}} c_{A,s}^{n-1} \frac{V}{F_s} \\ \beta &= \frac{(-\Delta H_R) k_0 e^{-\frac{E_A}{RT_s}} c_{A,s}^n V}{\rho c_p T_s} \frac{V}{F_s} \\ \gamma &= \frac{E_A}{RT_s} \\ \delta &= \frac{U A_w T_{j,s}}{\rho c_p T_s} \\ St &= \frac{U A_w}{F_s \rho c_p T_s} \end{aligned} \quad (5.6)$$

Then, all variables are changed to dimensionless forms for the purpose of frequency domain analysis. The definitions of all the dimensionless variables are as written in Table 5.1 where they show their relatives derivations from the steady state values.

Using all these parameters and the dimensionless variables, the material balance for the reactant A and the energy balance in (5.2)-(5.3) can be written

$$\begin{aligned} \frac{dC}{d\tau} &= (1 + \alpha)(\Phi + 1)(C_{in} + 1) - (\Phi + 1)(C + 1) - k_0 e^{-\frac{E_A}{RT_s(\theta+1)}} c_{A,s}^{n-1} \frac{V}{F_s} (1 + C)^n \\ \frac{d\theta}{d\tau} &= (1 + \beta + St - \delta)(\Phi + 1)(\theta_{in} + 1) - (\Phi + 1)(\theta + 1) - St(\theta + 1) + \delta(\theta_J + 1) \\ &\quad - \frac{\Delta H_R k_0 c_{A,s}^n V}{\rho c_p T_s F_s} e^{-\frac{E_A}{RT_s(\theta+1)}} (1 + C)^n \end{aligned} \quad (5.7)$$

Table 5.1: Definitions of the dimensionless variables.

Variable Name	Dimensionless form
Time	$\tau = \frac{t}{V/F_s}$
Frequency	$\omega = \omega_d \frac{V}{F_s}$
Inlet concentration of the reactant	$C_{in} = \frac{c_{A,in} - c_{Ain,s}}{c_{Ain,s}}$
Volumetric flow rate of the stream	$\Phi = \frac{F - F_s}{F_s}$
Outlet concentration of the reactant	$C = \frac{c_A - c_{A,s}}{c_{A,s}}$
Inlet temperature	$\theta_i = \frac{T_{in} - T_{in,s}}{T_{in,s}}$
Temperature in the CSTR	$\theta = \frac{T - T_s}{T_s}$
Temperatur of the heating or cooling fluid	$\theta_j = \frac{T_j - T_{j,s}}{T_{j,s}}$

The inlet concentration of the reactant,  $C_{in}$  is the periodic input of this system where its equation can be written as

$$C_{in} = 0.2(\cos(15t) - \cos(7t)), t \in (0, 20) \quad (5.8)$$

and Figure 5.1 shows the frequency for the inlet concentration of the reactant,  $C_{in}$

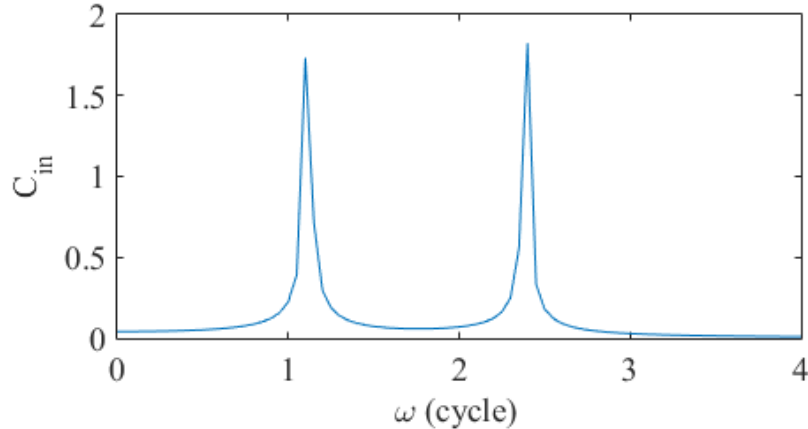


Figure 5.1: The frequency of the inlet concentration of the reactant,  $C_{in}$ .

To use this model in the new numerical method proposed in Chapter 4 of this thesis, the equation will be transform to Nonlinear Differential Equation(NDE) model where all the nonlinearities are in the polynomial form. The nonlinear terms will be expanding in the

Taylor series form. The Taylor series expansions for the nonlinear terms up to second order are

$$\begin{aligned}
 e^{-\frac{E_A}{RT_s(\theta+1)}} &= e^{-\frac{E_A}{RT_s}} + \theta \frac{E_A}{RT_s} e^{-\frac{E_A}{RT_s}} + \theta^2 \frac{-E_A}{RT_s} e^{-\frac{E_A}{RT_s}} + \frac{\theta^2}{2} \frac{-E_A}{RT_s} e^{-\frac{E_A}{RT_s}} + \dots \\
 &= e^{-\gamma} + \theta \gamma e^{-\gamma} - \theta^2 \gamma e^{-\gamma} + \frac{\theta^2}{2} \gamma e^{-\gamma} + \dots \\
 &= e^{-\gamma} (1 + \theta \gamma - \theta^2 \gamma + \frac{\theta^2}{2} \gamma + \dots) \\
 (1+C)^n &= 1 + nC + \frac{1}{2} n(n-1)C^2 + \dots \\
 (1+C)^n e^{-\frac{E_A}{RT_s(\theta+1)}} &= e^{-\gamma} (1 + \theta \gamma - \theta^2 \gamma + \frac{\theta^2}{2} \gamma + nC + nC\theta\gamma + \frac{1}{2} n(n-1)C^2 + \dots)
 \end{aligned} \tag{5.9}$$

and (5.7) are formed into

$$\begin{aligned}
 \frac{dC}{d\tau} &= (1+\alpha)(\Phi+1)(C_{in}+1) - (\Phi+1)(C+1) - \alpha \left( 1 + \theta \gamma - \theta^2 \gamma + \frac{\theta^2}{2} \gamma + nC + nC\theta\gamma + \frac{1}{2} n(n-1)C^2 \right) \\
 \frac{d\theta}{d\tau} &= (1+\beta+St-\delta)(\Phi+1)(\theta_{in}+1) - (\Phi+1)(\theta+1) - St(\theta+1) + \delta(\theta_J+1) \\
 &\quad - \beta \left( 1 + \theta \gamma - \theta^2 \gamma + \frac{\theta^2}{2} \gamma + nC + nC\theta\gamma + \frac{1}{2} n(n-1)C^2 \right)
 \end{aligned} \tag{5.10}$$

Expanding (5.10) and representing in the (4.1) form enables the coefficients for both subsystem to be determined easier.

$$\begin{aligned}
 \frac{dC}{d\tau} - \left( 1 + \alpha\Phi + \alpha + \Phi \right) C_{in} - \left( \alpha\Phi + \Phi - \alpha \right) - \left( \Phi + 1 - \alpha n \right) C + \alpha\gamma\theta \\
 + \alpha\gamma nC\theta + \alpha \frac{1}{2} n(n-1)C^2 + \left( \alpha\gamma - \alpha \frac{\gamma}{2} \right) \theta^2 &= 0 \\
 \frac{d\theta}{d\tau} - \left( \Phi + \Phi\beta + \Phi St - \Phi\delta \right) \theta_{in} - \left( \Phi\beta + \Phi St - \Phi\delta + \delta\theta_J \right) + \beta nC \\
 + \left( \Phi + 1 + St - \beta\gamma \right) \theta + \beta\gamma nC\theta - \left( \frac{\gamma}{2} - \gamma \right) \beta\theta^2 + \beta \frac{1}{2} n(n-1)C^2 &= 0
 \end{aligned} \tag{5.11}$$

The coefficients for the first subsystem are

$$\begin{aligned}
 c_{1,0}^1(1 : 1) &= 1, \\
 c_{1,0}^1(1 : 0) &= -\left(\Phi + 1 - \alpha n\right), \\
 c_{1,0}^2(1 : 0) &= \alpha\gamma, \\
 c_{2,0}^{1,1}(1 : 0, 0) &= \alpha\frac{1}{2}n(n-1), \\
 c_{2,0}^{1,2}(1 : 0, 0) &= \alpha\gamma n, \\
 c_{2,0}^{2,2}(1 : 0, 0) &= \alpha\gamma - \alpha\frac{\gamma}{2}, \\
 c_{0,1}^1(1 : 0) &= -\left(1 + \alpha\Phi + \alpha + \Phi\right)
 \end{aligned} \tag{5.12}$$

and the coefficients for the second subsystem are

$$\begin{aligned}
 c_{1,0}^2(2 : 1) &= 1, \\
 c_{1,0}^2(2 : 0) &= \Phi + 1 + St - \beta\gamma, \\
 c_{1,0}^1(2 : 0) &= \beta n, \\
 c_{2,0}^{1,1}(2 : 0, 0) &= \beta\frac{1}{2}n(n-1), \\
 c_{2,0}^{1,2}(2 : 0, 0) &= \beta\gamma n, \\
 c_{2,0}^{2,2}(2 : 0, 0) &= -\beta\left(\frac{\gamma}{2} - \gamma\right), \\
 c_{0,1}^2(2 : 0) &= -\left(\Phi + \Phi\beta + \Phi St - \Phi\delta\right)
 \end{aligned} \tag{5.13}$$

In this analysis, the values of all the model parameters used in the rest of the chapter are listed in (5.2) which defined an exothermic first order reaction and were taken from [49],[55].

From the parameters, the steady state solution that exists are  $c_{A,s} = 0.3466\text{kmol}/\text{m}^3$  and  $T_s = 388K$ . However, this steady state is not optimum. These values also had been tested with the stability analysis [55] and was found stable. It is important to determine if the system is a stable system as OFRF only works for stable system.

Table 5.2: Value for the physical parameters

Parameter	Value	Units
Reaction order, $n$	1	
Volume of the reactor, $V$	1	$m^3$
Preexponential factor of the reaction rate constant, $k_0$	$1 \times 10^{10}$	$1/min$
Activation energy, $E_A$	69 256	$kJ/kmol$
Heat of reaction, $\delta H_R$	-543 920	$kJ/kmol$
Heat of capacity, $\rho c_p$	$4.184 \times 10^3$	$kJ/K/m^3$
Steady state inlet concentration, $c_{A,i,s}$	2	$kmol/m^3$
Steady state inlet temperature, $T_{i,s}$	323	$K$
Steady state temperature of the coolant, $T_{i,s}$	365	$K$
Overall heat transfer coefficient, $U$	160	$W/m^2/K$
Surface area for heat exchange, $A_w$	240	$m^2$

The parameter of interest in this analysis is the steady state flow-rate,  $F_s$ . As a note, all the values discussed in this subsection will be used throughout the analysis in this chapter. For a better understanding of the system, Figure 5.2 shows the nonlinear nonisothermal CSTR with the a) dimensional parameters and b) dimensionless parameters.

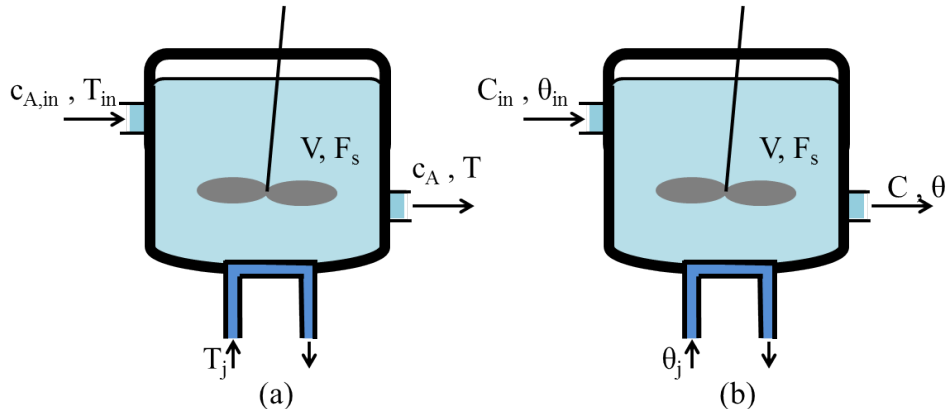


Figure 5.2: The nonlinear nonisothermal CSTR with the a) dimensional parameters and b) dimensionless parameters.

## 5.2.2 Output Frequency Response Functions(OFRF) representation for nonlinear non-isothermal CSTR

The next crucial step in this analysis is to determine OFRF representation for the nonlinear non-isothermal CSTR using the algorithm discussed in Section 4.2.2.1. Recall that OFRF is about the relationship between parameter that define the system nonlinearity and the outputs. However, in this system, the parameters define both the system linearity and nonlinearity. An assumption was made where the effect of the parameter of interest on the linear part has only small effect on the nonlinear system.

To determine the OFRF representation, first, the characteristic parameter vector of the system up to the third order can be determined by using the parametric characteristics analysis that was discussed in Chapter 4. The parameter of interest in this analysis is the steady state flow rate of the reaction,  $F_s$ . The result of parametric characteristics analysis of the systems are

$$\mathbf{M}_1 = [1] \quad \mathbf{M}_2 = \left[ \frac{1}{F_s} \right] \quad \mathbf{M}_3 = \left[ \frac{1}{F_s^2} \right] \quad (5.14)$$

Then, using the result from the parametric characteristic analysis, the OFRF representation of the system for each outputs can be written as

$$\begin{aligned} \hat{C}(j\omega) &= \hat{P}_{11}(j\omega) + \left[ \frac{1}{F_{s,nl}} \right] \hat{P}_{21}(j\omega) + \left[ \frac{1}{F_{s,nl}^2} \right] \hat{P}_{31}(j\omega) \\ \hat{\theta}(j\omega) &= \hat{P}_{11}(j\omega) + \left[ \frac{1}{F_{s,nl}} \right] \hat{P}_{21}(j\omega) + \left[ \frac{1}{F_{s,nl}^2} \right] \hat{P}_{31}(j\omega) \end{aligned} \quad (5.15)$$

The OFRF representation is the same for all outputs but the value of the OFRF "coefficients" are independent to the outputs. The value of the OFRF "coefficients" can be determined using the ALE that is derived in the next section.

### 5.2.3 Derivation of Associated Linear Equations(ALEs) for nonlinear non-isothermal CSTR

Chapter 4 has provided an algorithm to determine ALE for MIMO-NDE model in subsection 4.2.3.1. Using that algorithm, the ALEs for the nonlinear non-isothermal CSTR is derived. Rewritten (5.11) again for a better understanding of the process in this section.

$$\begin{aligned} \frac{dC}{d\tau} - & \left(1 + \alpha\Phi + \alpha + \Phi\right)C_{in} - \left(\alpha\Phi + \Phi - \alpha\right) - \left(\Phi + 1 - \alpha n\right)C + \alpha\gamma\theta \\ & + \alpha\gamma nC\theta + \alpha\frac{1}{2}n(n-1)C^2 + \left(\alpha\gamma - \alpha\frac{\gamma}{2}\right)\theta^2 = 0 \\ \frac{d\theta}{d\tau} - & \left(\Phi + \Phi\beta + \Phi St - \Phi\delta\right)\theta_{in} - \left(\Phi\beta + \Phi St - \Phi\delta + \delta\theta_J\right) + \beta nC \\ & + \left(\Phi + 1 + St - \beta\gamma\right)\theta + \beta\gamma nC\theta - \left(\frac{\gamma}{2} - \gamma\right)\beta\theta^2 + \beta\frac{1}{2}n(n-1)C^2 = 0 \end{aligned} \quad (5.16)$$

where

$$\begin{aligned} \alpha &= k_0 e^{-\frac{E_A}{RT_s}} c_{A,s}^{n-1} \frac{V}{F_s} \\ \beta &= \frac{(-\Delta H_R)k_0 e^{-\frac{E_A}{RT_s}} c_{A,s}^n V}{\rho c_p T_s} \frac{V}{F_s} \\ \gamma &= \frac{E_A}{RT_s} \\ \delta &= \frac{UA_w T_{j,s}}{\rho c_p T_s} \\ St &= \frac{UA_w}{F_s \rho c_p T_s} \end{aligned}$$

Next, rewrite (5.16) in the different form as (4.22)

$$\begin{aligned} D^1 C(\tau) - & \left(1 + \alpha\Phi + \alpha + \Phi\right)C_{in}(\tau) - \left(\alpha\Phi + \Phi - \alpha\right) - \left(\Phi + 1 - \alpha n\right)C(\tau) + \alpha\gamma\theta(\tau) \\ & + \alpha\gamma nC(\tau)\theta(\tau) + \alpha\frac{1}{2}n(n-1)C(\tau)^2 + \left(\alpha\gamma - \alpha\frac{\gamma}{2}\right)\theta(\tau)^2 = 0 \\ D^1 \theta(\tau) - & \left(\Phi + \Phi\beta + \Phi St - \Phi\delta\right)\theta_{in}(\tau) - \left(\Phi\beta + \Phi St - \Phi\delta + \delta\theta_J(\tau)\right) + \beta nC(\tau) \\ & + \left(\Phi + 1 + St - \beta\gamma\right)\theta(\tau) + \beta\gamma nC(\tau)\theta(\tau) - \beta\left(\frac{\gamma}{2} - \gamma\right)\theta(\tau)^2 + \beta\frac{1}{2}n(n-1)C(\tau)^2 = 0 \end{aligned} \quad (5.17)$$

Using the steps in the algorithm, set  $N_{max} = 3$ ,  $N = 1, 2, 3$ . Then, the general ALEs for every order up to 3rd-order can be written as

$$\begin{aligned} c_{1,0}^1(1:1)D^1y_{1,1}(\tau) + c_{1,0}^1(1:0)y_{1,1}(\tau) + c_{1,0}^2(1:0)y_{2,1}(\tau) &= c_{0,1}^1(1:0)u_1(\tau) + J_{1,1} - J_{1,0} \\ c_{1,0}^2(2:1)D^1y_{2,1}(\tau) + c_{1,0}^1(2:0)y_{1,1}(\tau) + c_{1,0}^2(2:0)y_{2,1}(\tau) &= c_{0,1}^2(1:0)u_2(\tau) + J_{2,1} - J_{2,0} \\ c_{1,0}^1(1:1)D^1y_{1,1}(\tau) + c_{1,0}^1(1:0)y_{1,1}(\tau) + c_{1,0}^2(1:0)y_{2,1}(\tau) &= J_{1,2} - J_{1,1} \\ c_{1,0}^2(2:1)D^1y_{2,1}(\tau) + c_{1,0}^1(2:0)y_{1,1}(\tau) + c_{1,0}^2(2:0)y_{2,1}(\tau) &= J_{2,2} - J_{2,1} \\ c_{1,0}^1(1:1)D^1y_{1,1}(\tau) + c_{1,0}^1(1:0)y_{1,1}(\tau) + c_{1,0}^2(1:0)y_{2,1}(\tau) &= J_{1,3} - J_{1,2} \\ c_{1,0}^2(2:1)D^1y_{2,1}(\tau) + c_{1,0}^1(2:0)y_{1,1}(\tau) + c_{1,0}^2(2:0)y_{2,1}(\tau) &= J_{2,3} - J_{2,2} \end{aligned} \tag{5.18}$$

where  $J_{1,0} = J_{2,0} = J_{1,1} = J_{2,1} = 0$ . Then, after solving  $J_{1,N}$  and  $J_{2,N}$ , the ALEs for the system up to 3rd-order can be written as

$$\begin{aligned} D^1C_1(\tau) - (\Phi + 1 - \alpha n)C_1(\tau) + \alpha\gamma\theta_1(\tau) \\ = (1 + \alpha\Phi + \alpha + \Phi)C_{in}(\tau) + (\alpha\Phi + \Phi - \alpha) \\ D^1\theta_1(\tau) + \beta nC_1(\tau) + (\Phi + 1 + St - \beta\gamma)\theta_1(\tau) \\ = (\Phi + \Phi\beta + \Phi St - \Phi\delta)\theta_{in}(\tau) + (\Phi\beta + \Phi St - \Phi\delta + \delta\theta_J(\tau)) \\ D^1C_2(\tau) - (\Phi + 1 - \alpha n)C_2(\tau) + \alpha\gamma\theta_2(\tau) \\ = \alpha\gamma nC_1(\tau)\theta_1(\tau) + \alpha\frac{1}{2}n(n-1)C_1(\tau)^2 + \left(\alpha\gamma - \alpha\frac{\gamma}{2}\right)\theta_1(\tau)^2 \\ D^1\theta_2(\tau) + \beta nC_2(\tau) + (\Phi + 1 + St - \beta\gamma)\theta_2(\tau) \\ = \beta\gamma nC_1(\tau)\theta_1(\tau) - \beta\left(\frac{\gamma}{2} - \gamma\right)\theta_1(\tau)^2 + \beta\frac{1}{2}n(n-1)C_1(\tau)^2 \end{aligned}$$

$$\begin{aligned}
& D^1 C_3(\tau) - (\Phi + 1 - \alpha n) C_3(\tau) + \alpha \gamma \theta_3(\tau) \\
&= \alpha \frac{1}{2} n(n-1) (2C_1(\tau)C_2(\tau) + C_2(\tau)^2) + \left( \alpha \gamma - \alpha \frac{\gamma}{2} \right) (2\theta_1(\tau)\theta_2(\tau) + \theta_2(\tau)^2) \\
&\quad + \alpha \gamma n (C_1(\tau)\theta_2(\tau) + C_2(\tau)\theta_1(\tau) + C_2(\tau)\theta_2(\tau)) \\
& D^1 \theta_3(\tau) + \beta n C_3(\tau) + (\Phi + 1 + St - \beta \gamma) \theta_3(\tau) \\
&= -\beta \left( \frac{\gamma}{2} - \gamma \right) (2\theta_1(\tau)\theta_2(\tau) + \theta_2(\tau)^2) + \beta \frac{1}{2} n(n-1) (2C_1(\tau)C_2(\tau) + C_2(\tau)^2) \\
&\quad + \beta \gamma n (C_1(\tau)\theta_2(\tau) + C_2(\tau)\theta_1(\tau) + C_2(\tau)\theta_2(\tau))
\end{aligned} \tag{5.19}$$

Solving (5.19) set by set for  $C_1(\tau), C_2(\tau), C_3(\tau), \theta_1(\tau), \theta_2(\tau)$  and  $\theta_3(\tau)$ . Then, the estimation of the outputs signal and the outputs spectrum for the system up to 3rd-order for both outputs thus can be written as

$$\begin{aligned}
\hat{C}(\tau) &= \hat{C}_1(\tau) + \hat{C}_2(\tau) + \hat{C}_3(\tau) \\
\hat{\theta}(\tau) &= \hat{\theta}_1(\tau) + \hat{\theta}_2(\tau) + \hat{\theta}_3(\tau)
\end{aligned} \tag{5.20}$$

and

$$\begin{aligned}
\hat{C}(j\omega) &= \hat{C}_1(j\omega) + \hat{C}_2(j\omega) + \hat{C}_3(j\omega) \\
\hat{\theta}(j\omega) &= \hat{\theta}_1(j\omega) + \hat{\theta}_2(j\omega) + \hat{\theta}_3(j\omega)
\end{aligned} \tag{5.21}$$

As a MIMO-NDE model, the estimation is independent for all outputs produced. The estimation of the output signal is the total of all ALEs responses for each outputs. In this nonlinear non-isothermal CSTR, there are two outputs which are outlet concentration of the reactant,  $C$  and temperature in the reactor,  $\theta$ . These outputs are in the dimensionless form and can be changed back to the dimension form using their steady state values. Figure 5.3 shows the comparison of the simulated results and the sum of the ALEs results in the dimensionless time domain form to indicate the significant of (5.20).

Then, from (5.21), which is the result of Fourier transform of (5.20), it is understandable that the ouput spectrum for each output can be approximated by the sum of the each outputs solutions of the ALE in the frequency domain. Figure 5.4 shows the comparison of the

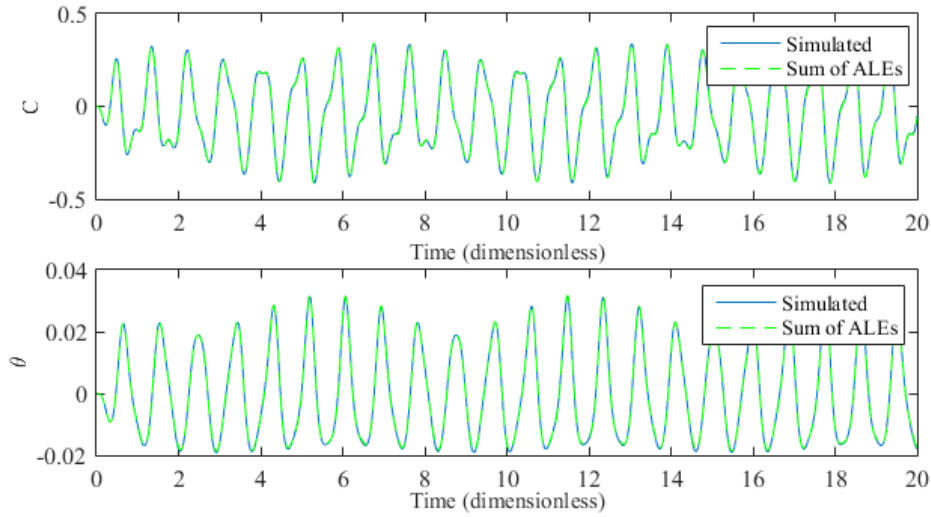


Figure 5.3: The simulated output signals for both outlet concentration of the reactant,  $C$  and temperature in the reactor,  $\theta$  and sum of the signals from the ALEs in the dimensionless time domain when  $F_s = 1$ .

simulated output spectrum and the sum of the solutions of the ALE in the frequency domain for each outputs, outlet concentration of the reactant,  $C$  and temperature in the reactor,  $\theta$ . From both Figure 5.3 and Figure 5.4, it can be said that the sum of the ALEs results in both

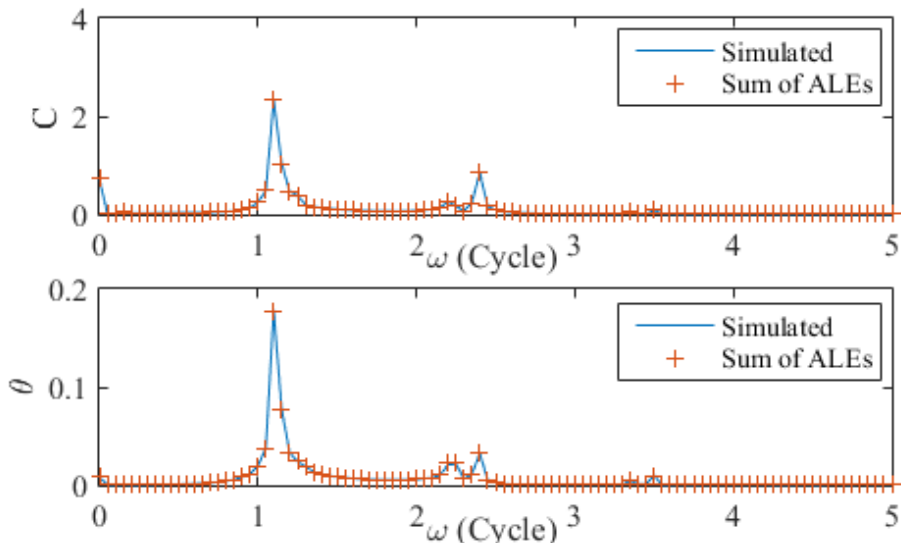


Figure 5.4: The simulated output signals for both outlet concentration of the reactant,  $C$  and temperature in the reactor,  $\theta$  of the system and sum of the signals from the ALEs when  $F_s = 1$ .

the time and frequency domain is in good accuracy to the simulated results for all the outputs in the system. Then, using the steady state values of the concentration of the reactor, the output signal changed to their dimensional form. Figure 5.5 shows the comparison of the simulated results and the sum of the ALEs results in the time domain.

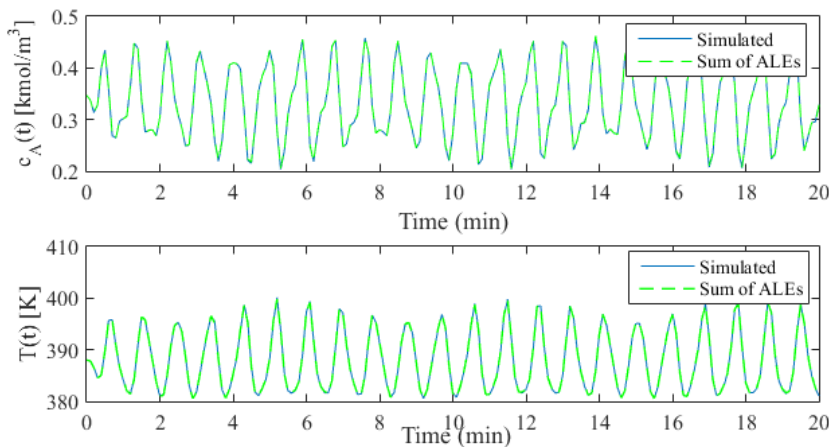


Figure 5.5: The simulated output signals for both outlet concentration of the reactant,  $c_A$  and temperature in the reactor,  $T$  and sum of the signals from the ALEs when  $F_s = 1$ .

Figure 5.5 shows that the ALEs derivation works for analysis in the dimensional form. These results shows the effectiveness of the ALEs determined using the algorithm discussed in Section 4.2.2.1. The estimation of the output spectrum up to 3rd-order for both outputs,  $C$  and  $\theta$  of the nonlinear non-isothermal CSTR that was determined in this subsection will be used in the next subsection.

### 5.2.4 Determination of OFRF of the nonlinear non-isothermal CSTR using ALEs

To determine the OFRF of the nonlinear non-isothermal CSTR, the algorithm derived in Section 4.2.4.1 will be used. First the OFRF representations for both dimensionless outputs, outlet concentration of the reactant,  $C$  and temperature in the reactor,  $\theta$  for the nonlinear non-isothermal CSTR was determined in subsection 5.2.2. The OFRF representations can be written as

$$\begin{aligned}\hat{C}(j\omega) &= \hat{P}_{11}(j\omega) + \left[ \frac{1}{F_s} \right] \hat{P}_{21}(j\omega) + \left[ \frac{1}{F_s^2} \right] \hat{P}_{31}(j\omega) \\ \hat{\theta}(j\omega) &= \hat{P}_{11}(j\omega) + \left[ \frac{1}{F_s} \right] \hat{P}_{21}(j\omega) + \left[ \frac{1}{F_s^2} \right] \hat{P}_{31}(j\omega)\end{aligned}\quad (5.22)$$

The OFRF representation is the same for both outputs but the OFRF "coefficients" for each outputs need to be calculated independently. Then, from the ALEs of the nonlinear non-isothermal CSTR that was determined in previous subsection, the estimation of the output spectrum up to 3rd-order for both outputs,  $C$  and  $\theta$  are

$$\begin{aligned}\hat{C}(j\omega) &= \hat{Y}_{1,1}(j\omega) + \hat{Y}_{1,2}(j\omega) + \hat{Y}_{1,3}(j\omega)) \\ \hat{\theta}(j\omega) &= \hat{Y}_{2,1}(j\omega) + \hat{Y}_{2,2}(j\omega) + \hat{Y}_{2,3}(j\omega)\end{aligned}\quad (5.23)$$

From these results, it can be understood that in using the method of determining OFRF using ALEs for this system, only one set of ALEs simulations using one value of  $F_s$  was needed to determine the OFRF of this nonlinear non-isothermal CSTR system. Combining both (5.22) and (5.23) produces

$$\hat{P}_{11}(j\omega) + \left[ \frac{1}{F_s} \right] \hat{P}_{21}(j\omega) + \left[ \frac{1}{F_s^2} \right] \hat{P}_{31}(j\omega) = \hat{Y}_{1,1}(j\omega) + \hat{Y}_{1,2}(j\omega) + \hat{Y}_{1,3}(j\omega)) \quad (5.24)$$

$$\hat{P}_{11}(j\omega) + \left[ \frac{1}{F_s} \right] \hat{P}_{21}(j\omega) + \left[ \frac{1}{F_s^2} \right] \hat{P}_{31}(j\omega) = \hat{Y}_{2,1}(j\omega) + \hat{Y}_{2,2}(j\omega) + \hat{Y}_{2,3}(j\omega) \quad (5.25)$$

where (5.24) corresponds to the first output, the outlet concentration of the reactant,  $C$  and (5.25) corresponds to the second output, the temperature in the reactor,  $\theta$ . Then, the solution for the OFRF "coefficients" for the outlet concentration of the reactant,  $C$  can be determined as

$$\begin{aligned}\hat{P}_{11}(j\omega) &= \hat{Y}_{1,1}(j\omega) \\ \hat{P}_{21}(j\omega) &= \left[ \frac{1}{F_s} \right]^{-1} \hat{Y}_{1,2}(j\omega) \\ \hat{P}_{31}(j\omega) &= \left[ \frac{1}{F_s^2} \right]^{-1} \hat{Y}_{1,3}(j\omega)\end{aligned}\quad (5.26)$$

whereas the OFRF "coefficients" for the temperature in the reactor,  $\theta$  can be determined as

$$\begin{aligned}\hat{P}_{11}(j\omega) &= \hat{Y}_{2,1}(j\omega) \\ \hat{P}_{21}(j\omega) &= \left[ \frac{1}{F_s} \right]^{-1} \hat{Y}_{2,2}(j\omega) \\ \hat{P}_{31}(j\omega) &= \left[ \frac{1}{F_s^2} \right]^{-1} \hat{Y}_{2,3}(j\omega)\end{aligned}\quad (5.27)$$

It is best to note again that the value of  $\hat{P}_{11}(j\omega)$ ,  $\hat{P}_{21}(j\omega)$  and  $\hat{P}_{31}(j\omega)$  are different for each outputs although the OFRF representation for the outputs are the same as represented in (5.22). Using the value of the parameter  $F_s = 1$ , OFRF of the system was determined. Using the OFRF determined, a comparison between the simulated output spectrum and the spectrum evaluated using OFRF for each outputs can be done.

Different value of  $F_s$  ( $F_s = 0.7, 0.8, 0.9$  and  $1.0 \text{ m}^3/\text{min}$ ) were used in the OFRF determined to show the effectiveness of the OFRF determined. Figure 5.6 shows the comparison of the amplitude of  $C(j\omega)$  and  $\hat{C}(j\omega)$  for four different value of  $F_s$ .

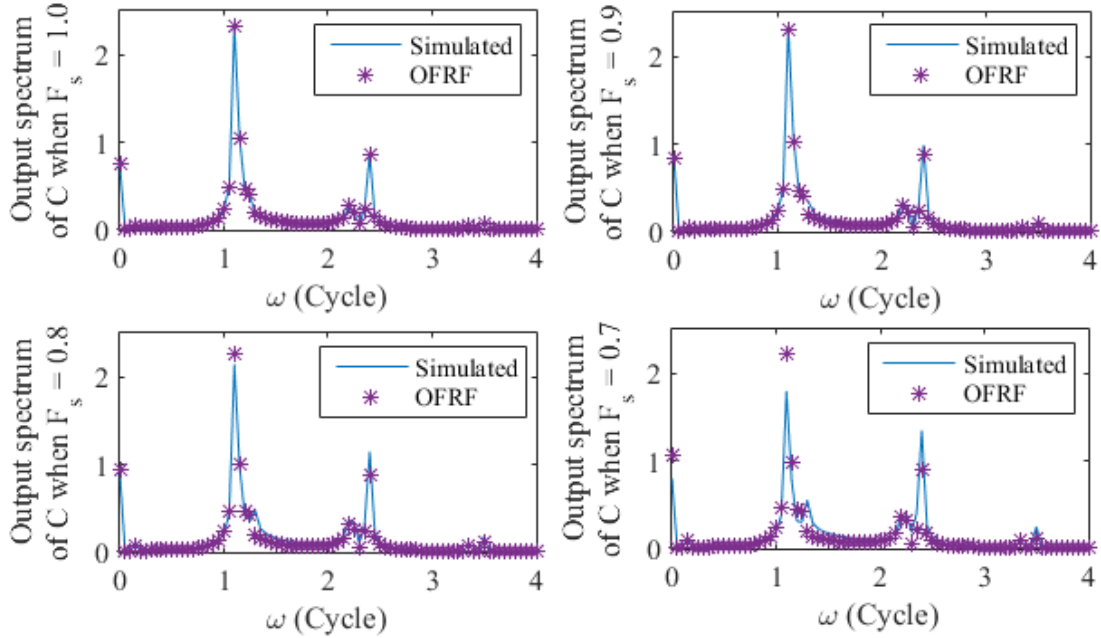


Figure 5.6: Comparison between the simulated output spectrum and the spectrum evaluated using OFRF for output  $C$  with different values of  $F_s$ .

From Figure 5.6, it can be seen that the OFRF can estimate the output spectrum of the outlet concentration of the reactant,  $C$ . However, it can be observed that the OFRF can only estimate the output spectrum well at certain frequency when  $F_s \neq 1.0\text{m}^3/\text{min}$ . Comparing the two results from both simulated output spectrum and the spectrum evaluated using OFRF for the four different values of  $F_s$ , it can be said that the output spectrum evaluated using OFRF had a limitation where the value of  $F_s$  used in the OFRF determination affected the results. The bigger the difference between the value of parameter used in the OFRF based analysis and the value of parameter used in the OFRF determined, the larger the error in the output spectrum evaluated using OFRF when compared with the simulated output spectrum.

The same relationship can be seen from the results for the second output,  $\theta$ , the temperature in the reactor in Figure 5.7. Figure 5.7 shows the comparison of the amplitude of  $\theta(j\omega)$  and  $\hat{\theta}(j\omega)$  for four different value of  $F_s$ .

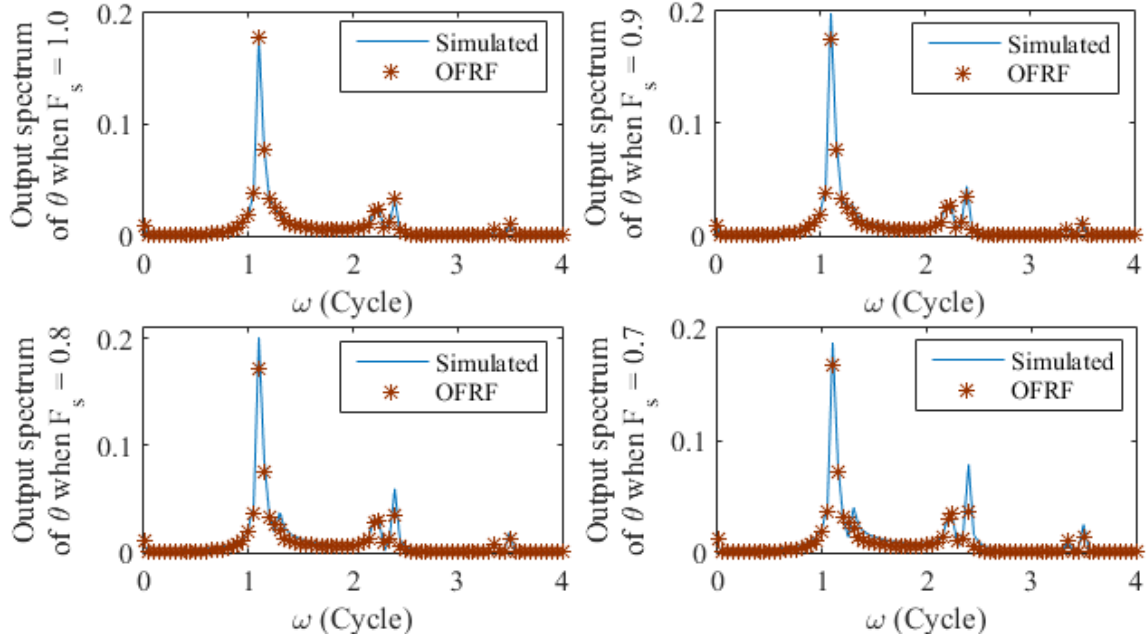


Figure 5.7: Comparison between the simulated output spectrum and the spectrum evaluated using OFRF for output  $\theta$  with different values of  $F_s$ .

Based on the results on both Figure 5.6 and Figure 5.7, it supported the assumption made at the beginning of this implementation. As OFRF can represent the simulated output spectrum well, it can be concluded that although the parameter of interest,  $F_s$  define both the linearity and the nonlinearity, the effect of the linear part is small on the nonlinear system.

### 5.2.5 OFRF based analysis for the nonlinear non-isothermal CSTR

Using the OFRF determined, two OFRF based analysis were done. First, using the fact from the current literature, OFRF will be used to check whether a periodic modulation of the input for the nonlinear non-isothermal CSTR system has a better average performance compared to the steady state operation due to the nonlinearities in the system. Second, using the OFRF, a function that can directly shows the relationship between the average value of output signal for dimensionless outlet concentration of the reactant and the nonlinear parameter will be presented to facilitate the analysis and design of nonlinear chemical process system.

For the first OFRF based analysis, by inverting the results of the OFRF estimated output spectrums, the data are converted to the time domain. Then, using the steady state values of the concentration of the reactant, the dimensionless data is converted to the real value output signal and the average of the output signals for the four different values of  $F_s$  can be calculated. Table 5.3 shows the mean value of the outlet concentration of the reactant,  $\bar{c}_A$  determined using numerical simulation and OFRF and their percentage error. In this comparison, the simulation time is constant and the starting conditions are the same.

Table 5.3: Comparison between mean values of the outlet concentration of the reactant,  $\bar{c}_A$  using numerical simulation and OFRF.

$F_s$ $m^3/min$	$\bar{c}_A$ using numerical simulation	$\bar{c}_A$ using OFRF	Percentage error (%)
0.7	0.3328	0.3282	1.38
0.8	0.3311	0.3304	0.21
0.9	0.3314	0.3321	0.21
1.0	0.3340	0.3335	0.15

From Table 5.3, it can be analysed that the bigger the flow rate, the smaller the mean values of the outlet concentration. This show the relationship between the parameter of interest, flow rate, which defines the system nonlinearity and the outputs of the system. Besides, all the mean values of the outlet concentration of the reactant,  $\bar{c}_A$  are less than the steady-state value ( $c_{A,s} = 0.3466 \text{ kmol/m}^3$ ) which are consistent with the fact that a periodic modulation of a nonlinear system will has a better average performance compared to the steady state due to the nonlinearities in the system.

The data in Table 5.3 also show that the percentage error between the result using OFRF and numerical simulation are small for each different value of  $F_s$  that were analysed. Thus, it is clear that OFRF can provide a good result in the analysis of a nonlinear non-isothermal CSTR system. In addition, it is also interesting to point out that the difference between the

mean values of the outlet concentration of the reactant,  $\bar{c}_A$  using numerical simulation and OFRF are bigger when  $F_s$  is smaller. This is because the OFRF that was used in this analysis was determined from the results of  $F_s = 1.0$ .

Then, the same concept was applied to the second output in the dimensional form and time domain, the temperature of the reactor,  $T$ . Table (5.4) shows the mean value of the temperature of the reactor,  $\bar{T}$  determined using numerical simulation and OFRF.

From table 5.4, the mean values of the temperature of the reactor are close to the steady

Table 5.4: Comparison between mean values of the temperature of the reactor,  $\bar{T}$  using numerical simulation and OFRF.

$F_s$	$\bar{T}$ using numerical simulation	$\bar{T}$ using OFRF
0.7	388.09	388.23
0.8	388.12	388.20
0.9	388.15	388.18
1.0	388.15	388.16

state value ( $T_s = 388K$ ). This show that  $F_s$  has small effect on the temperature of the reactor. In addition, the difference between the mean values of the temperature of the reactor,  $\bar{T}$  using numerical simulation and OFRF are bigger when  $F_s$  is smaller. This finding provides conclusive support that the estimation of the OFRF will has bigger deviation from the simulated result when the parameter analyzed had bigger difference from the parameter value that was used in the determination of the OFRF.

Next, for the second OFRF based analysis, a function that can directly shows the relationship between the average value of output signal for dimensionless outlet concentration of the reactant and the nonlinear parameter is needed. To determine this function, first, consider the OFRF that was determined for the non-isothermal CSTR.

$$\hat{C}(j\omega) = \hat{P}_{11}(j\omega) + \left[ \frac{1}{F_s} \right] \hat{P}_{21}(j\omega) + \left[ \frac{1}{F_s^2} \right] \hat{P}_{31}(j\omega) \quad (5.28)$$

Using (5.28), the average value of each functions can be determined as

$$\begin{aligned}
 & \frac{1}{\omega_2 - \omega_1} \int_{\omega_1}^{\omega_2} \hat{C}(j\omega) \hat{C}^*(j\omega) d\omega \\
 &= \frac{1}{\omega_2 - \omega_1} \int_{\omega_1}^{\omega_2} \left( \hat{P}_{11}(j\omega) + \left[ \frac{1}{F_s} \right] \hat{P}_{21}(j\omega) + \left[ \frac{1}{F_s^2} \right] \hat{P}_{31}(j\omega) \right. \\
 &\quad \times \left. \left( \hat{P}_{11}^*(j\omega) + \left[ \frac{1}{F_s} \right] \hat{P}_{21}^*(j\omega) d\omega + \left[ \frac{1}{F_s^2} \right] \hat{P}_{31}^*(j\omega) \right) d\omega \right. \\
 &= \frac{1}{\omega_2 - \omega_1} \int_{\omega_1}^{\omega_2} \left( \hat{P}_{11}(j\omega) \hat{P}_{11}^*(j\omega) + \left[ \frac{1}{F_s} \right] (\hat{P}_{21}(j\omega) \hat{P}_{11}^*(j\omega) + \hat{P}_{11}(j\omega) \hat{P}_{21}^*(j\omega)) \right. \\
 &\quad + \left. \left[ \frac{1}{F_s^2} \right] (\hat{P}_{31}(j\omega) \hat{P}_{11}^*(j\omega) + \hat{P}_{21}(j\omega) \hat{P}_{21}^*(j\omega) + \hat{P}_{11}(j\omega) \hat{P}_{31}^*(j\omega)) \right. \\
 &\quad + \left. \left[ \frac{1}{F_s^3} \right] (\hat{P}_{31}(j\omega) \hat{P}_{21}^*(j\omega) + \hat{P}_{21}(j\omega) \hat{P}_{21}^*(j\omega)) + \left[ \frac{1}{F_s^4} \right] (\hat{P}_{31}(j\omega) \hat{P}_{31}^*(j\omega)) \right) d\omega \\
 &= \frac{1}{\omega_2 - \omega_1} \int_{\omega_1}^{\omega_2} \hat{P}_{11}(j\omega) \hat{P}_{11}^*(j\omega) d\omega \\
 &\quad + \left[ \frac{1}{F_s} \right] \frac{1}{\omega_2 - \omega_1} \int_{\omega_1}^{\omega_2} (\hat{P}_{21}(j\omega) \hat{P}_{11}^*(j\omega) + \hat{P}_{11}(j\omega) \hat{P}_{21}^*(j\omega)) d\omega \\
 &\quad + \left[ \frac{1}{F_s^2} \right] \frac{1}{\omega_2 - \omega_1} \int_{\omega_1}^{\omega_2} (\hat{P}_{31}(j\omega) \hat{P}_{11}^*(j\omega) + \hat{P}_{21}(j\omega) \hat{P}_{21}^*(j\omega) + \hat{P}_{11}(j\omega) \hat{P}_{31}^*(j\omega)) d\omega \\
 &\quad + \left[ \frac{1}{F_s^3} \right] \frac{1}{\omega_2 - \omega_1} \int_{\omega_1}^{\omega_2} (\hat{P}_{31}(j\omega) \hat{P}_{21}^*(j\omega) + \hat{P}_{21}(j\omega) \hat{P}_{21}^*(j\omega)) d\omega \\
 &\quad + \left[ \frac{1}{F_s^4} \right] \frac{1}{\omega_2 - \omega_1} \int_{\omega_1}^{\omega_2} (\hat{P}_{31}(j\omega) \hat{P}_{31}^*(j\omega)) d\omega
 \end{aligned} \tag{5.29}$$

Then, using the relationship where

$$\int_{\omega_1}^{\omega_2} \hat{C}(j\omega) \hat{C}^*(j\omega) d\omega = \int_{\omega_1}^{\omega_2} |\hat{C}(j\omega)|^2 d\omega \tag{5.30}$$

and the Rayleigh's Theorem where the integral of the power spectrum equals the integral of the squared modulus of the function

$$\int_{-\infty}^{\infty} |\hat{f}(x)|^2 dx = \int_{-\infty}^{\infty} |\hat{f}(j\omega)|^2 d\omega \quad (5.31)$$

the relationship between the average value of the output spectrum for dimensionless outlet concentration of the reactant and the average value of output signal for dimensionless outlet concentration of the reactant can be written as

$$\frac{1}{\tau_2 - \tau_1} \int_{\tau_1}^{\tau_2} |\hat{C}(\tau)|^2 d\tau = \frac{1}{\omega_2 - \omega_1} \int_{\omega_1}^{\omega_2} |\hat{C}(j\omega)|^2 d\omega \quad (5.32)$$

Thus, using the OFRF determined, a relationship between the nonlinear parameters and the average value of outlet concentration output spectrum for dimensionless outlet concentration of the reactant can be written as

$$\begin{aligned} & \frac{1}{\omega_2 - \omega_1} \int_{\omega_1}^{\omega_2} |\hat{C}(j\omega)|^2 d\omega \\ &= \frac{1}{\omega_2 - \omega_1} \int_{\omega_1}^{\omega_2} \hat{P}_{11}(j\omega) \hat{P}_{11}^*(j\omega) d\omega \\ &+ \left[ \frac{1}{F_s} \right] \frac{1}{\omega_2 - \omega_1} \int_{\omega_1}^{\omega_2} \left( \hat{P}_{21}(j\omega) \hat{P}_{11}^*(j\omega) + \hat{P}_{11}(j\omega) \hat{P}_{21}^*(j\omega) \right) d\omega \\ &+ \left[ \frac{1}{F_s^2} \right] \frac{1}{\omega_2 - \omega_1} \int_{\omega_1}^{\omega_2} \left( \hat{P}_{31}(j\omega) \hat{P}_{11}^*(j\omega) + \hat{P}_{21}(j\omega) \hat{P}_{21}^*(j\omega) + \hat{P}_{11}(j\omega) \hat{P}_{31}^*(j\omega) \right) d\omega \\ &+ \left[ \frac{1}{F_s^3} \right] \frac{1}{\omega_2 - \omega_1} \int_{\omega_1}^{\omega_2} \left( \hat{P}_{31}(j\omega) \hat{P}_{21}^*(j\omega) + \hat{P}_{21}(j\omega) \hat{P}_{21}^*(j\omega) \right) d\omega \\ &+ \left[ \frac{1}{F_s^4} \right] \frac{1}{\omega_2 - \omega_1} \int_{\omega_1}^{\omega_2} \left( \hat{P}_{31}(j\omega) \hat{P}_{31}^*(j\omega) \right) d\omega \end{aligned} \quad (5.33)$$

This equation shows the relationship between the nonlinear parameters, the steady state flow rate,  $F_s$  and the average value of output spectrum for dimensionless outlet concentration of the reactant. Using (5.32), the relationship between the nonlinear parameters, the steady state

flow rate,  $F_s$  and the average value of output signal for dimensionless outlet concentration of the reactant can also be written as

$$\begin{aligned}
 & \frac{1}{\tau_2 - \tau_1} \int_{\tau_1}^{\tau_2} |\hat{C}(\tau)|^2 d\tau \\
 &= \frac{1}{\omega_2 - \omega_1} \int_{\omega_1}^{\omega_2} \hat{P}_{11}(j\omega) \hat{P}_{11}^*(j\omega) d\omega \\
 &\quad + \left[ \frac{1}{F_s} \right] \frac{1}{\omega_2 - \omega_1} \int_{\omega_1}^{\omega_2} (\hat{P}_{21}(j\omega) \hat{P}_{11}^*(j\omega) + \hat{P}_{11}(j\omega) \hat{P}_{21}^*(j\omega)) d\omega \\
 &\quad + \left[ \frac{1}{F_s^2} \right] \frac{1}{\omega_2 - \omega_1} \int_{\omega_1}^{\omega_2} (\hat{P}_{31}(j\omega) \hat{P}_{11}^*(j\omega) + \hat{P}_{21}(j\omega) \hat{P}_{21}^*(j\omega) + \hat{P}_{11}(j\omega) \hat{P}_{31}^*(j\omega)) d\omega \\
 &\quad + \left[ \frac{1}{F_s^3} \right] \frac{1}{\omega_2 - \omega_1} \int_{\omega_1}^{\omega_2} (\hat{P}_{31}(j\omega) \hat{P}_{21}^*(j\omega) + \hat{P}_{21}(j\omega) \hat{P}_{21}^*(j\omega)) d\omega \\
 &\quad + \left[ \frac{1}{F_s^4} \right] \frac{1}{\omega_2 - \omega_1} \int_{\omega_1}^{\omega_2} (\hat{P}_{31}(j\omega) \hat{P}_{31}^*(j\omega)) d\omega
 \end{aligned} \tag{5.34}$$

Both relationships allow a further analysis to be done using the OFRF. To show the effectiveness of this relationship, using the OFRF determined for the non-isothermal CSTR, this equation was produced

$$\begin{aligned}
 & \frac{1}{50-0} \int_0^{50} |\hat{C}(j\omega)|^2 d\omega \\
 &= 0.4407 + \left[ \frac{1}{F_s} \right] 0.0018 + \left[ \frac{1}{F_s^2} \right] 0.0116 + \left[ \frac{1}{F_s^3} \right] (7.8809 \times 10^{-4}) + \left[ \frac{1}{F_s^4} \right] 0.0020
 \end{aligned} \tag{5.35}$$

In this equation, only the frequency data for  $\omega = 0 - 50$  cycles is considered which is half of the output spectrum data. Using equation (5.33), the value of  $F_s$  that can produce a specified average value of output spectrum for dimensionless outlet concentration of the reactant can be determined. For example, if the average value of output spectrum for dimensionless outlet concentration of the reactant specified is 0.4589, the value of  $F_s$  can be determined by finding

the roots of this equation

$$0.4589 = 0.4407 + \left[ \frac{1}{F_s} \right] 0.0018 + \left[ \frac{1}{F_s^2} \right] 0.0116 + \left[ \frac{1}{F_s^3} \right] (7.7565 \times 10^{-4}) + \left[ \frac{1}{F_s^4} \right] 0.0020 \quad (5.36)$$

There are four roots for equation (5.36). From the four roots, only one can be used as the value of  $F_s$  because two roots are complex numbers while the other one root is negative number. As a result, the value of  $F_s$  calculated from (5.36) is  $0.9483 \text{ m}^3/\text{min}$ .

Comparing with the results from the numerical simulation using equation (5.16), the average value of output spectrum for dimensionless outlet concentration of the reactant is 0.4599 and the average value of output signal for dimensionless outlet concentration of the reactant is 0.4597 when the steady state flow rate,  $F_s$  is  $0.9483 \text{ m}^3/\text{min}$ . This result shows that (5.35) allows the determination of the steady state flow rate,  $F_s$  when the average value of output spectrum or output signal for dimensionless outlet concentration of the reactant are specified.

In this OFRF based analysis, the relationship between the nonlinear parameter and the output of the system can be determined. Using the current methodology and literature, only relationship between input and output of the system can be determined. In [55–57], the analysis of the same system, the nonlinear non-isothermal CSTR was done. It shows the effects of the periodic modulation input on the output of the system using nonlinear frequency response method. Thus, only relationship between the input and output can be understood. In this new OFRF based analysis, the relationship between the nonlinear parameter and the output can be understood and used for the manufacturing of chemical process design. This provides a new method for nonlinear chemical process system analysis and design.

### 5.3 Conclusion

In conclusion, this chapter has provided convincing evidence of how OFRF is useful in the chemical engineering process and may contribute to a further understanding of the relationship between the nonlinear parameters and the outputs of the system. In this analysis, an assumption where the parameter of interest in the linear part has a small effect on the nonlinear system had been made. The assumption allows the analysis using OFRF can be done as OFRF shows an explicit relationship between the nonlinear parameters and the outputs of the system.

This analysis also presented how the nonlinear system can be transformed to the NDE model using the expansion of the nonlinear terms in the Taylor series form technique. This transformation allowed the determination of OFRF for the nonlinear non-isothermal CSTR systems. Although this chapter only focuses on the specific case of non-isothermal CSTR, the same technique can be easily applied to other nonlinear CSTR. Besides, the same techniques also could be used in other types of reactor.

Based on the OFRF that was determined in this analysis, a different type of analysis and design can be done either in dimensionless or dimensional forms of the nonlinear non-isothermal CSTR. The process of transforming the dimensionless form results into the dimensional forms is by using the steady-state values of the system. This analysis provides a new insight for the nonlinear chemical process as the current research only provide a relationship between the inputs and the outputs of the system, but OFRF allows an explicit relationship between the parameter that describes the nonlinearities and the output of the system.

Using the OFRF that was determined using the new method, a new OFRF based analysis was done. The relationship between the steady state flow rate,  $F_s$  and the average value of the

output spectrum or the output signal for dimensionless outlet concentration of the reactant were presented. The nonlinear parameters can be calculated when the average value of the output spectrum or the output signal for dimensionless outlet concentration of the reactant is specified. This new OFRF based analysis shows the relationship between the nonlinear parameter and the output of the system and this analysis is useful for the chemical process design. Lastly, this method opens a new area for the understanding and development of chemical process system analysis and design.

# **Chapter 6**

## **Conclusion and Recommendation for Future Works**

### **6.1 Summary and Conclusion**

The purpose of this research was to develop a new and efficient numerical method in frequency domain analysis. Besides, this research aims to understand the relationship between the system output frequency response and parameters that define the system nonlinearity of nonlinear chemical engineering process systems.

In this research, the Volterra series theory in the frequency domain, the OFRF and the ALEs are reviewed. Then, the new numerical method for the determination of OFRF has been derived where it utilised the ALEs concept. The new numerical method increases the efficiency of the determination of OFRF for nonlinear systems by significantly reducing the number of numerical simulations and had been tested with SISO nonlinear systems. The OFRF based analysis and design were applied to a nonlinear passive engine mount system using the new numerical method derived in this research.

Understanding that most of nonlinear systems are not SISO and the need to has a numerical method to determine OFRF for MIMO nonlinear systems, the new numerical method concepts and techniques for the determination of OFRF using ALEs has been extended to the MIMO nonlinear systems. Detailed algorithms are derived for the determination of OFRF using ALEs for MIMO nonlinear system. The new numerical method to determine the OFRF for the MIMO nonlinear system opened a new journey to understanding the relationship between the nonlinear parameters and the output for MIMO nonlinear system. The new numerical method for the determination of OFRF for MIMO nonlinear system had been tested with MIMO nonlinear system. The OFRF based design of a building structure vibration isolation system has then be used to demonstrate how the new numerical method can be applied to implement a design for application in earthquake engineering.

Finally, the new numerical method proposed in this research have been applied to the analysis and design of nonlinear chemical engineering process system. The OFRF based analysis and design had been applied to the nonlinear non-isothermal CSTR. The results help in the understanding of the nonlinear chemical process identification and revealing the relationship between the system output frequency response and parameters that define the system nonlinearity.

## 6.2 Contributions of this research

This research makes several noteworthy contributions to the analysis and design on the nonlinear system in the frequency domain. The summary of the contributions of this works are as follows:

1. A new and efficient numerical method to determine OFRF using ALEs concept for the SISO nonlinear systems is proposed.

Three detailed algorithms for the new numerical method is presented in Chapter 3. These algorithms only work for SISO nonlinear system. The first algorithm is about the determination of the OFRF representation from the NDE model. Then, the second algorithm facilitates the derivation of ALEs for the nonlinear system. Finally, the last algorithm uses the results from the first and second algorithm and their relationship to determine the OFRF of the nonlinear system. The new numerical method increases the efficiency of determination of OFRF for a nonlinear system. The number of simulations needed to determine OFRF is less compared to the current literature [46].

2. A new numerical method to determine OFRF using ALEs for MIMO nonlinear systems is developed.

The concepts in the new numerical method to determine OFRF using ALEs for the SISO nonlinear model are extended to the MIMO nonlinear system. A better understanding of the relationship between the nonlinear parameters and the output for MIMO nonlinear system is achieved using the new numerical method to determine the OFRF using ALEs for the MIMO nonlinear systems developed in this research. This new numerical method also consists of three algorithms and is presented in Chapter 4. These algorithms use the same concept and techniques as the new numerical method to determine the OFRF using ALEs for the SISO nonlinear system. The first algorithm is an algorithm to determine the OFRF representation of the NDE MIMO nonlinear system. Then, the second algorithm is the derivation of ALEs for the MIMO nonlinear system. The second algorithm facilitates the process of determining the ALEs for the MIMO nonlinear system. The last algorithm is the determination of OFRF using ALEs.

3. Applications of the new numerical method to various nonlinear engineering problems.

The new numerical method proposed is applied to various nonlinear engineering problems. Different SISO nonlinear systems and MIMO nonlinear systems were tested and analysed using the new numerical method developed in this research. Simulation studies demonstrated the effectiveness of the new numerical method proposed in the determination of OFRF for both SISO and MIMO nonlinear systems. The OFRF based analysis and design were done on two different nonlinear systems; the passive engine mount system and the engineering earthquake system. This OFRF based analysis provide a better understanding of the relationship between the nonlinear parameters and the output for the nonlinear systems.

4. The application of OFRF approach to the analysis of the output frequency response of the nonlinear non-isothermal CSTR system.

The new numerical method proposed in this research is implemented and tested to the nonlinear non-isothermal CSTR system. The nonlinear non-isothermal CSTR system is transformed to the NDE model by expanding the nonlinear terms in the material and energy balance equation using the Taylor series concept. Then, the detailed algorithms presented and discussed in Chapter 4 are used to determine the OFRF for the nonlinear non-isothermal CSTR system. The OFRF provides a good solution to the nonlinear non-isothermal CSTR. Then, the OFRF based analysis was done using the OFRF determined. The relationship between the system output frequency response and parameters that define the system nonlinearity is analysed. In addition, as this system is a periodic operation system, the result of the OFRF based analysis was compared with the result in [49] where it analysed the same nonlinear system but in the steady-state operation. The result agrees with the current literature [19, 71, 73] where the periodic operation system improve the conversion of the product compared to the steady-state operation.

## 6.3 Future works

In the present research, a new numerical method to determine OFRF using ALEs for both SISO and MIMO nonlinear systems are developed. The application of the new numerical method to the nonlinear chemical process analysis and design also had been presented. However, there is abundant room for further research. It is recommended that further research is undertaken in the following area:

1. In this research, only application of OFRF into the CSTR is considered. It is interesting to apply the OFRF based analysis and design to other types of reactors such as batch reactor and PFR. The CSTR system that was analysed in this research is a nonlinear non-isothermal CSTR system that used Taylor series to be transformed to the NDE model. The same technique should applicable to other types of reactors. The OFRF concept provides an explicit analytical relationship between the output frequency response and the parameters that define the nonlinearity of the system. The relationship that can be determined by OFRF can help the researchers to optimise the reactors.
2. Besides applying the OFRF concepts to other types of reactors, the OFRF based analysis and design should also be implemented to different nonlinear chemical process systems such as adsorption and pH neutralisation processes. The derivation of NDE model from a current mathematical model that was used to describe these nonlinear chemical process systems might be a challenge. But, as OFRF can provide the analytical relationship between the output frequency response and the parameters that define the nonlinearity of the system, the results of this research can provide a new understanding to these nonlinear chemical process systems.
3. The results from the analysis and design of the nonlinear non-isothermal CSTR is based on the numerical simulation. It would be interesting to compare the results from the numerical simulation with the experimental data. Further experimental investigations

are needed to understand the relationship between the nonlinear parameters and the output frequency response of the nonlinear chemical process systems. These investigations can help in the designing process of the control system and the optimisation of the nonlinear system.

The recommended further research are focusing on the chemical engineering area. OFRF can show an explicit relationship between the system output frequency response and parameters that define the system nonlinearity while the current method in chemical process control is only focusing on the relationship between the input and the output of the nonlinear chemical process system. Therefore, this allows the OFRF based analysis to have an advantage in the nonlinear chemical process control analysis and design. This future works will provide new development in the chemical engineering process control area.

# References

- [1] R. Alkhatib, G. Nakhaie Jazarb, and M. F. Golnaraghi. Optimal design of passive linear suspension using genetic algorithm. *Journal of Sound and Vibration*, 275(3):665–691, 2004.
- [2] E. Bai. A blind approach to the Hammerstein – Wiener model identification. *Automatica*, 38:967–979, 2002.
- [3] E. Bai. Frequency Domain Identification of Hammerstein Models. *IEEE Transaction on Automatic Control*, 48(4):530–542, 2003.
- [4] E. Bai. Frequency Domain Identification of Wiener Models. *Automatica*, 39(9):1521–1530, sep 2003.
- [5] E W Bai. Identification of linear systems with hard-input nonlinearities of known structure. *Automatica*, 38:853–860, 2002.
- [6] D. Bauer and B. Ninness. Asymptotic properties of Hammerstein model estimates. *Proceedings of the 39th IEEE Conference on Decision and Control*, 3:2855–2860, 2000.
- [7] R. S. Bayma. *New Methods for Analysis of Nonlinear Systems in the Frequency Domain with Applications in Condition Monitoring and Engineering Systems*. PhD thesis, University of Sheffield, 2014.
- [8] R. S. Bayma and Z. Q. Lang. A New Method for Determining the Generalised Frequency Response Functions of Nonlinear Systems. *IEEE Transactions on Circuits and Systems - I*, 59(12):3005–3014, 2012.
- [9] B.W. Bequette. Nonlinear Control of Chemical Processes : A Review. *Ind. Eng. Chem. Res.*, (30):1391–1413, 1991.
- [10] N. Bhat and T. J. McAvoy. Use of Neural Nets for Dynamic Modeling and Control of Chemical Process Systems. *Computers & Chemical Engineering*, 14(4):573–583, 1990.
- [11] S. A. Billings and S. Y. Fakhouri. Identification of a class of nonlinear systems using correlation analysis. Technical report, Department of Control Engineering, University of Sheffield, 1977.

- [12] S. A. Billings and Z. Q. Lang. Nonlinear systems in the frequency domain: Energy transfer filters. Technical report, Department of Automatic Control and System Engineering, University of Sheffield, 2001.
- [13] S. A. Billings and J. C. Peyton Jones. Mapping non-linear integro-differential equations into the frequency domain. Technical report, 1989.
- [14] S. Boyd and L. Chua. Fading Memory and the Problem of Approximating Nonlinear Operators with Volterra Series. *IEEE Transactions on Circuits and Systems*, 32(11):1150–1161, 1985.
- [15] D. Brzić and M. Petkovska. Some Practical Aspects of Nonlinear Frequency Response Method for Investigation of Adsorption Equilibrium and Kinetics. *Chemical Engineering Science*, 82:62–72, 2012.
- [16] D. Brzić and M. Petkovska. Nonlinear frequency response analysis of nonisothermal adsorption controlled by macropore diffusion. *Chemical Engineering Science*, 118:141–153, 2014.
- [17] F. Caccavale, M. Iamarino, F. Pierri, and V. Tufano. *Control and Monitoring of Chemical Batch Reactors*. Springer-Verlag London, 2011.
- [18] A. Chatterjee and N. S. Vyas. Non-linear parameter estimation in multi-degree-of-freedom systems using multi-input Volterra series. *Mechanical Systems and Signal Processing*, 18:457–489, 2004.
- [19] C. C. Chen, C. Hwang, and R. Y. K. Yang. Optimal Periodic Forcing of Nonlinear Chemical Processes for Performance Improvements. *The Canadian Journal of Chemical Engineering*, 72(4):672–682, 1994.
- [20] S. Chen and S. A. Billings. Representation of non-linear systems: the NARMAX model. *International Journal of Control*, 49(3):1013–1032, 1989.
- [21] S. Cui and M. S. Chiu. A Multiple Model Approach to Nonlinear Internal Model Control Design. *Computers and Chemical Engineering*, 23(Supplement):S253–S256, 1999.
- [22] M. Dan and M. Kohiyama. System identification and control improvement of semi-active-controlled-base-isolated building using the record of the 2011 Great East Japan Earthquake. *Safety, Reliability, Risk and Life-Cycle Performance of Structure & Infrastructures*, pages 3842–3847, 2013.
- [23] M. F. Doherty and J. M. Ottino. Chaos in Deterministic Systems: Strange Attractors, Turbulence and Applications in Chemical Engineering. *Chemical Engineering Science*, 43(2):139–183, 1988.
- [24] J. M. Douglas. *Process Dynamics and Control Volume 2 Control System Synthesis*. Prentice-Hall Inc, Englewood Cliffs, New Jersey, 1972.

- [25] J. Du and T. A. Johansen. Integrated Multilinear Model Predictive Control of Nonlinear Systems Based on Gap Metric. *Industrial and Engineering Chemistry Research*, 54(22):6002–6011, 2015.
- [26] A. R. Garayhi and F. J. Keil. Determination of kinetic expressions from the frequency response of a catalytic reactor - theoretical and experimental investigations. *Chemical Engineering Science*, 56:1317–1325, 2001.
- [27] D. A. George. Continuous nonlinear systems. *Technical Report 355, MIT Research Laboratory of Electronics*, 1959.
- [28] P. Guo. *Damping System Designs using Nonlinear Frequency Analysis Approach*. PhD thesis, University of Sheffield, 2012.
- [29] M. A. Henson and D. E. Seborg. *Nonlinear Process Control*. Prentice-Hall PTR, NJ, USA, 1997.
- [30] F. J. M. Horn and R. C. Lin. Periodic processes : A variational approach. *Industrial & Engineering Chemistry Process Design and Development*, 6(1):21–30, 1967.
- [31] R. A. Ibrahim. Recent advances in nonlinear passive vibration isolators. *Journal of Sound and Vibration*, 314:371–452, 2008.
- [32] M. Ilić, M. Petkovska, and A. Seidel-Morgenstern. Determination of competitive adsorption isotherms applying the nonlinear frequency response method. Part II. Experimental demonstration. *Journal of Chromatography A*, 1216(33):6108–6118, 2009.
- [33] C. Jauberthie and L. Travé-Massuyès. A sufficient condition to test identifiability of nonlinear delayed-differential models with constant delays and multi-inputs. *Automatica*, 46(7):1222–1227, 2010.
- [34] G. N. Å Jazar, M Mahinfalah, and S Deshpande. Design of a piecewise linear vibration isolator for jump avoidance. *Proceedings of the Institution of Mechanical Engineers, Part K: Journal of Multi-body Dynamics*, 221(3):441–449, 2007.
- [35] X. Jing. Nonlinear Characteristic Output Spectrum for Nonlinear Analysis and Design. *IEEE/ASME Transactions on Mechatronics*, 19(1):1–13, 2012.
- [36] X. Jing and Z. Lang. *Frequency Domain Analysis and Design of Nonlinear Systems based on Volterra Series Expansion*. Springer, 2015.
- [37] X. J. Jing and Z. Q. Lang. The parametric characteristic of frequency response functions for nonlinear systems. *International Journal of Control*, 79(12):1552–1564, 2006.
- [38] X. J. Jing, Z. Q. Lang, and S. A. Billings. Mapping from parametric characteristics to generalized frequency response functions of non-linear systems. *International Journal of Control*, 81(7):1071–1088, 2008.

- [39] X. J. Jing, Z. Q. Lang, and S. A. Billings. Output frequency response function-based analysis for nonlinear Volterra systems. *Mechanical Systems and Signal Processing*, 22(1):102–120, jan 2008.
- [40] Xingjian Jing. Frequency domain analysis and identification of block-oriented nonlinear systems. *Journal of Sound and Vibration*, 330(22):5427–5442, oct 2011.
- [41] A. Kalafatis, N. Arifin, L. Wang, and W. R. Cluett. A New Approach to the Identification of PH Processes Based on the Wiener Model. *Chemical Engineering Science*, 50(23):3693–3701, 1995.
- [42] L. B. Koppel. Input Multiplicities in Nonlinear, Multivariable Control Systems. *AICHE Journal*, 28(6):935–945, 1982.
- [43] Z. Q. Lang and S. A. Billings. Output Frequency Characteristics of Nonlinear Systems. *International Journal of Control*, 64:1049–1067, 1996.
- [44] Z. Q. Lang and S. A. Billings. Output Frequencies of Nonlinear Systems. *International Journal of Control*, 67(5):713–730, jan 1997.
- [45] Z. Q. Lang and S. A. Billings. Energy transfer properties of non-linear systems in the frequency domain. *International Journal of Control*, 78(5):345–362, mar 2005.
- [46] Z. Q. Lang, S. A. Billings, R. Yue, and J. Li. Output frequency response function of nonlinear Volterra systems. *Automatica*, 43(5):805–816, may 2007.
- [47] O. Levenspiel. *Chemical Reaction Engineering*. Wiley, New York, 1999.
- [48] A. G. J. Macfarlane. Perspectives The Development of Frequency-Response Methods in Automatic Control. *IEEE Transaction on Automatic Control*, AC-24(2):250–265, 1979.
- [49] E. T. Marlin. *Process Control: Designing Processes and Control Systems for Dynamic Performance*. McGraw Hill, New York, 2nd editio edition, 2000.
- [50] D. Q. Mayne, J. B. Rawlings, C. V. Rao, and P. O. M. Scokaert. Constrained model predictive control : Stability and optimality. *Automatica*, 36:789–814, 2000.
- [51] I. S. Metcalfe. *Record Details and Options Chemical reaction engineering : a first course*. Oxford University Press, New York, 1997.
- [52] G. Nakhaie Jazar, A.. Narimani, M. F.. Golnaraghi, and D. A. Swanson. Practical Frequency and Time Optimal Design of Passive Linear Vibration Isolation Mounts Practical Frequency and Time Optimal Design of Passive Linear Vibration Isolation Mounts. *Vehicle System Dynamics*, 39(6):437–466, 2003.
- [53] K. S. Narendra and P. G. Gallman. An Iterative Method for the Identification of Nonlinear Systems Using a Hammerstein Model. *IEEE Transaction on Automatic Control*, 11:546–550, 1966.

- [54] N. N. N Nik Ibrahim and Z. Q. Lang. A new and efficient method for the determination of Output Frequency Response Function of nonlinear vibration system. In *Proceedings of the International Conference on Smart Infrastructure and Construction*, pages 447–452, 2016.
- [55] D. Nikoli, A. Seidel-Morgenstern, and M. Petkovska. Nonlinear frequency response analysis of forced periodic operation of non-isothermal CSTR using single input modulations . Part I : Modulation of inlet concentration or flow-rate. *Chemical Engineering Science*, 117:71–84, 2014.
- [56] D. Nikoli, A. Seidel-Morgenstern, and M. Petkovska. Nonlinear frequency response analysis of forced periodic operation of non-isothermal CSTR using single input modulations . Part II : Modulation of inlet temperature or temperature of the cooling / heating fluid. *Chemical Engineering Science*, 117:31–44, 2014.
- [57] D. Nikoli, A. Seidel-Morgenstern, and M. Petkovska. Nonlinear frequency response analysis of forced periodic operation of non-isothermal CSTR with simultaneous modulation of inlet concentration and inlet temperature. *Chemical Engineering Science*, 137:40–58, 2015.
- [58] Z. K. Peng and Z. Q. Lang. On the convergence of the Volterra-series representation of the Duffing’s oscillators subjected to harmonic excitations. *Journal of Sound and Vibration*, 305:322–332, 2007.
- [59] Z. K. Peng and Z. Q. Lang. The effects of nonlinearity on the output frequency response of a passive engine mount. *Journal of Sound and Vibration*, 318(1-2):313–328, nov 2008.
- [60] Z. K. Peng, Z. Q. Lang, and S. A. Billings. Non-linear output frequency response functions for multi-input non-linear Volterra systems. *International Journal of Control*, 80(6):843–855, jun 2007.
- [61] Z. K. Peng, Z. Q. Lang, S. A. Billings, and G. R. Tomlinson. Comparisons between harmonic balance and nonlinear output frequency response function in nonlinear system analysis. *Journal of Sound and Vibration*, 311:56–73, 2008.
- [62] Z. K. Peng, Z. Q. Lang, C. Wolters, S. A. Billings, and K. Worden. Feasibility study of structural damage detection using NARMAX modelling and Nonlinear Output Frequency Response Function based analysis, 2011.
- [63] M. Petkovska and D. D. Do. Nonlinear Frequency Response of Adsorption Systems. *Chemical Engineering Science*, 53(17):3081–3097, 1998.
- [64] M. Petkovska and D. D. Do. Nonlinear Frequency Response of Adsorption Systems: Isothermal Batch and Continuous Flow Adsorbers. *Chemical Engineering Science*, 53(17):3081–3097, 1998.

- [65] J. C. Peyton Jones. Simplified computation of the Volterra frequency response functions of non-linear systems. *Mechanical Systems and Signal Processing*, 21:1452–1468, apr 2007.
- [66] T. Proll and M. N. Karim. Model-predictive PH Control using Real-time Narx Approach. *AICHE Journal*, 40(2):269–282, 1994.
- [67] S. Rahman and J. Ahmed. *Handbook of Food Process Design*. John Wiley & Sons, 2012.
- [68] N. S. Rajbman and V. M. Chadeev. *Identification of Industrial Processes*. North-Holland, New York, 1980.
- [69] B. Ravindra and A. K. Mallik. Performance of nonlinear vibration isolators under harmonic excitation. *Journal of Sound and Vibration*, 170(3):325–337, 1994.
- [70] A. K. Ray. Performance improvement of a chemical reactor by non-linear natural oscillations. *The Chemical Engineering*, 59:169–175, 1995.
- [71] A. Renken. The use of periodic operation to improve the performance stirred tank reactors. *Chemical Engineering Science*, 27:1925–1932, 1972.
- [72] W. J. Rugh. *Nonlinear system theory - the Volterra/Wiener approach*. John Hopkins University Press, Baltimore, MD, 1981.
- [73] K. Schadlich, U. Hoffman, and H. Hofmann. Periodical operation of chemical processes and evaluation of conversion improvements k. *Chemical Engineering Science*, 38(9):1375–1384, 1983.
- [74] M. Schetzen. *The Volterra and Wiener Theories of Nonlinear Systems*. John Wiley, 1980.
- [75] M. Schetzen. Nonlinear System Modeling Based on the Wiener Theory, 1981.
- [76] D. E. Seborg, T. F. Edgar, and D. A. Mellichamp. *Process dynamics and control*. Wiley, Hoboken, N.J., 3rd ed., i edition, 2011.
- [77] T. Si and J. W. Blackburn. Importance of reaction structure in the periodic operation of six industrial chemical reactions. *Chemical Engineering Communications*, 169(1):111–136, 1998.
- [78] P. L. Silverston. Periodic operation of chemical reactors - a review of the experimental literature. *Sandhana*, 10:217–246, 1987.
- [79] P. Silveston, R. R. Hudgins, and A. Renken. Periodic operation of catalytic reactors - introduction and overview. *Catalysis Today*, 25:91–112, 1995.
- [80] P. Stoica. On the Convergence of an Iterative Algorithm Used for Hammerstein System Identification. *IEEE Transaction on Automatic Control*, 26(4):967–969, 1981.

- [81] S. W. Sung, J. Lee, and I. B. Lee. *Process Identification and PID Control*. Wiley-IEEE Press, 2009.
- [82] H Tong. *Non-Linear Time Series*. Oxford University Press, New York, 1990.
- [83] A. Uppal, W. H. Ray, and A. B. Poore. On the Dynamic Behavior of Continuous Stirred Tank Reactors. *Chemical Engineering Science*, 29(4):967–985, 1974.
- [84] J. A. Vazquez Feijoo, K. Worden, and R. Stanway. System identification using associated linear equations. *Mechanical Systems and Signal Processing*, 18(3):431–455, may 2004.
- [85] J. A. Vazquez Feijoo, K. Worden, and R. Stanway. Associated Linear Equations for Volterra operators. *Mechanical Systems and Signal Processing*, 19(1):57–69, jan 2005.
- [86] J. A. Vazquez Feijoo, K. Worden, and R. Stanway. Analysis of time-invariant systems in the time and frequency domain by associated linear equations (ALEs). *Mechanical Systems and Signal Processing*, 20(4):896–919, 2006.
- [87] F. Wang, K. Xing, X. Xu, and H Liu. *An identification approach of Hammerstein model*. 2010.
- [88] D. D. Weiner and J. E. Spina. *Sinusoidal Analysis and Modeling of Weakly Nonlinear Circuits with Application to Nonlinear Interference Effects*. Van Nostrand Reinhold, 1980.
- [89] Y. Yasuda. Frequency response method for study of kinetic details of a heterogeneous catalytic reaction of gases. 1. Theoretical treatment. *Journal of Physical Chemistry*, 97:3314–3318, 1993.
- [90] A. V. Zakharov, H. S. Bosman, and S. L. Jamsa-Jounela. Two-Phase Model Predictive Control and Its Application to the Tennessee Eastman Process. *Industrial and Engineering Chemistry Research*, 52(36):12937–12949, 2013.
- [91] Z. Zou, M. Yu, Z. Wang, X. Liu, Y. Guo, F. Zhang, and N. Guo. Nonlinear model algorithmic control of a pH neutralization process. *Chinese Journal of Chemical Engineering*, 21(4):395–400, 2013.



## Appendix A

# Results for the quadratic nonlinear MIMO system

### A.1 Comparison between the simulated output and the sum of ALEs

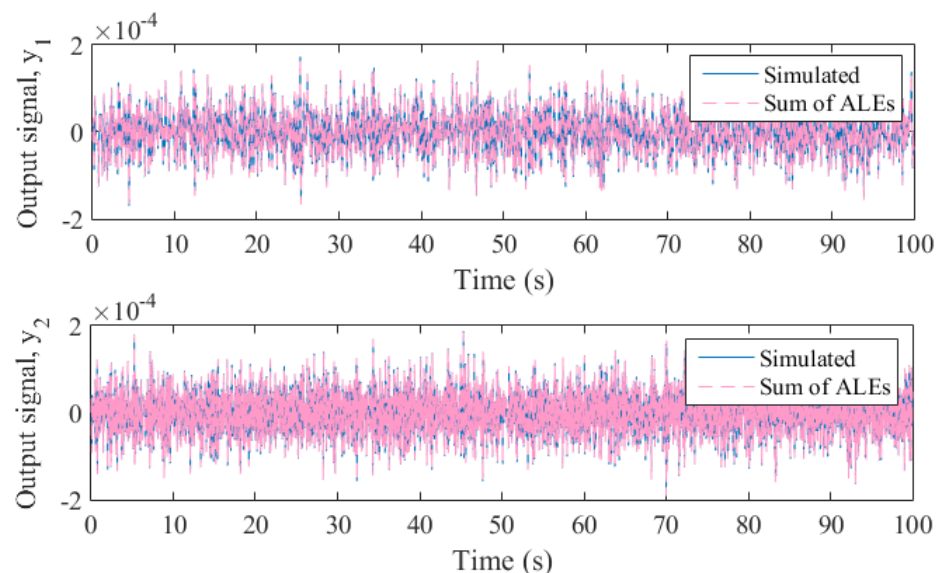


Figure A.1: The simulated output signals for both  $y_1$  and  $y_2$  of the system and sum of the signals from the ALEs in the time domain when  $a = 50$  and  $b = 150$ .

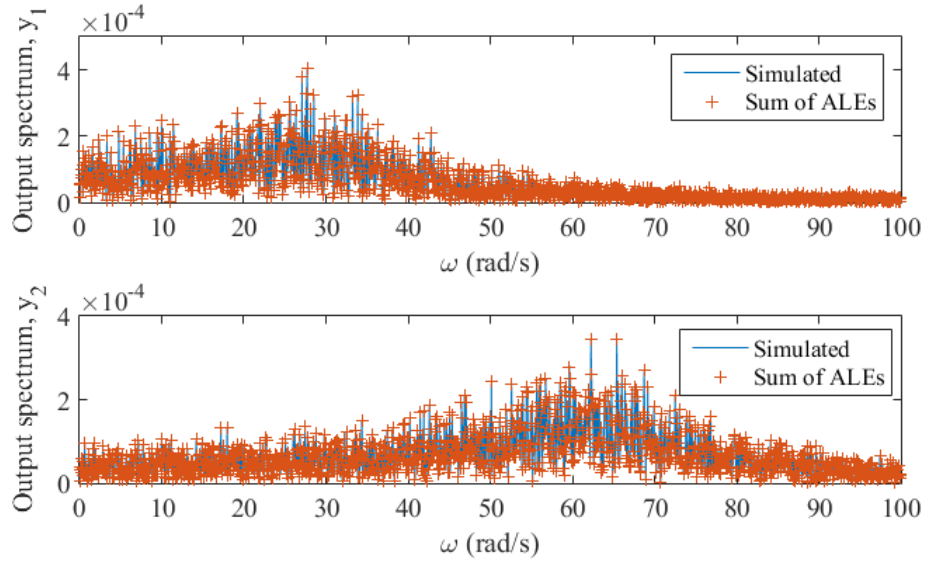


Figure A.2: The simulated output spectrum of the system and sum of the output spectrum from the ALEs in the frequency domain when  $a = 50$  and  $b = 150$  for both  $y_1$  and  $y_2$ .

## A.2 Comparison between the simulated output spectrum and the spectrum evaluated using OFRF

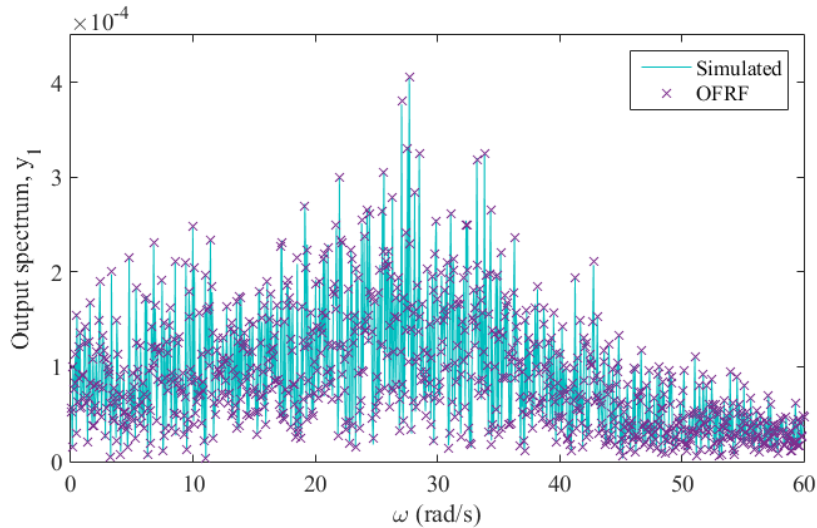


Figure A.3: Comparison between the simulated output spectrum and the spectrum evaluated using OFRF for output  $y_1$  when  $a = 90$  and  $b = 240$ .

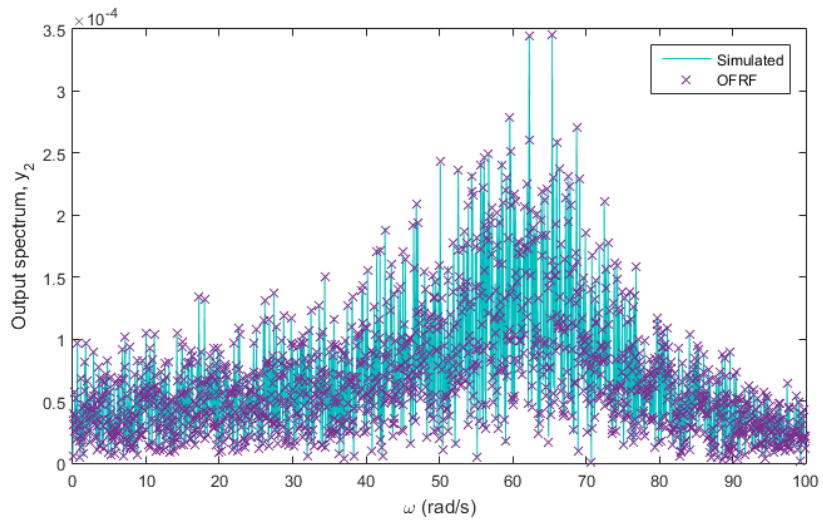


Figure A.4: Comparison between the simulated output spectrum and the spectrum evaluated using OFRF for output  $y_2$  when  $a = 90$  and  $b = 240$ .





## Appendix B

# OFRF based analysis for the application in the earthquake engineering

### B.1 The derivation of ALEs for the building system

In order to use the algorithm, rewrite the building system (4.42) in the different form as

$$\begin{aligned}
 m_1 D^2 x_1(t) + (c_1 + c_2) D^1 x_1(t) - c_2 D^1 x_2(t) + (k_1 + k_2) x_1(t) - k_2 x_2(t) \\
 = (C_1 + C_2 x_1(t)^2) D^1 x_1(t) + (K_1 + K_2 x_1(t)^2) x_1(t) - m_1 \ddot{z}(t) \\
 m_2 D^2 x_2(t) - c_2 D^1 x_1(t) + (c_2 + c_3) D^1 x_2(t) - c_3 D^1 x_3(t) - k_2 x_1(t) + (k_2 + k_3) x_2(t) - k_3 x_3(t) \\
 = -m_2 \ddot{z}(t) \\
 m_3 D^2 x_3(t) - c_3 D^1 x_2(t) + (c_3 + c_4) D^1 x_3(t) - c_4 D^1 x_4(t) - k_3 x_2(t) + (k_3 + k_4) x_3(t) - k_4 x_4(t) \\
 = -m_3 \ddot{z}(t) \\
 m_4 D^2 x_4(t) - c_4 D^1 x_3(t) + (c_4 + c_5) D^1 x_4(t) - c_5 D^1 x_5(t) - k_4 x_3(t) + (k_4 + k_5) x_4(t) - k_5 x_5(t) \\
 = -m_4 \ddot{z}(t) \\
 m_5 D^2 x_5(t) - c_5 D^1 x_4(t) + (c_5 + c_6) D^1 x_5(t) - c_6 D^1 x_6(t) - k_5 x_4(t) + (k_5 + k_6) x_5(t) - k_6 x_6(t) \\
 = -m_5 \ddot{z}(t) \\
 m_6 D^2 x_6(t) - c_6 D^1 x_5(t) + (c_6 + c_7) D^1 x_6(t) - c_7 D^1 x_7(t) - k_6 x_5(t) + (k_6 + k_7) x_6(t) - k_7 x_7(t) \\
 = -m_6 \ddot{z}(t) \\
 m_7 D^2 x_7(t) - c_7 D^1 x_6(t) + (c_7 + c_8) D^1 x_7(t) - c_8 D^1 x_8(t) - k_7 x_6(t) + (k_7 + k_8) x_7(t) - k_8 x_8(t) \\
 = -m_7 \ddot{z}(t)
 \end{aligned}$$

$$\begin{aligned}
& m_8 D^2 x_8(t) - c_8 D^1 x_7(t) + (c_8 + c_9) D^1 x_8(t) - c_9 D^1 x_9(t) - k_8 x_7(t) + (k_8 + k_9) x_8(t) - k_9 x_9(t) \\
& = -m_8 \ddot{z}(t) \\
& m_9 D^2 x_9(t) - c_9 D^1 x_8(t) + (c_9 + c_{10}) D^1 x_9(t) - c_{10} D^1 x_{10}(t) - k_9 x_8(t) + (k_9 + k_{10}) x_9(t) \\
& - k_{10} x_{10}(t) = -m_9 \ddot{z}(t) \\
& m_{10} D^2 x_{10}(t) - c_{10} D^1 x_9(t) + c_{10} D^1 x_{10}(t) - k_{10} x_9(t) + k_{10} x_{10}(t) \\
& = -m_{10} \ddot{z}(t)
\end{aligned} \tag{B.1}$$

Using the steps in the algorithm, set  $N_{max} = 3$ ,  $N = 1, 2, 3$ . Then, the ALEs for every order up to 5th-order can be written as

$$\begin{aligned}
& m_1 D^2 x_{1,1}(t) + (c_1 + c_2) D^1 x_{1,1}(t) - c_2 D^1 x_{2,1}(t) + (k_1 + k_2) x_{1,1}(t) - k_2 x_{2,1}(t) \\
& = -m_1 \ddot{z}(t) \\
& m_2 D^2 x_{2,1}(t) - c_2 D^1 x_{1,1}(t) + (c_2 + c_3) D^1 x_{2,1}(t) - c_3 D^1 x_{3,1}(t) - k_2 x_{1,1}(t) + (k_2 + k_3) x_{2,1}(t) \\
& - k_3 x_{3,1}(t) = -m_2 \ddot{z}(t) \\
& m_3 D^2 x_{3,1}(t) - c_3 D^1 x_{2,1}(t) + (c_3 + c_4) D^1 x_{3,1}(t) - c_4 D^1 x_{4,1}(t) - k_3 x_{2,1}(t) + (k_3 + k_4) x_{3,1}(t) \\
& - k_4 x_{4,1}(t) = -m_3 \ddot{z}(t) \\
& m_4 D^2 x_{4,1}(t) - c_4 D^1 x_{3,1}(t) + (c_4 + c_5) D^1 x_{4,1}(t) - c_5 D^1 x_{5,1}(t) - k_4 x_{3,1}(t) + (k_4 + k_5) x_{4,1}(t) \\
& - k_5 x_{5,1}(t) = -m_4 \ddot{z}(t) \\
& m_5 D^2 x_{5,1}(t) - c_5 D^1 x_{4,1}(t) + (c_5 + c_6) D^1 x_{5,1}(t) - c_6 D^1 x_{6,1}(t) - k_5 x_{4,1}(t) + (k_5 + k_6) x_{5,1}(t) \\
& - k_6 x_{6,1}(t) = -m_5 \ddot{z}(t) \\
& m_6 D^2 x_{6,1}(t) - c_6 D^1 x_{5,1}(t) + (c_6 + c_7) D^1 x_{6,1}(t) - c_7 D^1 x_{7,1}(t) - k_6 x_{5,1}(t) + (k_6 + k_7) x_{6,1}(t) \\
& - k_7 x_{7,1}(t) = -m_6 \ddot{z}(t)
\end{aligned}$$

$$\begin{aligned}
& m_7 D^2 x_{7,1}(t) - c_7 D^1 x_{6,1}(t) + (c_7 + c_8) D^1 x_{7,1}(t) - c_8 D^1 x_{8,1}(t) - k_7 x_{6,1}(t) + (k_7 + k_8) x_{7,1}(t) \\
& \quad - k_8 x_{8,1}(t) = -m_7 \ddot{z}(t) \\
& m_8 D^2 x_{8,1}(t) - c_8 D^1 x_{7,1}(t) + (c_8 + c_9) D^1 x_{8,1}(t) - c_9 D^1 x_{9,1}(t) - k_8 x_{7,1}(t) + (k_8 + k_9) x_{8,1}(t) \\
& \quad - k_9 x_{9,1}(t) = -m_8 \ddot{z}(t) \\
& m_9 D^2 x_{9,1}(t) - c_9 D^1 x_{8,1}(t) + (c_9 + c_{10}) D^1 x_{9,1}(t) - c_{10} D^1 x_{10,1}(t) - k_9 x_{8,1}(t) \\
& \quad + (k_9 + k_{10}) x_{9,1}(t) - k_{10} x_{10,1}(t) = -m_9 \ddot{z}(t) \\
& m_{10} D^2 x_{10,1}(t) - c_{10} D^1 x_{9,1}(t) + c_{10} D^1 x_{10,1}(t) - k_{10} x_{9,1}(t) + k_{10} x_{10,1}(t) \\
& \quad = -m_{10} \ddot{z}(t)
\end{aligned} \tag{B.2}$$

$$\begin{aligned}
& m_1 D^2 x_{1,3}(t) + (c_1 + c_2) D^1 x_{1,3}(t) - c_2 D^1 x_{2,3}(t) + (k_1 + k_2) x_{1,3}(t) - k_2 x_{2,3}(t) \\
& \quad = -C_2 x_{1,1}(t)^2 \dot{x}_{1,1}(t) - K_2 x_{1,1}(t)^3 \\
& m_2 D^2 x_{2,3}(t) - c_2 D^1 x_{1,3}(t) + (c_2 + c_3) D^1 x_{2,3}(t) - c_3 D^1 x_{3,3}(t) - k_2 x_{1,3}(t) + (k_2 + k_3) x_{2,3}(t) \\
& \quad - k_3 x_{3,3}(t) = 0 \\
& m_3 D^2 x_{3,3}(t) - c_3 D^1 x_{2,3}(t) + (c_3 + c_4) D^1 x_{3,3}(t) - c_4 D^1 x_{4,3}(t) - k_3 x_{2,3}(t) + (k_3 + k_4) x_{3,3}(t) \\
& \quad - k_4 x_{4,3}(t) = 0 \\
& m_4 D^2 x_{4,3}(t) - c_4 D^1 x_{3,3}(t) + (c_4 + c_5) D^1 x_{4,3}(t) - c_5 D^1 x_{5,3}(t) - k_4 x_{3,3}(t) + (k_4 + k_5) x_{4,3}(t) \\
& \quad - k_5 x_{5,3}(t) = 0 \\
& m_5 D^2 x_{5,3}(t) - c_5 D^1 x_{4,3}(t) + (c_5 + c_6) D^1 x_{5,3}(t) - c_6 D^1 x_{6,3}(t) - k_5 x_{4,3}(t) + (k_5 + k_6) x_{5,3}(t) \\
& \quad - k_6 x_{6,3}(t) = 0 \\
& m_6 D^2 x_{6,3}(t) - c_6 D^1 x_{5,3}(t) + (c_6 + c_7) D^1 x_{6,3}(t) - c_7 D^1 x_{7,3}(t) - k_6 x_{5,3}(t) + (k_6 + k_7) x_{6,3}(t) \\
& \quad - k_7 x_{7,3}(t) = 0
\end{aligned}$$

$$\begin{aligned}
& m_7 D^2 x_{7,3}(t) - c_7 D^1 x_{6,3}(t) + (c_7 + c_8) D^1 x_{7,3}(t) - c_8 D^1 x_{8,3}(t) - k_7 x_{6,3}(t) + (k_7 + k_8) x_{7,3}(t) \\
& \quad - k_8 x_{8,3}(t) = 0 \\
& m_8 D^2 x_{8,3}(t) - c_8 D^1 x_{7,3}(t) + (c_8 + c_9) D^1 x_{8,3}(t) - c_9 D^1 x_{9,3}(t) - k_8 x_{7,3}(t) + (k_8 + k_9) x_{8,3}(t) \\
& \quad - k_9 x_{9,3}(t) = 0 \\
& m_9 D^2 x_{9,3}(t) - c_9 D^1 x_{8,3}(t) + (c_9 + c_{10}) D^1 x_{9,3}(t) - c_{10} D^1 x_{10,3}(t) - k_9 x_{8,3}(t) \\
& \quad + (k_9 + k_{10}) x_{9,3}(t) - k_{10} x_{10,3}(t) = 0 \\
& m_{10} D^2 x_{10,3}(t) - c_{10} D^1 x_{9,3}(t) + c_{10} D^1 x_{10,3}(t) - k_{10} x_{9,3}(t) + k_{10} x_{10,3}(t) \\
& \quad = 0
\end{aligned} \tag{B.3}$$

$$\begin{aligned}
& m_1 D^2 x_{1,5}(t) + (c_1 + c_2) D^1 x_{1,5}(t) - c_2 D^1 x_{2,5}(t) + (k_1 + k_2) x_{1,5}(t) - k_2 x_{2,5}(t) \\
& = -C_2 (2x_{1,1}(t)x_{1,3}(t)\dot{x}_{1,1} + x_{1,3}(t)^2\dot{x}_{1,1} + x_{1,1}(t)^2\dot{x}_{1,3} + 2x_{1,1}(t)x_{1,3}(t)\dot{x}_{1,3} \\
& \quad + x_{1,3}(t)^2\dot{x}_{1,3}) - K_2 (3y_1(t)^2y_3(t) + 3y_1(t)y_3(t)^2 + y_3(t)^3) \\
& m_2 D^2 x_{2,5}(t) - c_2 D^1 x_{1,5}(t) + (c_2 + c_3) D^1 x_{2,5}(t) - c_3 D^1 x_{3,5}(t) - k_2 x_{1,5}(t) + (k_2 + k_3) x_{2,5}(t) \\
& \quad - k_3 x_{3,5}(t) = 0 \\
& m_3 D^2 x_{3,5}(t) - c_3 D^1 x_{2,5}(t) + (c_3 + c_4) D^1 x_{3,5}(t) - c_4 D^1 x_{4,5}(t) - k_3 x_{2,5}(t) + (k_3 + k_4) x_{3,5}(t) \\
& \quad - k_4 x_{4,5}(t) = 0 \\
& m_4 D^2 x_{4,5}(t) - c_4 D^1 x_{3,5}(t) + (c_4 + c_5) D^1 x_{4,5}(t) - c_5 D^1 x_{5,5}(t) - k_4 x_{3,5}(t) + (k_4 + k_5) x_{4,5}(t) \\
& \quad - k_5 x_{5,5}(t) = 0 \\
& m_5 D^2 x_{5,5}(t) - c_5 D^1 x_{4,5}(t) + (c_5 + c_6) D^1 x_{5,5}(t) - c_6 D^1 x_{6,5}(t) - k_5 x_{4,5}(t) + (k_5 + k_6) x_{5,5}(t) \\
& \quad - k_6 x_{6,5}(t) = 0 \\
& m_6 D^2 x_{6,5}(t) - c_6 D^1 x_{5,5}(t) + (c_6 + c_7) D^1 x_{6,5}(t) - c_7 D^1 x_{7,5}(t) - k_6 x_{5,5}(t) + (k_6 + k_7) x_{6,5}(t) \\
& \quad - k_7 x_{7,5}(t) = 0
\end{aligned}$$

$$\begin{aligned}
& m_7 D^2 x_{7,5}(t) - c_7 D^1 x_{6,5}(t) + (c_7 + c_8) D^1 x_{7,5}(t) - c_8 D^1 x_{8,5}(t) - k_7 x_{6,5}(t) + (k_7 + k_8) x_{7,5}(t) \\
& \quad - k_8 x_{8,5}(t) = 0 \\
& m_8 D^2 x_{8,5}(t) - c_8 D^1 x_{7,5}(t) + (c_8 + c_9) D^1 x_{8,5}(t) - c_9 D^1 x_{9,5}(t) - k_8 x_{7,5}(t) + (k_8 + k_9) x_{8,5}(t) \\
& \quad - k_9 x_{9,5}(t) = 0 \\
& m_9 D^2 x_{9,5}(t) - c_9 D^1 x_{8,5}(t) + (c_9 + c_{10}) D^1 x_{9,5}(t) - c_{10} D^1 x_{10,5}(t) - k_9 x_{8,5}(t) \\
& \quad + (k_9 + k_{10}) x_{9,5}(t) - k_{10} x_{10,5}(t) = 0 \\
& m_{10} D^2 x_{10,5}(t) - c_{10} D^1 x_{9,5}(t) + c_{10} D^1 x_{10,5}(t) - k_{10} x_{9,5}(t) + k_{10} x_{10,5}(t) \\
& \quad = 0
\end{aligned} \tag{B.4}$$

(B.2) is the first order ALEs for the system while (B.3) and (B.4) are the third and fifth order ALEs for the system.

## B.2 Comparison between the simulated output spectrum and the spectrum evaluated using OFRF for even floors

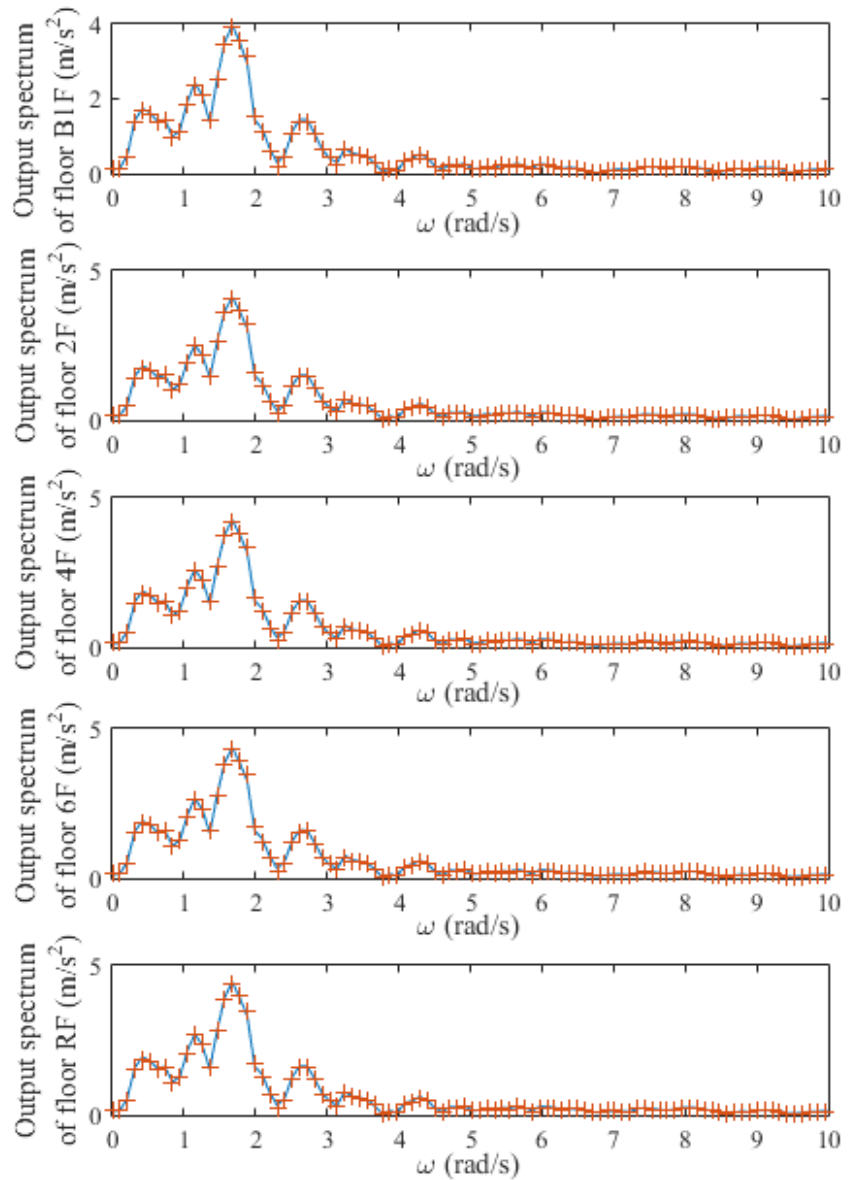


Figure B.1: Comparison between the simulated output spectrum and the spectrum evaluated using OFRF for the even floors when  $C_2 = 120 \times 10^5$  and  $K_2 = 40 \times 10^5$ .